The copyright of this thesis vests in the author. No quotation from it or information derived from it is to be published without full acknowledgement of the source. The thesis is to be used for private study or non-commercial research purposes only.

Published by the University of Cape Town (UCT) in terms of the non-exclusive license granted to UCT by the author.

University of Cape Town

Synthesis of *Mycobacterial* Ergothioneine biosynthetic pathway metabolites

Lutete Peguy Khonde

University of Cape Town

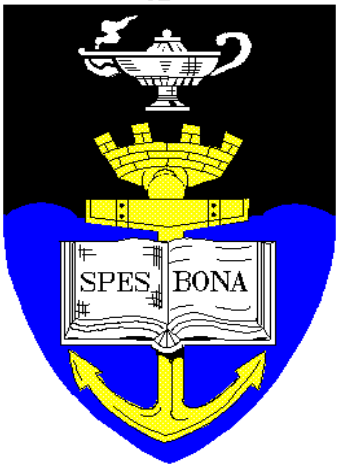

UNIVERSITY OF CAPE TOWN

2013

Synthesis of *Mycobacterial* Ergothioneine biosynthetic pathway metabolites

By

Lutete Peguy Khonde

A thesis submitted in fulfilment of the requirements for the degree of Master in Science of chemistry

University of Cape Town

Department of Chemistry

University of Cape Town

South Africa

Supervisor: Dr Anwar Jardine

February 2013

Declaration

I declared that "**Synthesis of *Mycobacterial* Ergothioneine biosynthetic pathway metabolites"** is my own work and that all sources of information used herein are cited, acknowledged and completely referenced at the end of each chapter.

University of Cape Town

Lutete Peguy Khonde (KHNLUT001) Date

Acknowledgements

I would like to express my profound gratitude and appreciation to the following individuals for their contribution to the preparation of this thesis, without their support this research project would not have been possible:

First and foremost, my Lord and my Sovereign God for the unconditional love and grace to carry out this work.

My supervisor, Dr Anwar Jardine, for his guidance, support, enthusiasm, patience, encouragement, support and invaluable training throughout the course of my Master studies.

Carine Sao, Bienyameen Baker (Tygerberg Stellenbosch University, Cape Town, South Africa) our collaborators for their assistance in the preparation of crude *Mycobacterium smegmatis* enzyme lysate.

Mr Pete Roberts and Noel Hendrick for recording of NMR spectra. Mr Piero Benincasa for EI-MS. Dr. Zac Mcdonald (Molecular and Cell biology, University of Cape Town, South Africa) for LCMS studies.

My colleagues in the UCT Chemistry Department; particularly the Jardine research group, James Sehata, Dorothy Semenya, Shakeela Sayed, Gaynor Manuel, the Gammon research group, Denis Ngumbu Muhunga, Freddy Munganza Munyololo, Nick Watermeyer, the Chibale research group, Dennis ongarora, Faith Riziki, and Nicholas Njuguma for their helpful discussions.

The University of Cape Town (Postgraduate Funding office) for funding.

And finally, I dedicate this thesis to my family, Tsimba Khonde Joseph (*father*), Ngoma Yezi Hortence (*mother*), Fanny, Rebecca, Josue, Rachel, Priscille (*siblings*), Precieux (*nephew*), Eunice, Ara (*nieces*), Bijou Kapinga (*my wife*) and Samuella Lutete (*my love*), thank you all for the constant love and encouragements throughout my life.

University of Cape Town

Abstract

Many gram positive bacteria, such as *Mycobacterium tuberculosis*, lack the redox protective molecule, glutathione and produce mycothiol (MSH) and ergothioneine (ESH) as their principal low molecular mass thiol instead. Ergothioneine has been known for a while as an anti-oxidant; however its role as a protective thiol in *Mycobacterium tuberculosis* is still undefined. Present knowledge indicates that ergothioneine may play a critical role in the *in vivo* and *in vitro* survival of Mycobacteria, hence enzymes involved in ESH synthesis can be considered as potential drug targets.

Ergothioneine is synthesized by the sequential action of five enzymes, encoded by the genes *egtA, egtB, egtC, egtD* and *egtE*. Three of these enzymes implicated in the ergothioneine synthesis have been expressed and purified. The last step catalyzed by EgtE, a pyridoxal 5-phosphate (PLP)-dependent β-lyase convert the *S*-(*β*-amino-*β*-carboxyethyl) ergothioneine sulfoxide to ergothioneine. This thesis describes the synthesis of ESH pathway enzyme substrates, with the main focus on the synthesis of the EgtE enzyme substrate, ESH biosynthetic precursor, *R*- and *S*-(*β*-amino-*β*-carboxyethyl) ergothioneine sulfoxide. In order to prove that synthesized compounds are indeed mycobacterium ESH pathway enzyme substrates, crude *M. smeg* cell free lysate enzyme was used to convert substrates to ESH. Enzymatic transformation was followed by LCMS analysis.

One of two synthetic routes studied, required sufficient quantities of ESH and were therefore thoroughly reviewed. An improved synthetic procedure for ESH was obtained.

Deuterated hercynine and ESH was prepared, which will serve as a valuable internal standards and probes for ergothioneine metabolic studies. Enantioselective sulfoxidation of EgtE enzyme substrate precursor, hercynyl cysteine sulfide gave the required hercynyl cysteine sulfoxide derivative and in same cases the hercynyl cysteine sulfone. Crude enzyme mediated transformation of substrates indicated that the hercynyl cysteine sulfide undergoes efficient conversion to ESH.

University of Cape Town

Abbreviations

AcOH	Acetic acid glacial
aq.	Aqueous
Ar	Aromatic
BnBr	Benzyl Bromide
Boc	*Tert-butyl* dicarbonate
br.	Broad
brs	Broad singlet
BSH	Bacillithiol
Bz	Benzoyl
BzCl	Benzoyl chloride
c	Concentration (g/100 ml)
cat.	Catalytic
CF_3COOH	Trifluoroacetic acid
CH_2Cl_2	Dichloromethane / Methylene chloride
CH_3CN	Acetonitrile
Conc	Concentrated
C=O	Carbonyl
CPO	Chloroperoxidase
°	Degree
°C	Degree Celcius
δ	Chemical shift in ppm
d	Doublet
DCM	Dichloromethane
dec	Decomposition
dd	Doublet of doublet
dt	Doublet of triplet
DMSO	Dimethyl sulfoxide

University of Cape Town

DMF	Dimethyl formamide
DNA	Deoxyribonucleic acid
EDTA	Ethylene diamine tetracetic acid
EI^+	Electron impact (positive mode)
EIC	Extract ion chromatogram
ESH	Ergothioneine
ESI^+	Electro spray ionization (positive mode)
Et_3N	Triethylamine
Et_2O	Diethyl ether
EtOAc	Ethyl acetate
EtOH	Ethanol
eq.	Equivalent
FAD	Flavin adenine dinucleotide
FTIR	Fourier Transform Infrared
g	Gram(s)
GSH	Glutathione
H_2O_2	Hydrogen peroxide
HCl	Hydrochloric acid
HPLC	High pressure liquid chromatography
hr.	Hour
HRMS	High resolution mass spectrometry
Hz	Hertz
IR	Infrared
J	Coupling constant
Lit.	Literature
m	Meta
m	Multiplet
*m*CPBA	Meta-chloroperoxybenzoic acid
MeOH	Methanol

University of Cape Town

Me_2SO_4	Dimethyl sulfate
mg	Milligram(s)
$[M]^+$	Molecular ion
MHz	Mega Hertz
ml	Milliliter(s)
mmol	Millimole(s)
Mp	Melting point
MS	Mass spectrum
MSH	Mycothiol
m/z	Mass to charge ratio
NMR	Nuclear magnetic resonance
$NaBH(OAc)_3$	Sodium triacetoxyborohydride
Lit	Literature
o	Ortho
p	Para
PG	Protecting group
Pd/C	Palladium-on-carbon
Pet Ether	Petroleum ether
Ph	Phenyl
PLP	Pyridoxal 5'-phosphate
%	Percentage
PPh_3	Triphenylphosphine
$(PPh_3)_4P$	Tetrakis(triphenylphosphine)palladium
RNA	Ribonucleic acid
rt	Room temperature
R_t	Retention time
$RhCl(PPh_3)_3$	Chlorotris(triphenylphosphine)rhodium (I)
s	Singlet
S_N1	Unimolecular nucleophilic substitution

University of Cape Town

S_N2	Bimolecular nucleophilic substitution
t	Triplet
TCT	2, 4, 6-Trichloro-[1, 3, 5]triazine
td	Triplet of doublets
TEA	Triethylamine
THF	Tetrahydrofuran
TIC	Total ion chromatogram
TFA	Trifluoroacetic acid
TLC	Thin layer chromatography
TSH	Trypanothione
q	Quartet
UV	Ultra violet
w/v	Weight by volume
v/v	Volume by volume

University of Cape Town

Conference contributions

Synthesis of *R/S*-(*β*-amino-*β*-carboxyethyl) ergothioneine sulfoxide, the biosynthetic precursor of ergothioneine, 12th Frank Warren Conference (organic chemistry), University of Free State, Bloemfontein, South Africa, 15 -18th April, **2012.**

Khonde, P.L. and Jardine, A.M. (Poster)

Total synthesis of *L*-ergothioneine, Workshop and dfiscussion forum on Mycothiol drug development, Pine Lake Marina, Sedgefield, South Africa, 16 -18th April, **2011**.

Khonde, P.L. and Jardine, A.M. (Oral)

University of Cape Town

Table of contents

University of Cape Town

University of Cape Town

University of Cape Town

Chapter 1 Introduction

1.1. Tuberculosis

Tuberculosis (TB) is a global infectious disease caused by the pathogenic gram positive bacterium *Mycobacterium tuberculosis.*[1] Despite the availability of chemotherapy for many decades, tuberculosis remains a major global threat and a leading cause of mortality in the developing world.[2]

1.2. The burden of disease caused by tuberculosis

The disease was declared by World Health Organisation (WHO) as a global health emergency in 1993; however the rapid growth of the global population, the deterioration of the living conditions within developing countries and the spread of HIV drastically affected the magnitude of tuberculosis problem.

Tuberculosis kills one person every 10 seconds,[3] each year 1% of the global population is infected and an estimated one billion more people will be infected and 700 million killed by 2020. In 2010 most of cases of TB occurred in Asia (57%) and Africa (26%), but a smaller incidence of TB has occurred in Eastern Mediterranean countries (7%), Europe (5%) and America (3%). [4] According to WHO (2010 statistics) the five countries with the highest TB incidence were India (2.0-2.5 million), China (0.9 million-1.2 million), South Africa (0.40 million – 0.59 million), Indonesia (0.37 million – 0.54 million) and Pakistan (0.33 million – 0.48 million) as shown in Figure 1.1.

University of Cape Town

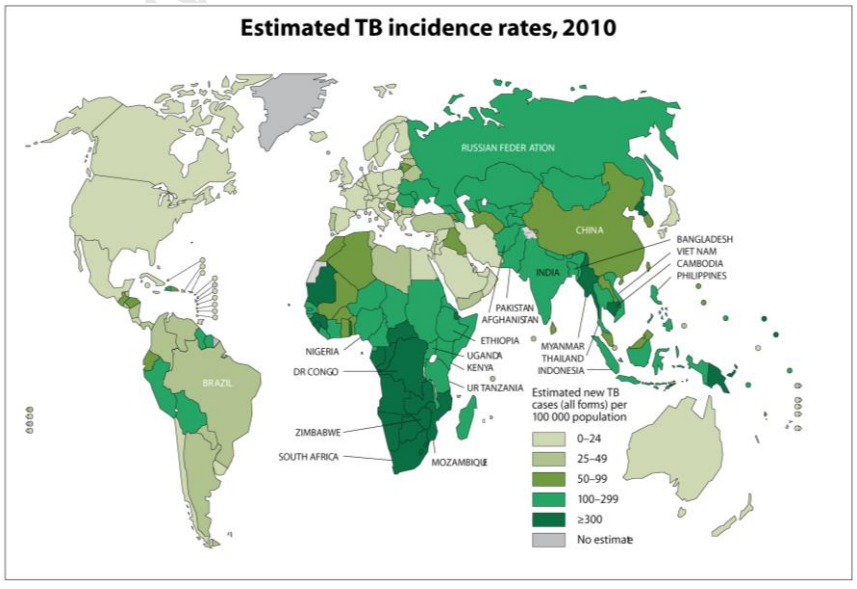

Figure 1.1 Estimated TB incidence rates, WHO, 2010.[5]

According to statistics released by WHO in October 2011, there were an estimated 8.8 million cases of TB reported globally in 2010, 1.1 million deaths amongst them 0.35 millions were HIV positive.[4] Africa still has the highest reported incidence of TB patients co-infected with HIV, an overall 82 % was estimated (Figure 1.2).

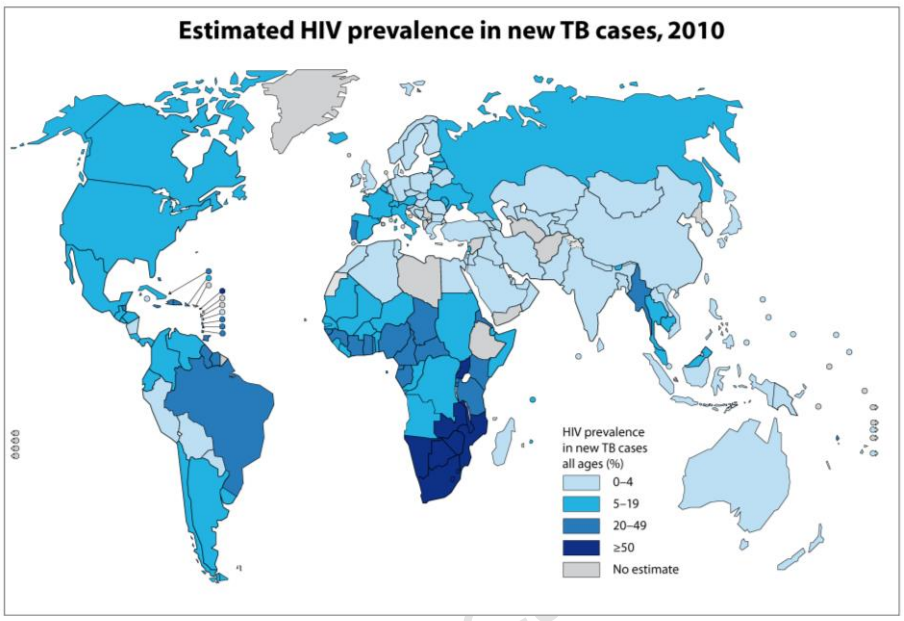

Figure 1.2. Estimated HIV prevalence in new TB cases, WHO, 2010.[5]

1.3. Mycobacterium tuberculosis (M. tb)

Mycobacterium tuberculosis (*M. tb*) (Figure 1.3) has been found to mainly cause disease in humans. *M. tb* is a rod shaped bacterium, 2-4 µm long and 0.2-0.5 µm wide. It is an obligate aerobic pathogen, for this reason usually found in the lung in particular the well aerated parts. *M.tb* is a facultative intracellular parasite that has a very slow growth rate; it divides every 15-20 hours which is a physiological characteristic that may contribute to its virulence.

M. tb is classified as acid-fast bacteria due to the structure of its cell wall containing peptidoglycan although rich in lipids (over 60%). The cells wall consists of three components, mycolic acid, cord factor and wax-D.[6]

University of Ca

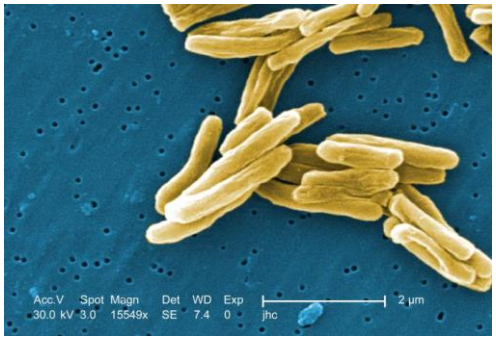

Figure 1.3 *Mycobacterium tuberculosis* scanning electron micrograph.[6]

1.4. Drug treatment against tuberculosis

The treatment of tuberculosis is difficult due to two major factors, persistence (survival of *M. tuberculosis* despite the use of antibiotics) and complete resistance. Because of the persistence of *M .tb*, drug treatment is extended between 6-9 months and even requires a combination of at least 3 effective drugs to cure the patients completely and prevent relapse.[3]

In year 2000, an estimated 3.2% of all TB cases were multi-drug resistant. The resistance is due to a genetic mutation resulting in altered affinity of the target or the activator of the drug. Multidrug-resistant strains (MDR) are resistant to first line drugs; isoniazid (INH) and rifampicin (RFP), other strains carry even a greater level of drug resistance, called extensively drug-resistant (XDR) displaying resistance to fluoroquinolones and at least one of the injectable antibiotics (streptomycin, kanamycin, capreomycin) (Figure 1.4).[7]

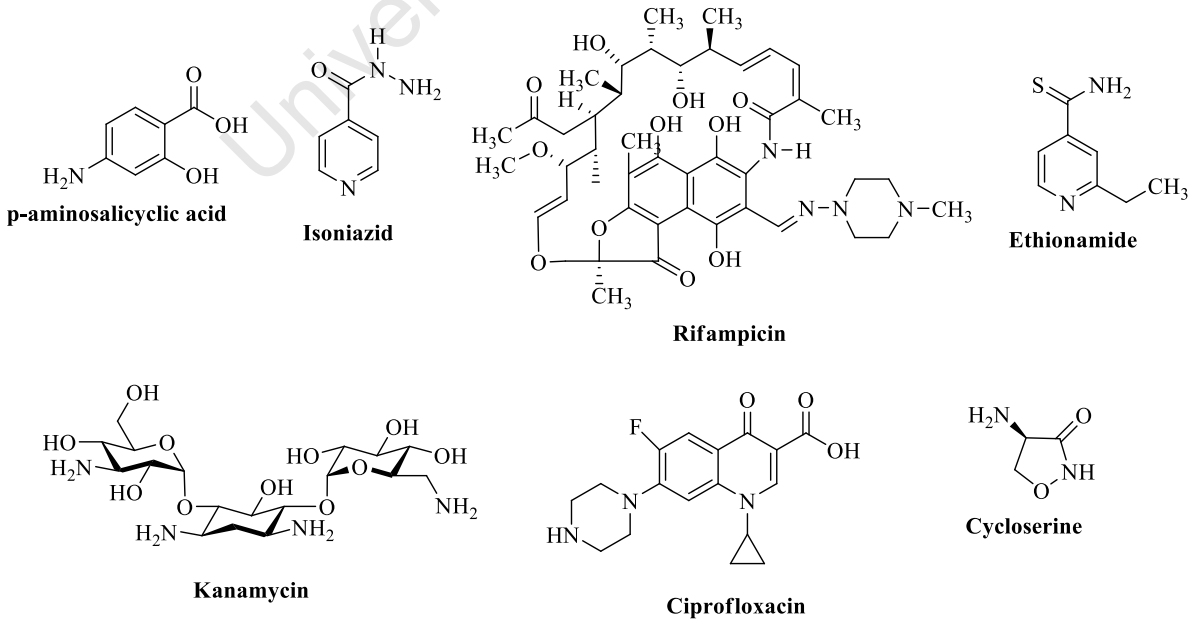

Figure 1.4 Structures of some antitubercular Drugs.[7]

University of Cape Town

The second and third-line TB drugs are less effective, more toxic, and more expensive than the first line drugs. It is necessary to revert to 2nd line drugs when the patient either does not respond to the first line or does not tolerate them. Understanding the *M. tb* mechanism of defence (detoxification / xenotification) is an alternative approach to battle the disease (Figure 1.5).

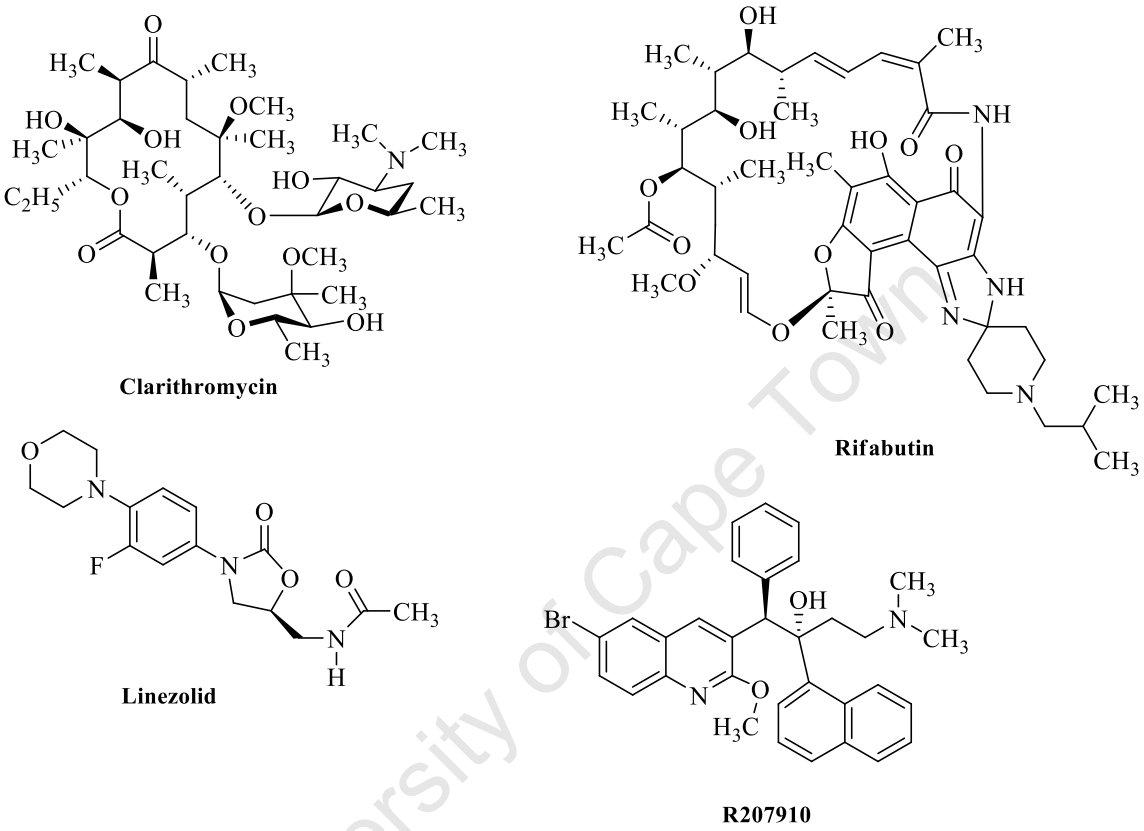

Figure 1.5 Structures of some examples of third-line TB drugs

1.5. Challenges in tuberculosis drug discovery.

TB treatment faces many problems, high cost and very long (6 to 9 months) treatment. Resistance of *M. tb* toward current drugs, toxicity, and TB / HIV co-infection etc, warrants the development of new more efficient, safe and affordable drugs.

Existent TB drugs possess various mechanisms of action. The first-line antitubercular drug, isoniazid (INH) inhibits mycolic acid biosynthesis, one of the essential components of the mycobacterial wall cell. Pyrazinamide, which is structurally similar to INH, is a prodrug that target the ribosomal protein S1.[8]

University of Cape Town

Rifampicin, acts on replicating and non-replicating mycobacteria by inhibiting bacterial RNA synthesis through binding to the β-subunit of the DNA-dependent polymerase.[8, 9]

In the last decade, many promising drug candidates have entered clinical trials. These efforts gave rise to the fluoroquinolones; gatifloxacin and moxifloxacin (phase 3), oxazolidinone linezolid and nitroimidazole metronidazole (phase 2) have been repurposed for tuberculosis treatment. New chemical entities have also progressed in clinical development based on the optimization of known chemical scaffolds such as nitro-imidazole derivatives (oxazolidinones) and diaryquinolines (a new class of antitubercular drug).[8]

Most of the abovementioned drugs target the cell wall; hence they are more susceptible to develop resistance. Therefore, modern drug discovery programs targets the metabolome, in search of essential metabolites. Low molecular thiols are metabolites that play a key role in maintaining a redox balance in mycobacteria and are responsible for the survival of *M. tb*.[10]

The future of TB drug discovery is promisisng. Researches toward funding new biological targets, funding analogues of existing drug more effective and less toxic, disturbing the redox homeostasis of *M. tb* by inhibiting its protective anti oxidant thiol (MSH, ESH), as well as improvement of method of screening and testing of drugs candidates, etc are leading the future of TB drug discovery, [9, 11] as summarised in Figure 1.6.

University of Cape Town

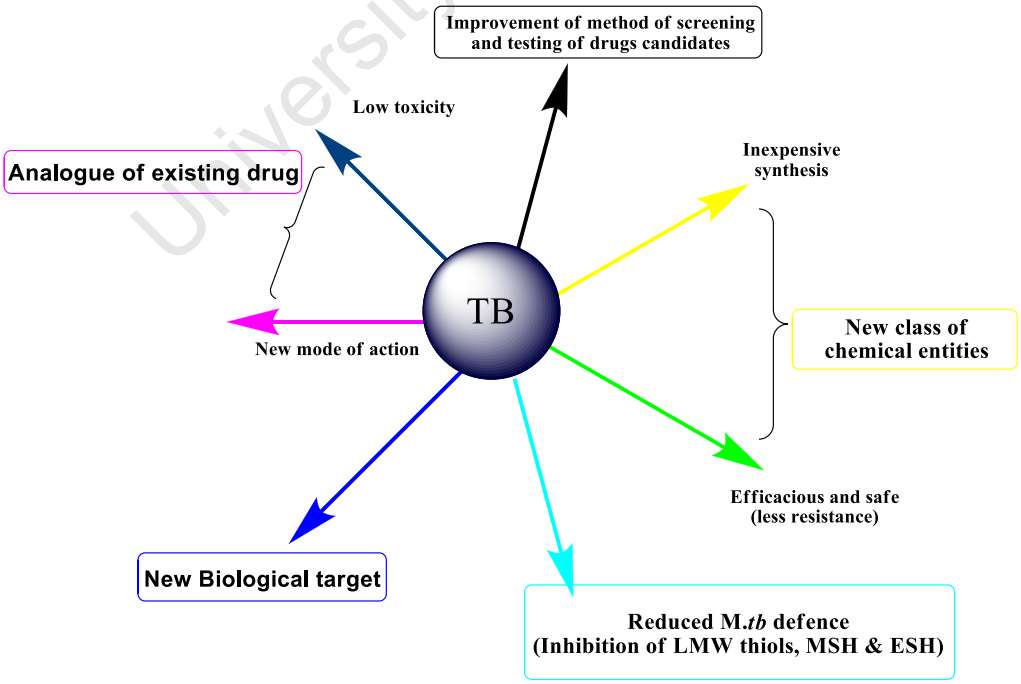

Figure 1.6 Future of TB drug discovery.[9]

1.6. Low Molecular Weight (LMW) thiols

Low Molecular Weight (LMW) thiols play an essential role in the survival of many pathogenic microorganisms, acting as redox buffers, maintaining the redox homeostasis within the cells,[12] and can defend the cells from damage inflicted by reactive oxygen and nitrogen species[13] (Figure 1.7)

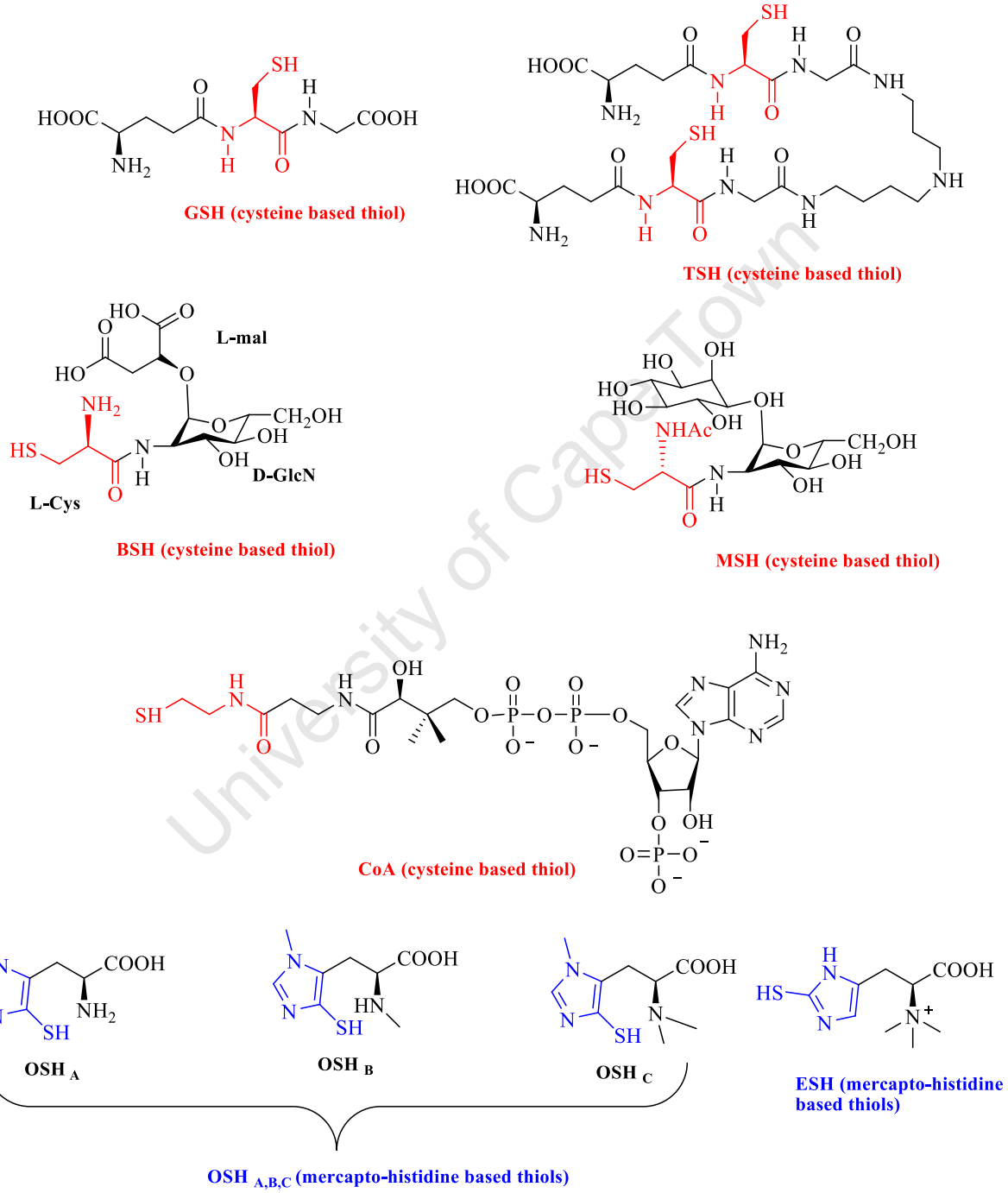

University of Cape Town

Figure 1.7 Chemical structure of Low Molecular Weight Thiol (Cysteine and mercapto-histidine based thiols).[14]

The principal thiol in most organisms (eukaryote and gram negative bacteria) including human is glutathione (GSH), a cysteine-based thiol. Most gram positive bacteria lack GSH, but produce a range of alternate LMW thiols. *Trypanosoma* and *Leishmania* produce trypanothione (TSH) and ovothiols ($OSH_{A, B \& C}$) which belong to the cysteine and mercapto-histidine based thiol classes respectively. Bacilithiol (BSH) and co-enzyme A (CoA), also both cysteine based thiols were established to act as protective thiols in *Bacillus* and *Staphylococcus.*[15, 16]

Many gram-positive bacteria like *Staphylococcus aureus* do not produce GSH; instead they do rely on CoA as their principal protective thiol. It has been shown that *Staphylococcus aureus* produces millimolar levels of reduced CoA, a unique redox thiol / disulfide redox system.[17]

Interest in CoA is growing, searching for antibiotics capable to kill *Staphylococcus aureus*, the agent causal of nosocomial infections. Research toward finding effective therapy against MRSA (Methyllicin multi-drug Resistance strains of *Staphylococcus aureus)* is still big challenge and CoA, the protective unique thiol of *S. aureus*, emerges as the new potential drug target.[48]

Very recently due to emergence of multi drug resistant *M. tb* strains (XDR) against TB drug, targeting the CoA pathway appear to be promising in TB drug discovery.[19]

1.6.1. Trypanothione (TSH).

TSH was identified in *trypanosomatids*, the causal agent of sleeping sickness, in the 1980s. TSH consists of 2 molecules of GSH linked covalently to spermidine.[20] In *trypanosoma cruzi* the concentration of $T(SH)_2$ depends on the parasite life stage, about 1.5-2.1 mM in epimastigotes cultured in presence of polyamines, 0.5 mM in trypomastigotes and 0.12 mM in amastigotes; this variation in concentration may be attributed to the biosynthesis pathway (Figure 1.8).

University of Cape Town

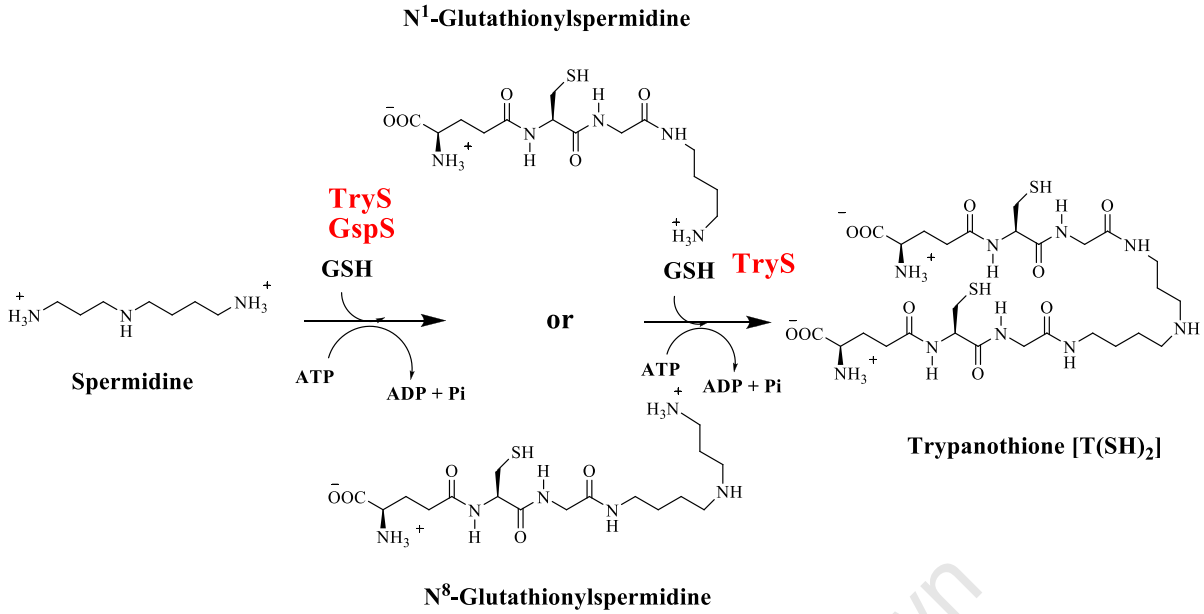

Figure 1.8 Biosynthesis of $T(SH)_2$.[20]

1.6.2. Sleeping sickness and drug discovery based on the TSH biosynthesis pathway

Sleeping sickness, called also Human African Trypanosomiasis (HAT), is one the most neglected diseases, because it affects the poorest of African populations, making any drug development economically unattractive for pharmaceutical industries.[21, 22]

It is caused by unicellular flagellated parasite subspecies *Trypanosoma bruccei*, transmitted in Africa via an infected tsetse fly. Clinically there are two forms of diseases, the first known as West African sleeping disease, chronic disease caused by *T. gambiense.* Although the second form, known as East Africa sleeping disease, is caused by *T. rhodesiense,* which is more virulent and endemic in East and Central Africa.[22, 23]

For over 50 years, chemotherapy of sleeping sickness disease has evolved and currently there are five drugs widely used against HAT, depending on the stage of the disease. These drugs include; suramin, pentamidine, melasorprol, nifurtimox and difluoromethylornithine (Figure 1.9). In comparison to all available drugs, the most efficacious of all are difluoromethylornithine (DFMO). This is the only example of a successful, clinically available, mechanism-based inhibitor across the spectrum of species of LMW thiol producing organisms.

University of Cape Town

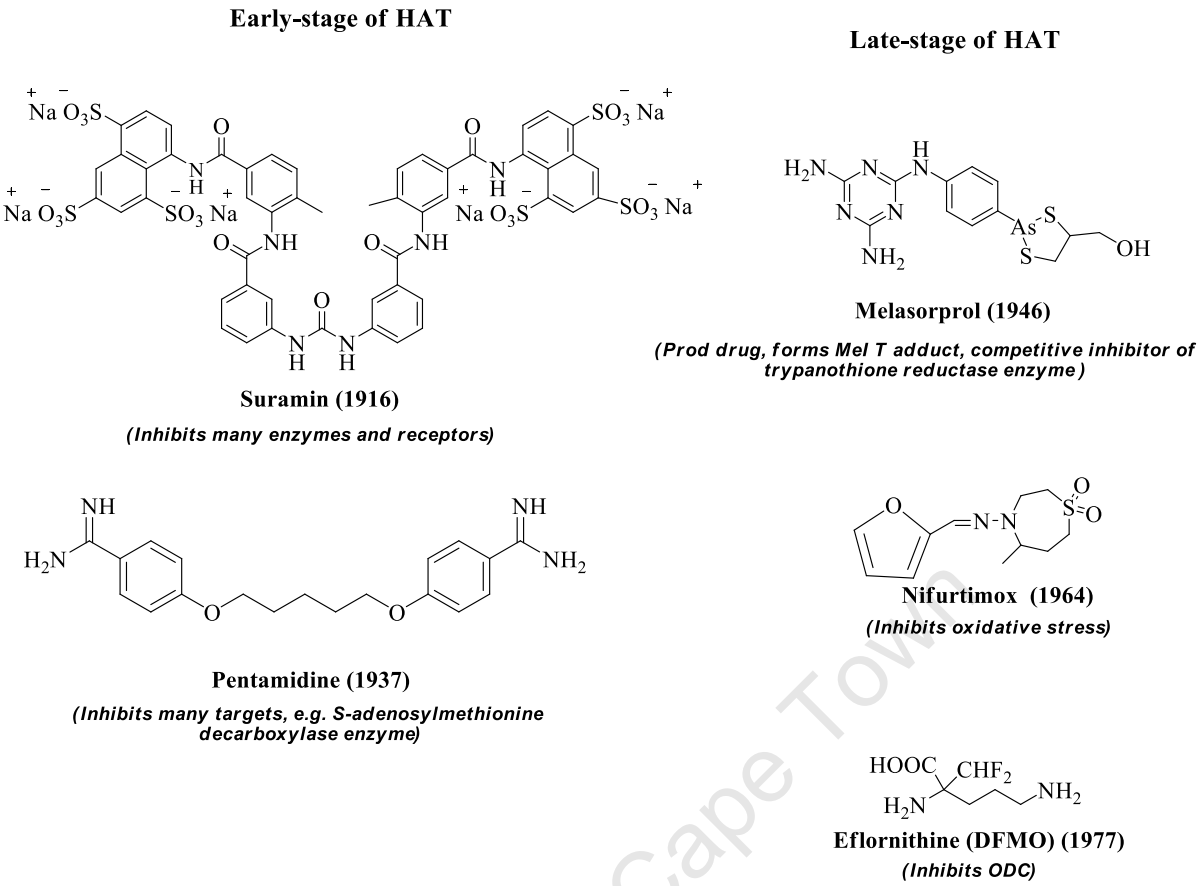

Figure 1.9 Current Drugs against HAT.[21]

DFMO irreversibly inhibit ornithine decarboxylase (ODC), a PLP-dependent enzyme implicated in the first step of the biosynthesis of polyamines (Figure 1.10).

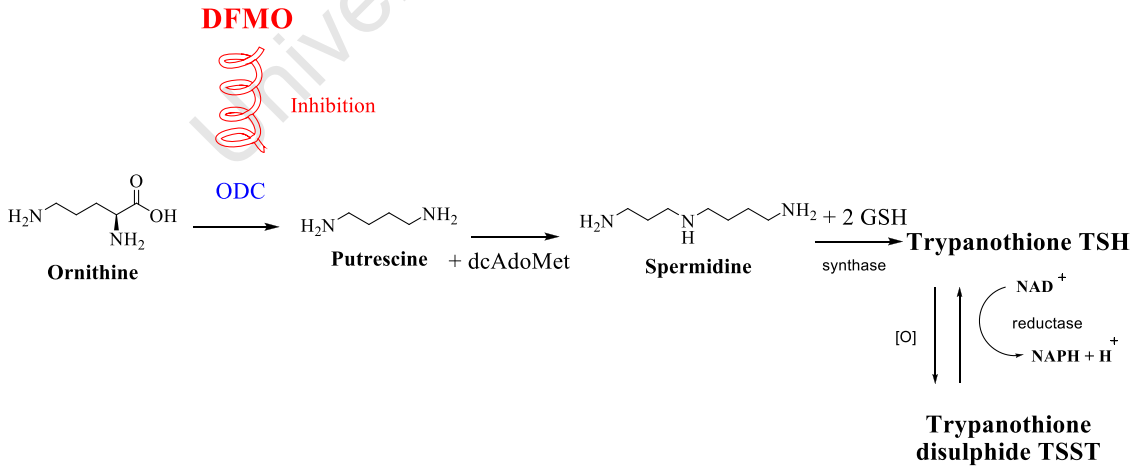

Figure 1.10 DFMO inhibition of ODC in TSH biosynthetic.[21]

University of Cape Town

1.6.3. Bacillithiol (BSH)

BSH was isolated by treating *Deinococcus radiodurans* cell extracts with monobromobimane (mBBr) and its structure was elucidated as the corresponding fluorescently labelled *S*-bimane derivate (BSmB) (Figure 1.11).

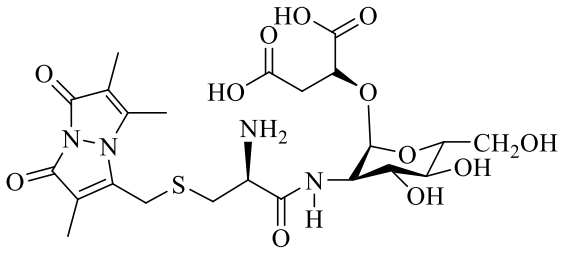

BSmB

Figure 1.11 Structure of Bacilithiol-*S*-Bimane.[24]

It has since been found that BSH plays an important role in many metabolic regulation processes including sporulation, acid and salt resistance and detoxification of electrophilic xenobiotics such as fosfomycin.[24]

The interest in BSH is still growing due to the fact that BSH occurs in several clinically important pathogens like *Bacillus anthracis, Bacillus cereus, Staphylococcus aureus, Staphylococcus saprophyticus* and *Staphylococcus agalactiae*, all of which do not produce MSH or GSH. The biosynthesis and the first total synthesis of BSH were very recently established by *Hamilton et al.*[25]

1.6.4. Mycothiol (MSH)

Mycobacterium tuberculosis produces mycothiol (MSH) and ergothioneine (ESH) which belong to the cysteine and mercapto-histidine based thiol classes respectively. It has been established that MSH plays a crucial role in the growth and survival of *M. tb*.

In *M. tb*, MSH function, as redox buffer, is involved in detoxification of electrophilic compounds such as alkylating agents and antibiotics. The latter occurs by means of conjugation and subsequent expulsion as a mercapturic acid.[12, 13] The level of MSH in *M. tb* is still the highest (millimolar levels) observed, compared to any microorganism.[14] MSH is biosynthesized by sequential action of four enzymes, *Msh* A, *Msh* B, *Msh* C, and *Msh* D.

University of Cape Town

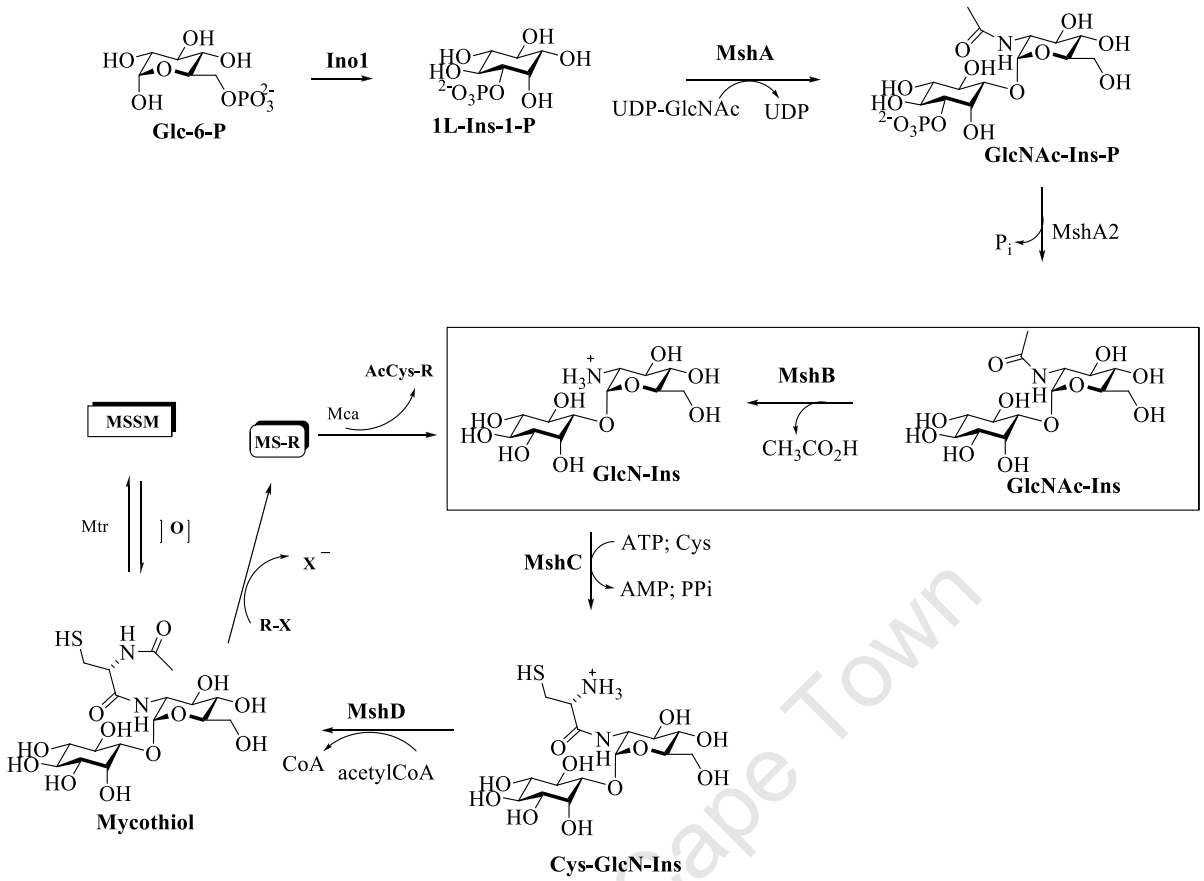

Figure 1.12 Biosynthesis of MSH.[12]

Two enzymes, Mtr (mycothiol disulfide reductase) and Mca (mycothiol *S*-conjugate amidase) play the important end stage functional role in the MSH biosynthesis pathway (Figure 1.12). As mentioned before, these enzymes are responsible for redox homeostasis and detoxification respectively.

Many studies were conducted on mycothiol biosynthesis in *M. tb* as well as *M.smeg.* mutants, bearing mutations of *mshB* and *mshD* resulting in the production of low levels of MSH, thus making these organisms more sensitive to oxidatives stress.[13]

Efforts to clone *Mycobacterium tuberculosis* lacking *mshA* and *mshC* genes were unsuccessful, but recently, a *Mycobacterial tuberculosis msh* A mutant were isolated, suggesting that *mshA, mshC* and mtr (mycothiol reductase) genes are essential in *M. tb.* However, the bacteria can adapt to the lost of mycothiol presumeably due to the presence of ESH. Furthermore it has been shown that mycothiol is not essential for the growth of *Mycobacterial smegmatis*.[15]

University of Cape Town

However after deleting mycothiol synthesis *in vitro* or *in vivo*, the *M. tb* still survives suggesting that the bacterium does have an alternative low molecular weight thiol (LMW), which compensate for the lost of mycothiol (MSH).

Recently *Fahey et al* found a drastic increase of ergothioneine in MSH- deficient strains, 30 fold for *msh*A strain and 20 fold for *msh*C strain, suggesting the effective up regulation. Despite numerous papers dealing with ergothioneine, its role in *Mycobacteria* is still not fully understood.[13]

Mycothiol (MSH) and ergothioneine (ESH) are the principal small molecule thiols produced by *M. tb.* It was shown through specific deletion mutations of enzymes along the biosynthetic pathway of these small molecule thiols that such mutant bacteria are vulnerable to existing drugs.[13] Thus, the enzymes involved in the biosynthesis of small molecule thiols can be considered as a novel targets for antitubercular drug discovery antitubercular drug.

1.7. Redox homeostasis in mycobacteria.

It has been known for more than a hundred years that *M. tb* is an obligate aerobe, although research has shown that *M. tb* can survive *in vitro* under anaerobic conditions for many decades.

The redox balance in *M. tb* can be disturbed by many factors intra-or extracellularly, which allow the bacteria, through unknown mechanisms, to subvert the immune system and to cause TB. Isoniazid (INH), ethionamide (ETA) and the nitro-imidazole drug, PA-824, need bioreductive activation. Hence, a redox imbalance affects the efficacy of such TB drugs. Furthermore, studies demonstrated that the increase in the NADH / NAD^+ ratio could also be responsible for INH resistance.[26] *Mycobacteria* with deletion mutations in MSH biosynthesis demonstrated resistance to INH and ETA.[27] However, the mechanism used by *M. tb* to maintain the redox homeostasis, their role in drug susceptibly and efficiency remain poorly understood.

M. tb lack the GSH redox couple (GSSG / 2GSH) and instead contains the mycothiol redox couple (MSSM / 2MSH) as major redox buffer in millimolar quantities. Although its redox potential has not been determined, many studies are limited to determine the ratio of MSSM / 2MSH. In addition *M. tb* contains other redox couples such as thioredoxin (TrxSS / Trs $(SH)_2$).

University of Cape Town

FAD-binding mycothione reductase catalyses the reduction of mycothiol disulfide using NADPH as a cofactor as depicted in equation (1)

$$NADPH + H^{+} + MSSM \longrightarrow 2\,MSH + NADP^{+} \quad (1)$$

It has been proven that MSH deletion mutants are sensitive to oxidative stress caused by H_2O_2, cumene hydroperoxide and $O_2^{\cdot -}$.

The redox couple of ESH_{ox}/ESH_{red} (E^{O} = - 60 mV) and its role as protective thiol is not well known, however it has been shown to protect mammalian cells against oxidative stress.[28]

Understanding the redox homeostasis in the mycobacteria and how it influences drug efficacy remains the key to control TB. Is MSH the major redox buffer in *M. tb* and what role does ESH play in the maintenance of redox homeostasis in *M. tb* and in disease progression?

1.8. Mercaptohistidine based Low Molecular Weight Thiols

Ergothioneine (ESH) and ovothiols ($OSH_{A, B \& C}$) belong to the mercaptohistidine based LMW class and they differ from each other by the position of –SH and the degree of *N*-methylation of the amino acid.

1.8.1. Ovothiols.

Ovothiol or *N*-methyl *S*-thiohistidine contain a relatively acidic thiol group (pk_a = 1.4) (Figure 1.13). Unlike ESH, ovothiol readily undergoes oxidation by H_2O_2 or atmospheric oxygen to form the disulfide. OSH was first isolated in the late 1970s from the eggs of *S. purpuratus*. Since then research were conducted to understand its biochemistry and biosynthesis. Recently, the discovery of OSH in pathogenic *Trypanosoma and Leishmania*, has raised the interest in trypanosomal drug discovery.[29]

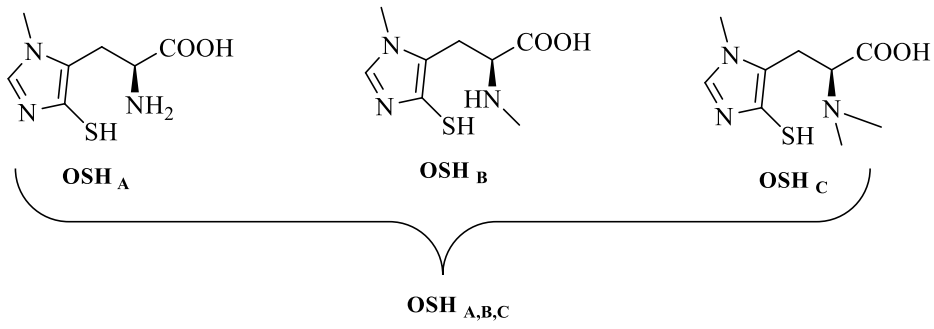

Figure 1.13 Structures of ovothiols (OSH_s)

University of Cape Town

OSH plays an important role as an anti-oxidant in the redox defence of a number of organisms. Marine organisms produce a high amount of OSH, for example sea urchin eggs contain several millimolar OSH_C, required to protect eggs during oxidative envelope maturation.[29, 30, 31]

1.8.2. Ergothioneine (ESH).

ESH was first isolated by Tanret in 1909 from ergot (*Claviceps purpurea*), the fungal infection of rye grain. Since that discovery numerous studies has been conducted to understand its role as protecting thiol in *mycobacteria.* Although many hypotheses have been suggested, its natural function in *M. tb* cells is still not fully unravelled.

1.8.2.1. Structure and distribution

ESH is a histidine derivative (2-mercaptohistidine *N*,*N*,*N*-trimethyl betaine) with a thiol group attached to the C-2 position of the imidazole ring. ESH is an unique natural C2-thio-imidazole containing amino acid.[14] (Figure 1.14.)

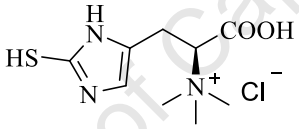

Figure 1.14 Structures of Ergothioneine (ESH).

In aqueous solution the thiol form **(III)** is more abundant than the thione form **(I),** although at physiological pH (7.4), the thione form **(I)** appears to be predominant (Figure 1.15).

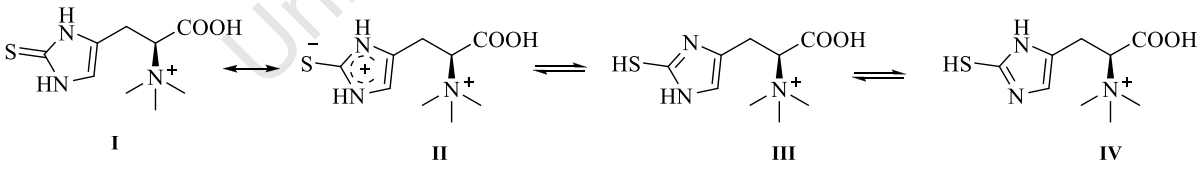

Figure 1.15 Possible tautomeric structures of ESH

This characteristic distinguishes ESH from other biological LMW thiols and explains the fact that ESH is stable and is not easily auto-oxidized unlike other alkylmercaptans.[14, 32]

ESH is synthesized mostly by some bacteria and fungi in the soil at a level of 0-5 μmol per g and is easily absorbed by plants through the roots. The level of ESH has been measured in *Actinoplanes philippinensis, Nocardia asteroides* strains *(Actinomycetes)* and in three species of *Streptomycetes.*[32, 33]

University of Cape Town

Animals as well as humans do not synthesize ESH; instead they acquire it from their diet. Foods rich in ESH include mushrooms, corn, oats and meat. ESH concentrates in specific tissues or cells such as erythrocytes, liver, kidney, central nervous system, heart, seminal fluids, red bloods cells and ocular tissues.[34] It has been shown that the concentration of ESH in human red blood cells is 1.5- 3.7 mg/100 ml, while the human lens contains 68-115 mg/100 g.[35]

ESH protects spermatozoa against oxidative stress and confers to it viability during storage. It has displayed a critical protective role in seminal fluid as it is the predominant thiol compound in a human, pig and horse semen.[36]

Recently, a cation transporter (OCTN1) with high substrate specificity for ESH has been discovered. OCTN1 is now established as the ESH transporter and is responsible for the non uniform distribution of ESH in different cells within the same species.

1.8.2.4. Antioxidant activity

It has been shown that ESH protects rats *in vivo* against hepatic injury (damage occurs through the formation of lipid peroxides). [37] ESH is widely used in cosmetics as an active UV protectant; it has been proven to block the formation of various reactive oxygen species including singlet molecular oxygen, superoxide, hydroxide radical, protecting then the skin against any form of UV damage (skin cancer). Amongst other thiols such cysteine, *N*-acetyl-cysteine, glutathione, ESH emerges to be the most efficient UV skin protectant and offers ten fold greater protection than glutathione.[32, 38]

1.8.2.3. Biosynthesis of ergothioneine

The attempt to elucidate the biosynthesis of ergothioneine has started some decades ago. In 1956, *Heath et al* elucidated ESH biosynthesis in *Claviceps purpurea*. He demonstrated that histidine or a compound closely related to histidine might be a precursor of ESH.[39]

The same year, *Melville et al* investigated the ergothioneine biosynthesis pathway in *Neurospora crassa*, an organism selected for this study because of its high concentration in ergothioneine. Using the classical radio isotopic labelling (^{14}C and ^{35}S) method, *Melville et al* found that histidine is the precursor for ergothioneine biosynthesis, the introduction of a sulfhydryl group is provided by cysteine, and at least one of the three methyl groups of ergothioneine is derived from methionine.[40] The same year, *Heath et al* established that histidine is indeed a precursor of ESH.[40, 41]

University of Cape Town

In 1962, *Melville et al* published the biosynthetic sequence of ergothioneine biosynthesis, which involved histidine, thio-histidine and hercynine as intermediates whereby cysteine is the source of the introduced thiol to the imidazole moiety and methionine is responsible for the trimethylation of the amino acid moiety (Figure 1.16).[40]

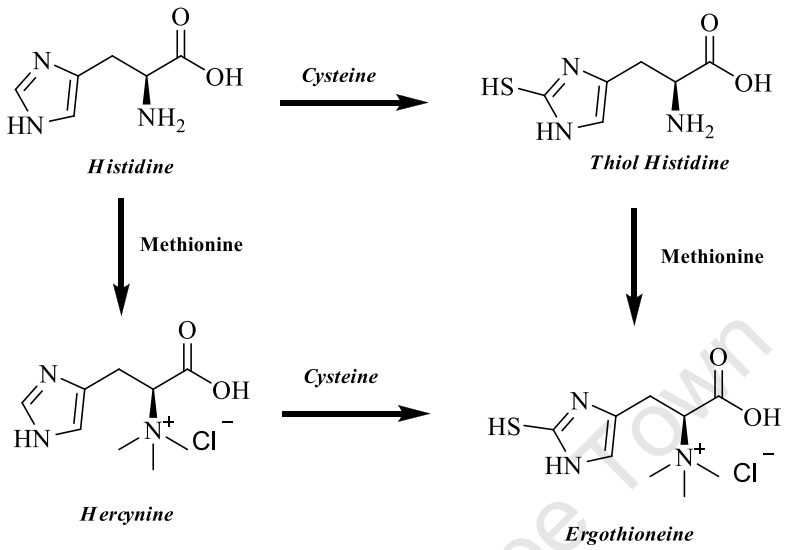

Figure 1.16 Ergothioneine biosynthesis sequence.[30]

Five years after the *Melville* study, *Genghof et al*[42] confirmed that endogenous hercynine is the ESH biosynthetic precursor in *Mycobacterium smegmatis*. They also found that the addition of cysteine in their preparation caused the formation of 100 to 200 µg of ESH per g of dry cells after only 2.5 to 3 hours of incubation, thus supporting that cysteine is the direct source of sulphur in *M. smeg* ESH.[40, 42]

Recently, Seebeck was the first to publish the gene cluster (*egtABCDE*) encoding for ESH biosynthesis in *Mycobacterium smegmatis* (Figure 1.17). All these enzymes were examined but not studied in detail yet; EgtA was identified as a glutamyl cysteine synthetase, EgtB as a FGE (Formylglycine Generating Enzyme) like protein, EgtC as a glutamine amidotransferase, EgtD as a methyl transferase and EgtE as a PLP binding enzyme.[43]

University of Cape Town

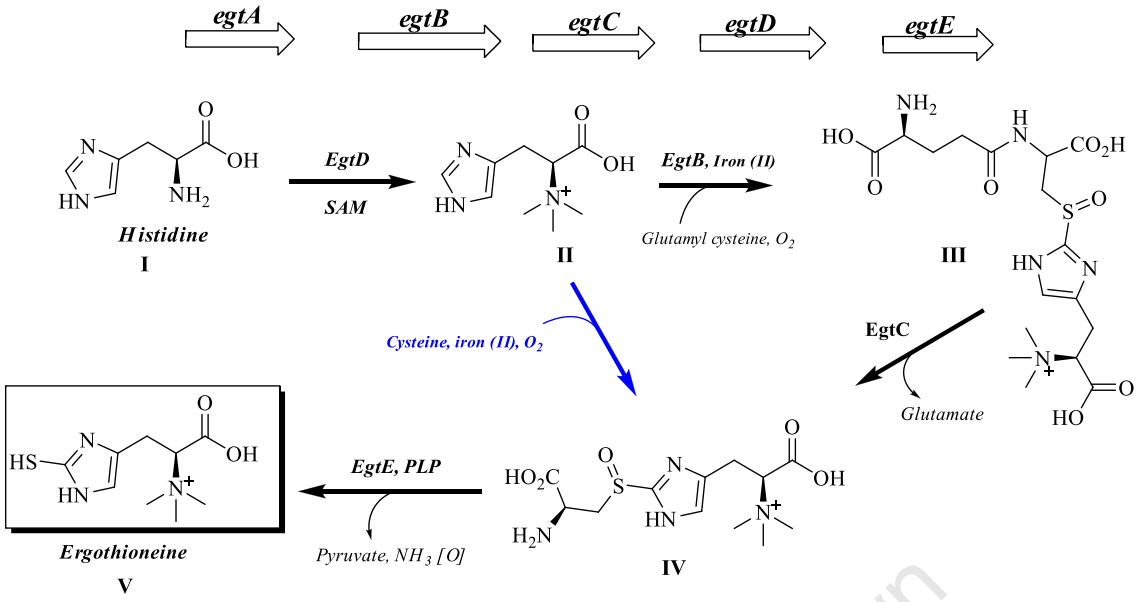

Figure 1.17 (Top) *Mycobacterial* ergothioneine gene cluster, (Bottom) Reaction sequence of ESH biosynthesis.[43]

The biosynthesis started with the trimethylation of histidine **(I)** by a *S*-Adenosyl Methionine (SAM) dependent enzyme EgtD to form hercynine **(II)** as the first intermediate in the biosynthesis. The second step involved the condensation and oxidation of hercynine **(I)** with glutamyl cysteine, yielding glutamyl cysteine sulfoxide **(III),** catalyzed by an iron II dependent oxidase enzyme (EgtB). The latter enzyme could also catalyze the direct coupling of hercynine **(II)** and cysteine to form hercynyl cysteine sulfoxide **(IV)** as the second intermediate in the biosynthesis; this alternative route was previously suggested by *Ishikawa et al.*[44]

Finally the last step is catalyzed by a PLP–dependent β-lyase enzyme EgtE, involved the cleavage of the sulfoxide intermediate **(IV)** to form ergothioneine **(V).** Seebeck *et al* [43] expressed and characterized all the enzymes implicated in the pathway except EgtE because of an expressed protein solubility problem, a common problem for cofactor dependent enzymes of slow growing organisms.[43]

Higher eukaryotes lack the genes for ESH biosynthesis, which is produced in a wide range of Actinobacteria, in particular *Mycobacteria* and therefore may represent a novel target for tuberculosis drug discovery.

University of Cape Town

1.9. Objectives of the study

Very recently Bello *et al* [45] found that ESH is the major low molecular weight thiol in conidia of Ascomycetes C. *graminicola* and N. *crassa*. By using two strains of conidia, wild type and *NcΔEgt-1* (conidia mutant lacking ESH), they demonstrated that endogenous ESH is responsible for the protection of plants against peroxide toxicity during the germination process.

Unpublished work conducted by our collaborators Sao, C. and Baker B., University of Stellenbosch, Tygerberg, South Africa has highlighted that ESH is essential for the survival of *M. smeg*, as demonstrated by the increased sensitivity of ESH deficient mutants toward antitubercular drugs.

Amongst all the ESH pathway enzymes, EgtE and EgtD implicated in the first and last step respectively, seem to be indispensable to the biosynthesis of ESH. Based on these findings, the research in this thesis aims to:

(i) Provide improved synthetic methods to produce significant amounts of EgtD *and* EgtE *substrates in order to allow further investigation of the pathway enzymes, in particular* EgtE*, which is hitherto unavailable.*

(ii) In the absence of expression systems for EgtE*, the groundwork for classical protein purification methods will be established utilising crude* EgtE *enzyme from Mycobacterial smegmatis.*

(iii) Establish LCMS methods to monitor conversion of EgtD *and* EgtE *substrates to ESH using crude enzyme extracts from M. smegmatis*

(iv) Synthesize stable isotopically labelled substrates for metabolomic studies and drug discovery. Ultimately, these tools will be used to develop a multiwell plate assay for the discovery of inhibitors of the ESH biosynthesis pathway.

University of Cape Town

1.10. References

1. *Core Curriculum on Tuberculosis*, Fifth Edition, **2011**, National Center for HIV/AIDS, Viral Hepatitis, STD, and TB Prevention, http://www.cdc.gov/tb.
2. Weyand, S.; Kefala, G. and Weiss, M.S., *J. Mol. Biol.*, **2007**, 367, 825.
3. Sacchettini, J.C.; Rubin, E. J. and Freundlich, J.S., *Nat. Rev. Microbiol.*, **2008**, 6, 41.
4. Global Tuberculosis control, WHO report, **2011**
5. http://textbookofbacteriology.net/tuberculosis.html.
6. http://www.who.int/gho/map_gallery/en/.
7. Janin, Y.L., *Biorg. Med. Chem*, **2007**, 15, 2479.
8. Villemagne, B.; Crauste, C.; Flipo, M.; Banlard, A.R.; Deprez, B.; Willard, N., *Eur. J. Med. Chem.*, **2012**, 1.
9. Zhang, Y., *Annu. Rev. Pharmacol. Toxicol.*, **2005**, 45, 529.
10. Kumar, A.; Farhana, A.; Guidry, L.; Saini, V.; Hondalus, M.; Steyn, A.J., *Expert Rev. Mol. Med*., **2011**, 1.
11. Xu, J.; and Yadan, J.C., *J. Org. Chem*., **1995**, 60, 6296.
12. Bornemann, C.; Jardine, A. M. and Steenkamp, D. J., *Biochem J.*, **1997**, 325(3), 623.
13. Ta, P.; Buchmeier, N.; Newton, G.L.; Rawat, M. and Fahey, R.C., *J. Bacteriol.*, **2011**, 8, 1981.
14. Fahey, R.C., *Annu. Rev. Microbiol.*, **2001**, 55, 333.
15. Sharma, S.V.; Jothivasan, V.K.; Newton, G.L.; Upton, H.; Wakabayashi, J.I.; Kane, M.G.; Roberts, A.A.; Rawat, M.; La Clair, J.J. and Hamilton, C.J., *Angew. Chem. Int. Ed.*, **2011**, 50, 7101.
16. Vilcheze, C; Av-Gay, Y.; Attarian, R.; Liu, Z.; Hazbón, M.H.; Colangeli, R.; Chen, B.; Liu, W.; Alland, D.; Sacchettini, J.C.; Jacobs, W. R., *Mol. Biol*., **2008**, 69, 1316.
17. Daugherty, M.; Polanuyer, M.F.; Scholle, M.; Lykidis, A.; De cresy, L.V.; and Osterman, A., *J. Biol. Chem.*, **2002**, 24, 21431.
18. Delcardayre, S.B.; Stock, K.P.; Newton, G.L.; Fahey, R.C.; and Davies, E.J., *J. Biol. Chem.*, **1998**, 10, 5744.
19. Ambaby, A.; Awasthy, D.; Yadav, R.; Basuthkas, S.; Seshadri, K.; Sharma, U.; *Tuberculosis*, **2012**, 92, 521.
20. Irigoin, F.; Cibils, L.; Comini, M.A.; Wilkinson, S.R.; Flohe, L.; Radi, R. , *Free Rad. Biol. & Med.*, **2008**, 45, 733.
21. Alain, H.F., *Trends. Parasitol.*, **2003**, 19, 488.

University of Cape Town

22. Denise, H. and Barrett, M.P., *Bioch. Pharmacol.*, **2001**, 61, 1.
23. Wenzler, T.; Boykin, D.W.; Ismail M.A.; Hall, J.E.; Tidwell, R.R. and Brun, R., *Antimicrob. Agents Chemother*., **2009**, 53, 4185.
24. Sharma, S.V.; Jothivasan, V.K.; Newton, G.L.; Upton, H.; Wakabashi, J.I.; Kane, M.G.; Roberts, A.A.; Rawat, M.; La clair, J.J. and Hamilton, C.J., *Angew. Chem. Int. Ed.*, **2011**, 50, 7101.
25. Fahey, R.C.; and Sundquist, A.R., *Adv. Enzymol.*, **1991**, 64, 1.
26. Vilcheze, C.; Weisbrod, T.R. ; Chen B. ; Kremer, L. ; Hazbón, M.H. ; Wang, F. ; Alland, D.; Sacchettini, J.C. and Jacobs Jr, W.R., *Antimicrob. Agents Chemother*., **2005**, 49, 708.
27. Xu, X , *Antimicrob. Agents Chemother.*, **2005**, 55, 3133.
28. Paul, B.D.; and Snyder, S.H., *Cell Death and differentiation*, **2009**, 17, 1134.
29. Braunshausen, A.; Seebeck, F., *J. Am. Chem. Soc*., **2011**, 133, 1757.
30. Holler, T.P.; Ruain, F.; Spaltenstein, A. and Hopkins, P., *J. Org. Chem*., **1989**, 54, 4570.
31. Turner, E.; Klevit, R.; Hager, L.J. and Shapiro, B.M., *Biochemistry*, **1987**, 26, 4028.
32. http://www.oxisresearch.com/ergo/l-ergothioneine_monograph.pdf
33. Braunshausen, A.; Seebeck, F.P., *J. Am. Chem. Soc.*, **2011**, 133, 1757.
34. Hartman, P.E., *Methods Enzymol.*, **1990**, 186, 310.
35. Hand, C.E.; and Honek, J.F., *J. Nat. Prod*., **2005**, 68, 293.
36. Mann, T.; and Leone, E., *Biochem. J.*, **1953**, 53, 140.
37. Kawano, H.; Murata, H.; Iriguchi, S.; Mayumi, T. and Hama, T., *Chem. Pharm. Bull*., **1983**, 31, 1676.
38. Hans, J.S., *Mutation Research*, **1992**, 22, 77.
39. Heath H.; Wildy, J., *Biochem. J.*, **1957**, 65, 220.
40. Melville, D.B.; Eich, S.; Ludwig, M.L., *J. Biol. Chem.*, **1957**, 224, 871.
41. Askari, A.; Melville, D.B., *J. Biol. Chem.*, **1962**, 237, 1615.
42. Genghof, D.S.; and Van Damme, O., *J. Bacteriol*., **1962**, 95, 340.
43. Seebeck, F.P., *J. Am. Chem. Soc*., **2010**, 132, 6632.
44. Ishikawa, Y.; Israel, S.E.; Melville, D.B., *J. Biol. Chem.*, **1974**, 249, 4420.
45. Bello, M.V.; Barrera, P.V.; Morin, D. and Epstein, L., *Fungal gen. & boil.*, **2012**, 160.

University of Cape Town

Chapter 2 Total synthesis of Ergothioneine

2.1. Introduction

ESH have been studied for almost a century as it has been detected in most plants and animals. Although its quantification in fresh tissues was hindered through lack of standardized methods of detection.[1]

A range of submillimolar to millimolar concentrations of ESH has been found in the cornea, bone marrow and seminal fluid (where it is the highest level). ESH was also found in central nervous system and ranged from 0.36 to 0.03 mg/100gm depending on the brain region and type of animal examined.[2, 3]

Due to increasing commercial interest, a scaleable synthetic process for *L*-ergothioneine is valuable. Research quantities is commercially available, but very expensive (**5767. 98 ZAR per 25 mg Sigma Aldrich**).[4] ESH synthesis holds unique process challenges, despite its apparently simple structure, many procedures has been developed to date, but only three of the published methods emerged as efficient.

2.2 Retrosynthetic Analysis

The retrosynthesis leads to commercially available *L*-histidine that affords hercynine through *N*-methylation as well as thionation using different approaches depending on the nature of the sulfur sources utilized (Scheme 2.1). According to this strategy, thiation requires the imidazole ring to be activated.

University of Cape Town

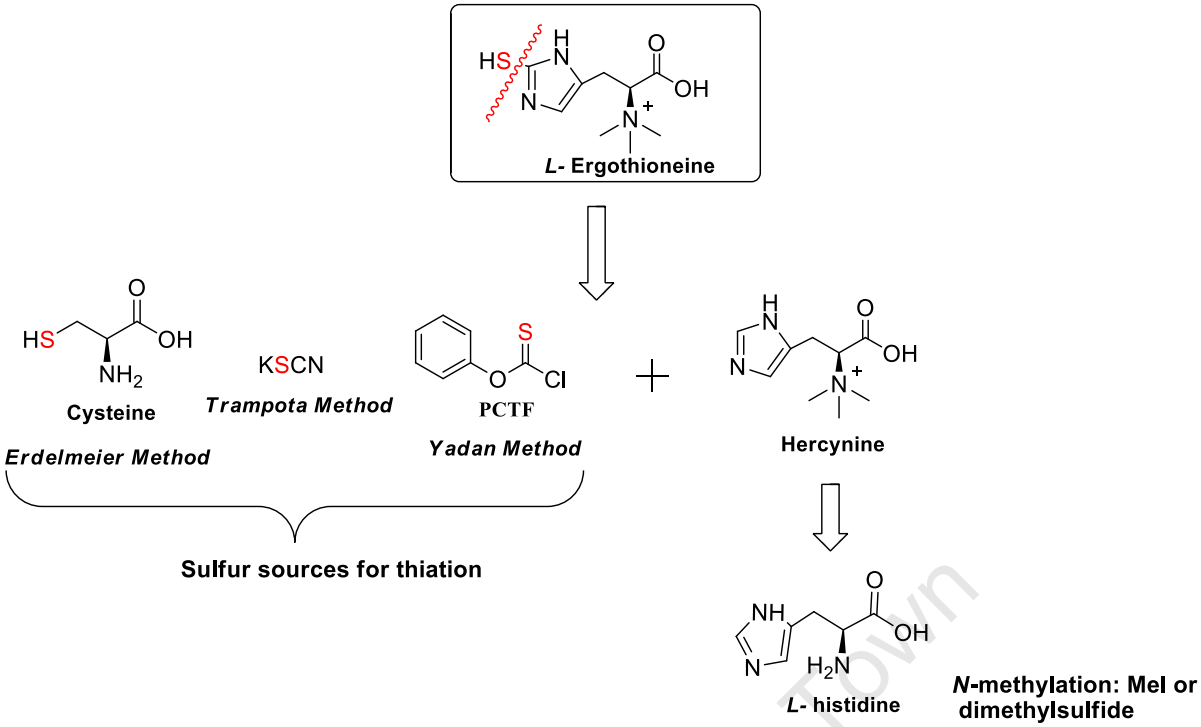

Scheme 2.1 Retrosynthetic strategy of *L*-ergothioneine synthesis**.**

2.3. Synthesis of *L*-ergothioneine using the *Yadan* approach

Yadan et al [5] published the first total synthesis of *L*-ergothioneine in five steps (Scheme 2.2). This synthesis starts by the esterification of the commercially available *L*-histidine **(1)** to obtain the *L*-histidine methyl ester (**2**), which was dimethylated via reductive amination affording the *N*, *N*-dimethyl histidine methyl ester (**3**).

The key step of this synthesis is the thiation which was performed by reacting intermediate (**3**) with phenyl chlorothionoformate (PCTF) under basic conditions ($NaHCO_3$). The sulfur and nitrogen of the imidazole ring of the *N*,*N*-dimethyl mercapto histidine **(4)** intermediate was protected by reacting it with ethyl chloroformate prior to quaternarization of the amine to afford *N*- and *S*-protected ergothioneine (**6**). Acid mediated deprotection yield the target, *L*-ergothioneine (**7**) (Scheme 2.2).

University of Cape Town

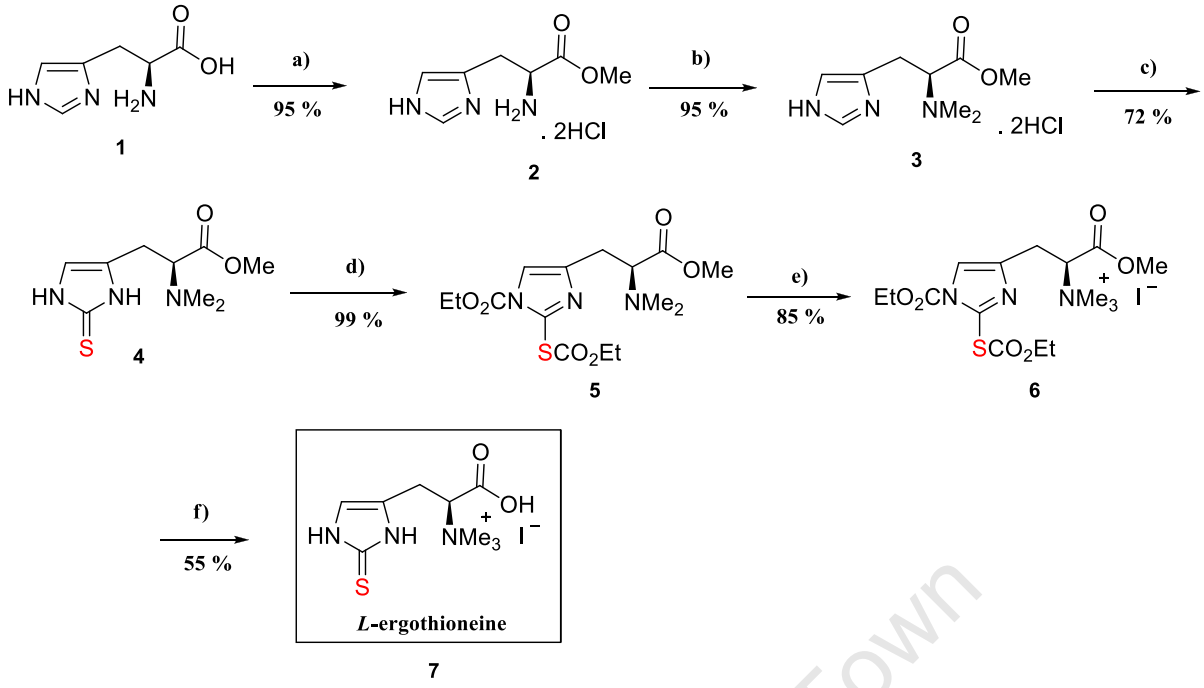

Scheme 2.2 *Yadan* ergothioneine Synthesis [5] reagent and conditions (a) MeOH, gaseous HCl; (b) 37 % aqueous CH_2O, H_2, 10 % Pd/C , rt; (c) (i). PCTF, $NaHCO_3$, H_2O / Et_2O, (ii) TEA, MeOH, rt (d) $ClCO_2Et$, TEA, CH_2Cl_2, 10 °C; (e) MeI, THF , rt; (f) Conc HCl, 75 equiv $HSCH_2CH_2CO_2H$

According to the *Yadan* method *L*-ergothioneine was synthesized in 6 steps, used tedious chromatographic purification methods and resulted in a high degree of racemisation of the final product. The overall yield was low (34 %) and difficult to reproduce.

This synthesis required the use of many toxic reagents such as thiophosgene ($CSCl_2$) to synthesize PCTF *in situ*. This method also required the use of considerable amounts of halogenated organic solvent and concentrated hydrochloric acid, which generates a large amount of harmful waste for the environment.

Considering all the disadvantages mentioned above, *Trampota* developed another synthetic route.

2.4. Attempted synthesis of ergothioneine using the *Trampota* method

A decade later, *Trampota et al* [6] patented the second total synthesis, similar to the *Yadan* method. The major improvement in this approach was the introduction of sulfur in the imidazole ring using KSCN via the Bamberger imidazole cleavage reaction, followed by *t-butyl* protection of sulfur prior to methylation of the amino group.

University of Cape Town

After careful evaluation of the available synthetic procedures, it was decided to attempt the *Trampota* method. *L*-Ergothioneine was synthesized in 7 steps from commercially available histidine methyl ester (**1)** (Scheme 2.4). The Bamberger imidazole cleavage method gave in a number of sequences, subsequent intermediate, the (*S*)-2,3-diamino-4-oxopentanoic acid (**4a)** thiation using KSCN affords mercapto histidine (**4)**, which was further transformed into ergothioneine **(8)** as outlined in the Scheme 2.3. The detailed report of this synthesis follows.

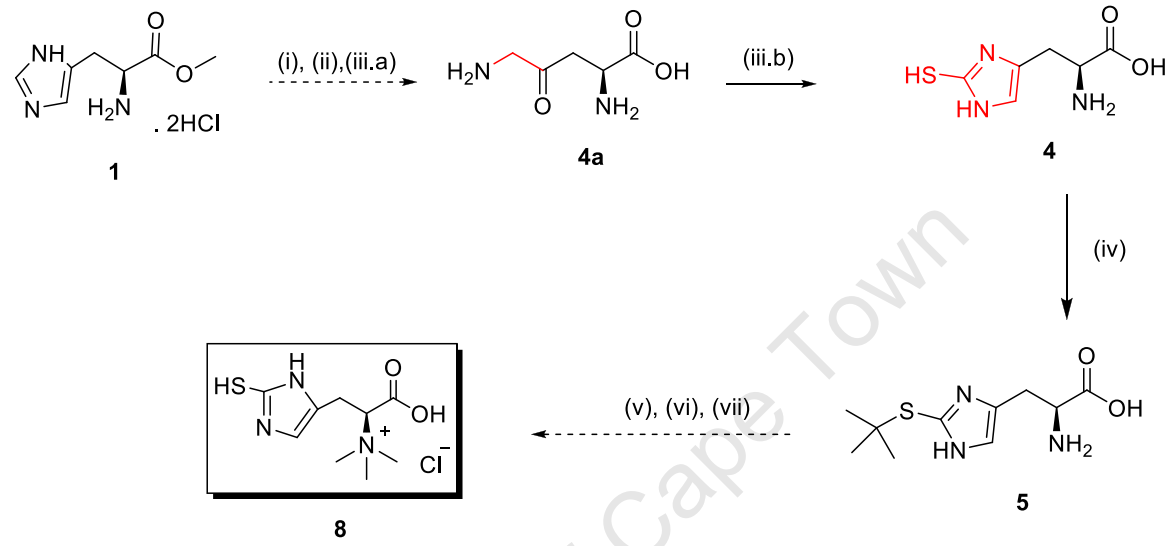

Scheme 2.3 Synthesis of (8). Reagents and conditions: (i) $NaHCO_3$, BzCl / THF:H_2O 10:90 18-24 h at rt (82%); (ii) MeOH / HCl 5 hr at rt (95.5%); (iii) a. HCl 15 h at 90-93°C; b. KSCN 4-5 hrs at 80-90°C (87.8%); (iv) *t*-BuOH / HCl reflux for 3-4 h (62.7%); (v) Formalin, sodium triacetoxyborohydride / THF, 6-8 h at 10°C (33.7 %); (vi) NH_4OH, CH_3I / MeOH 24 h at rt; (vii) HCl, 2-mercaptoprionic acid refluxed for 21h (27.3 % over 2 steps).

2.4.1. Synthesis of (*S, Z*)-methyl 2, 4, 5-tris (benzamido) pent-4-enoate (2), the Bambeger imidazole cleavage.

Commercially available histidine methyl ester dihydrochloride (**1)** was *N*-benzoylated using benzoyl chloride under basic conditions ($NaHCO_3$) in a mixture of THF and H_2O as a solvent. The reaction was monitored by TLC, showing complete disappearance of starting material after 24 hours.

The product (**2)** was isolated in 82 % yield (Scheme 2.4).

University of Cape Town

Scheme 2.4 Synthesis of (2) : reagents and condition. $NaHCO_3$, BzCl / THF: H_2O (10:90), 18-24 h at rt (82%)

2.4.1.1. Mechanism of Bamberger imidazole cleavage.

Bamberger et al [7] reported in 1893 that imidazole in the presence of an acylating agent such as an acyl chloride in an alkaline medium ($NaHCO_3$ aq) and an inert solvent, underwent a hydrolytic ring cleavage to give a *N*,*N*-diamino acyl-substituted alkene.[7] Since this discovery the reaction has found many applications in organic synthesis involving the preparation of 1,2-diamino vicinal alkenes. It has also been used as a method of detection of imidazole and histidine components.

Later, Pratt *et al* [8] and Avaera[9] as well as Vliegenthart[10] systematically investigated its mechanism and proved that the imidazole ring cleavage is possible under mild conditions. The mechanism involves the reaction of 3 mol equivalents of benzoyl chloride with the carboxylic acid ester **(1)** to form species **(i),** which is hydrated to form hydro imidazole **(ii)**. The intermediate **(ii)** undergoes imidazole ring cleavage to yield **(iii)**, finally deformylation of **(iii)** affords the *N*,*N*-diaminoacyl product **(iv)**. At higher concentration of an acyl chloride, the rate-determining step was the breakdown of tetrahedral 2-hydroxy-4-imidazoline (**ii)** (scheme 2.5). *Pratt et al* noted that it is possible to end up with a mixture of **(iii)** and **(iv)** in almost equal proportions, but performing the reaction at higher pH and much for longer time would afford the final product **(iv)** in moderate yield.[8]

University of Cape Town

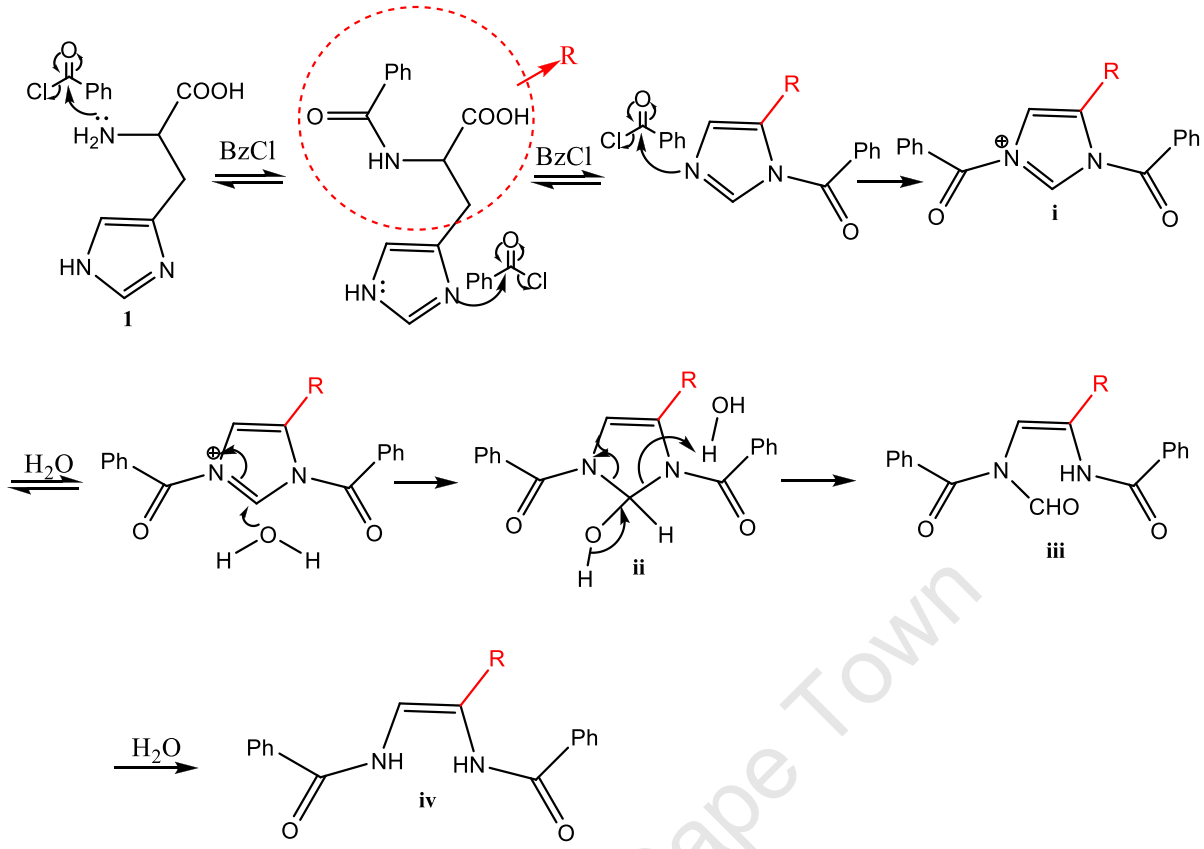

Scheme 2.5 Proposed mechanism of Bamberger imidazole cleavage.[8]

2.4.1.2. Characterisation of Bamberger imidazole intermediate, the *(S, Z)*-methyl 2, 4, 5-tris (benzamido) pent-4-enoate (2)

Evidence for the formation of the Bamberger intermediate **(2)** was obtained by spectroscopic methods. The ^{1}H NMR spectrum in $CDCl_3$ displayed three distincts deshielded ortho sets of aromatic resonances integrating for two protons each and a multiplet in the aromatic region (δ_H 7.60 to 7.39 ppm) integrating for 9 protons (meta and para), thus confirming the introduction of two benzoyl-groups. All three NH protons were also established to be down field at δ_H 9.91 (d, J = 8.7 Hz, 1H, NH-7), δ_H 8.84 (s, 1H, NH) ppm in close proximity to two carbonyl groups. Hence the two NH protons were more deshielded one slightly shifted up field at δ_H 7.16 (d, J = 6.8 Hz, 1H, NH) ppm. The characteristic methyl ester resonated up field at δ_H 3.82 (s, 3H, OCH_3-6) ppm as shown in the Figure 2.1.

University of Cape Town

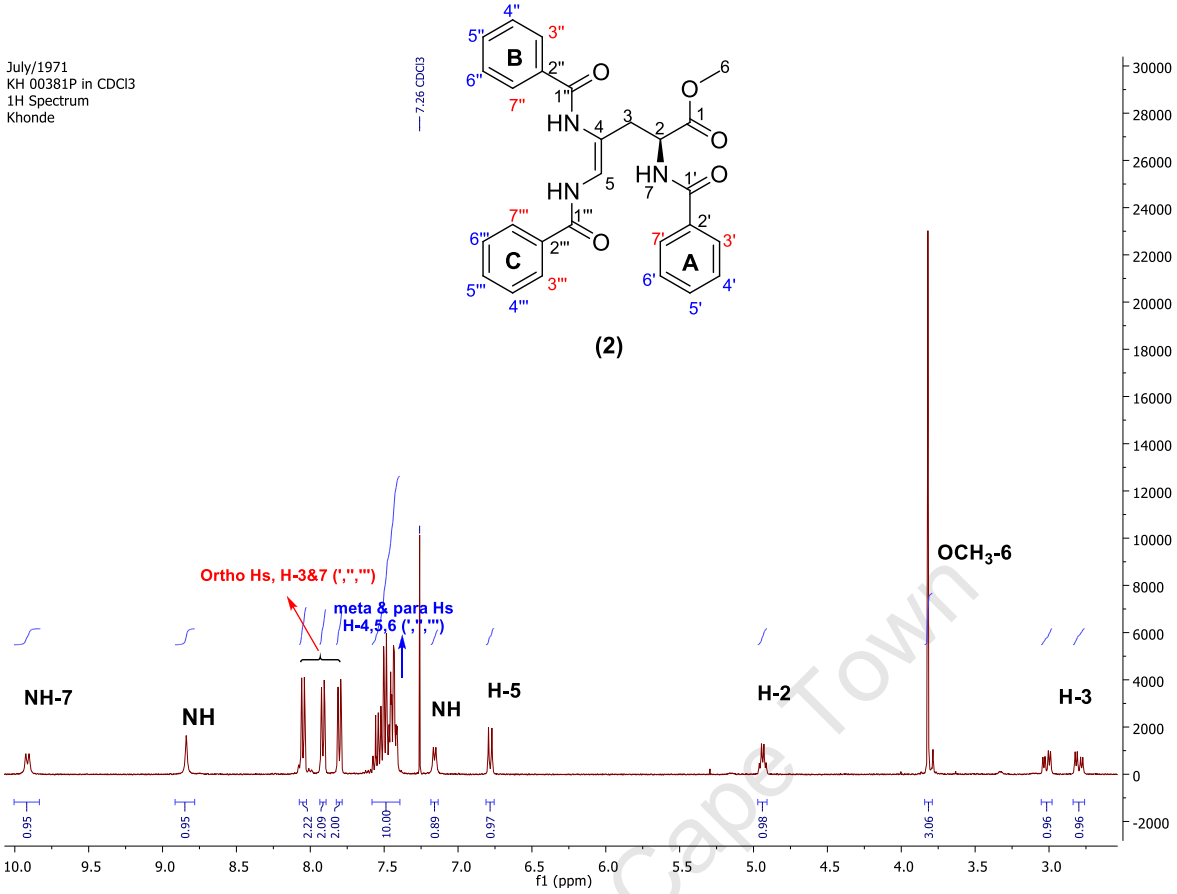

Figure 2.1 ^{1}H NMR spectrum of (**2**) in $CDCl_3$ at 400 MHz

The ^{13}C NMR spectrum of the Bamberger intermediate (**2**) displayed four carbonyl signals, twelve aromatic resonances, displaying the introduction of three benzoyl groups, two vinyl resonances respectively at δ_C 115.8 to 115.0 ppm showing clearly that imidazole ring was cleaved, and the correct number of carbon resonances, thus confirming the carbon skeleton of product (**2**).

In addition, the FTIR spectrum in KBr showed a diagnostic absorption band at 804 cm^{-1} confirming the presence of the phenyl moiety and strong absorption band at 1671 cm^{-1} proving the insertion of the benzoyl group.

Finally the EI^+ mass spectrum displayed a molecular ion at *m/z* 471.1 $([M+H])^+$ calculated for $C_{27}H_{26}N_3O_5$: 471.2 supporting the assigned structure of **(2)**.

2.4.2. Synthesis of *(S, Z)*-methyl 2,5-bis(benzamido)-4-hydroxypent-4-enoate (3b).

This step required anhydrous HCl for the deaminative cleavage of one of the three benzamide groups of compound (**2**). Hence, HCl gas was prepared *in situ* in an ice cold water bath (0-5°C) by the treatment of excess methanol with acetyl chloride. TLC indicated complete

University of Cape Town

hydrolysis of product (**2)** after 24 hours and the recovery of product (**3)** in an excellent yield of 95 % after recrystallization (Scheme 2.6).[11, 12]

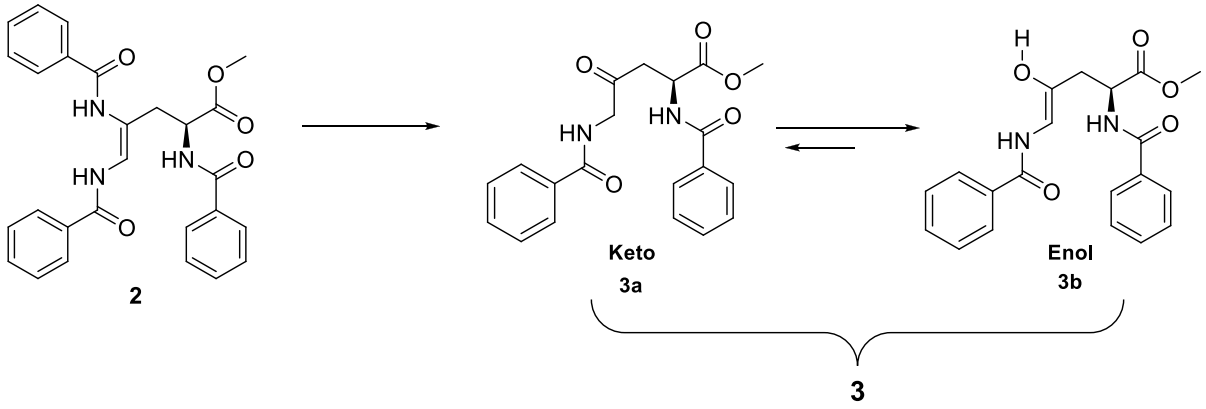

Scheme 2.6 Synthesis of (3) reagent and condition: MeOH / HCl 5 h at rt (95.5 %)

Shinkwin et al[13] showed in their report that the enol tautomer form of ethyl 4-oxotetrahydrothiophene-3-carboxylate was the most predominant tautomer at equilibrium in chloroform-d_3 and the only form visible in the ^{1}H NMR spectrum. This phenomenon was ascribed to the intramolecular hydrogen bonding that arises with an ester in its vicinity. Hence, this explains the presence of a singlet at δ_H 6.81 ppm which wasn't coupling to any other proton suggesting fast proton delocalization between the methylene and ketone carbonyl (Scheme 2.7) and the appearance of OH signal as a broad singlet at δ_H 7.14 ppm.

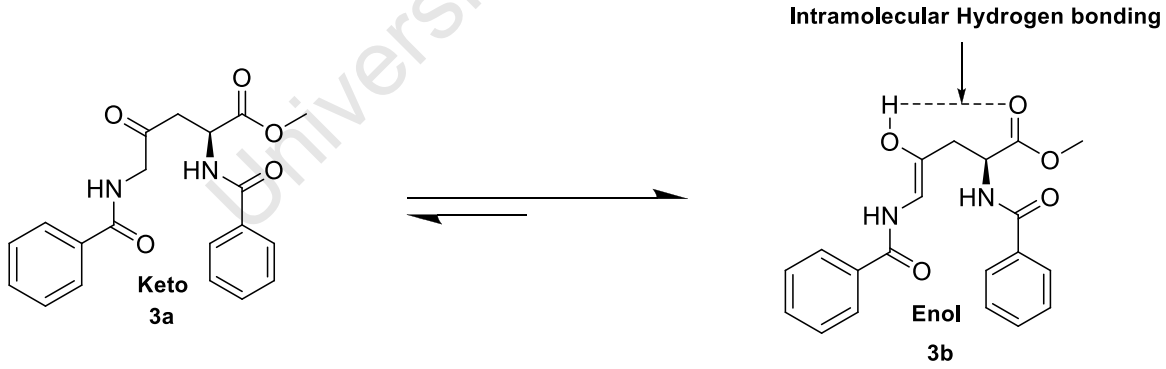

Scheme 2.7 Proposed tautomeric forms of (**3)** in equilibrium between *(S)*-methyl 2,5-bis(benzamido)-4-oxopentanoate **(3a)** and *(S,Z)*-methyl 2,5-bis(benzamido)-4-hydroxypent-4-enoate **(3b)**

Evidence for the formation *(S, Z)*-methyl 2,5-bis(benzamido)-4-hydroxypent-4-enoate **(3b)** was obtained by ^{1}H NMR spectra analysis as well as EI-MS. The proton NMR revealed 10 aromatic resonances, a multiplet in the aromatic region from δ_H 8.21 to 7.72 ppm integrating for 4 protons (two ortho protons), and a multiplet from δ_H 7.49 to 7.44 ppm integrating for 6

University of Cape Town

protons (two meta and four para protons) compared to (**2)** which was revealed at about the same chemical shift, thus indicating the disappearance of one benzoyl ring. The methyl ester proton signal resonated as a singlet at δ_H 3.83 ppm and the methylene signal resonated as a multiplet, slightly shielded, at δ_H 2.95 ppm suggesting close proximity to the carbonyl group thus supporting the assigned structure of (**3)** (Figure 2.2).

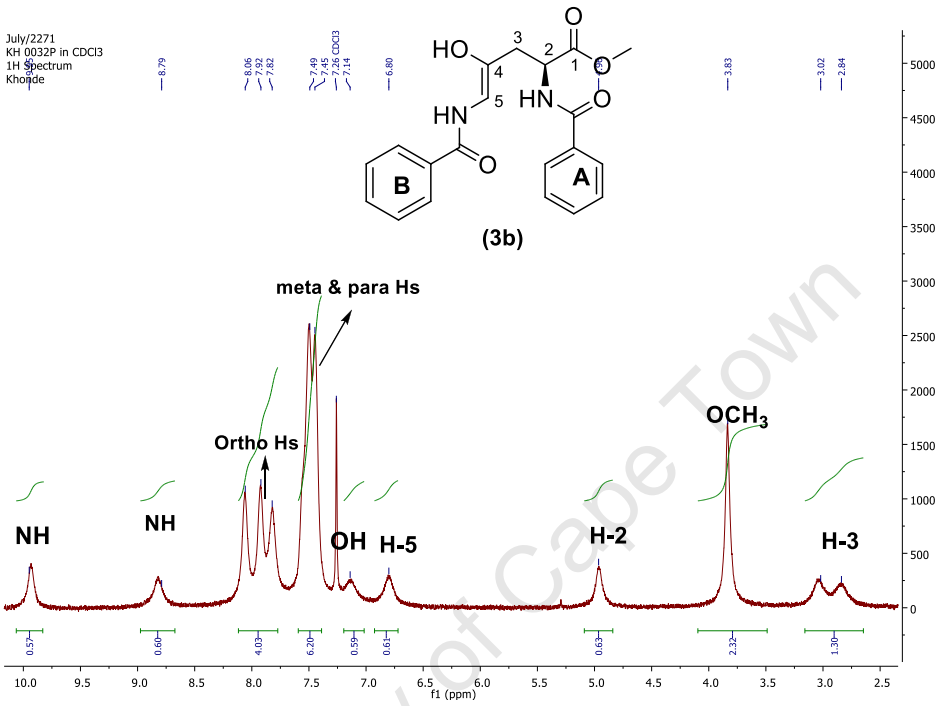

Figure 2.2. ^{1}H NMR spectrum of (**3b)** in $CDCl_3$ at 400 MHz

The melting point of (**3)** was in agreement with that reported in the literature.[6] Finally the EI^+ mass spectrum displayed a molecular ion at *m/z* 367.8 calculated for $C_{20}H_{20}N_2O_5$: 368.1 supporting the assigned structure of **(3).**

2.4.3. Synthesis of 2*(S)*-2-amino-3-(2-mercapto-1*H*-imidazol-4-yl) propanoic acid (4)

The *(2S)*-2-amino-3-(2-mercapto-1*H*-imidazol-4-yl) propanoic acid **(4)** was a key intermediate toward the synthesis of our target, because it only required *N*-methylation to get to the target, ergothioneine. The intermediate (**4)** was synthesized in two sequential steps. First, the acid hydrolysis of (**3)**, yielding the formation of *(2S)*-2,5-diamino-4-oxopentanoic acid (**4a**) giving benzoic acid as a by product which was removed by filtration. The intermediate (**4a)** was used directly in the next step without further purification. Finally (**4a)** was reacted with 2.8 mol equivalents of KSCN at 80-90 °C for 4-5 hours for the construction

University of Cape Town

of the mercapto imidazole ring. The product (**4)** was isolated as a white powder after freeze drying and in a good yield of 88 % (Scheme 2.8).

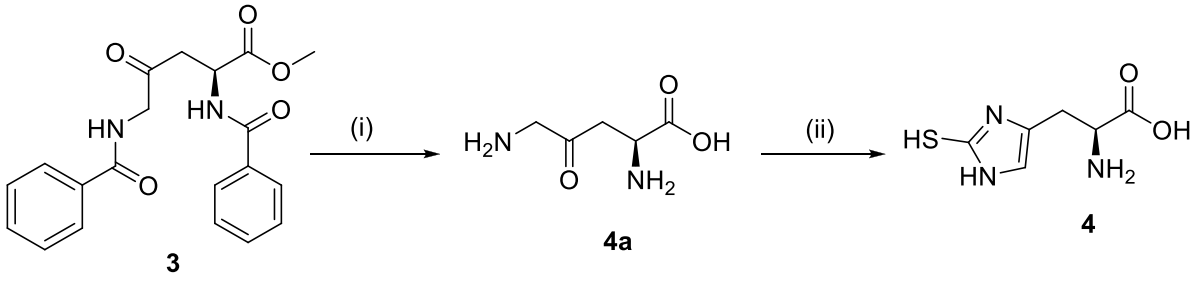

Scheme 2.8 Synthesis of (4).reagent and condition (i) HCl 15 h at 90 - 93°C, (ii) KSCN 4 - 5 h at 80 - 90°C (88%)

The ^{1}H NMR spectrum of *(2S)*-2-amino-3-(2-mercapto-1*H*-imidazol-4-yl) propanoic acid **(4)** in deuterium oxide displayed a characteristic aromatic signal for proton H-5' resonating as a singlet at δ_H 6.87 ppm indicative of the formation of the mercapto ring. Other keys signals were the α-amino acid proton H-2 resonating as a triplet at δ_H 4.31 (J = 6.6 Hz) ppm, suggesting coupling with the neighbouring methylene protons, and a set of two doublet of doublets resonances at δ_H 3.28 (J = 16.1, 6.6 Hz) and δ_H 3.17 (J = 16.1, 6.6 Hz) for proton H-3a and H-3b respectively, confirming the presence of an amino acid moiety. The NH, OH, and SH protons were not observed in the spectrum, presumably all exchanged with deuterium as D_2O was used as NMR solvent (Figure 2.3).

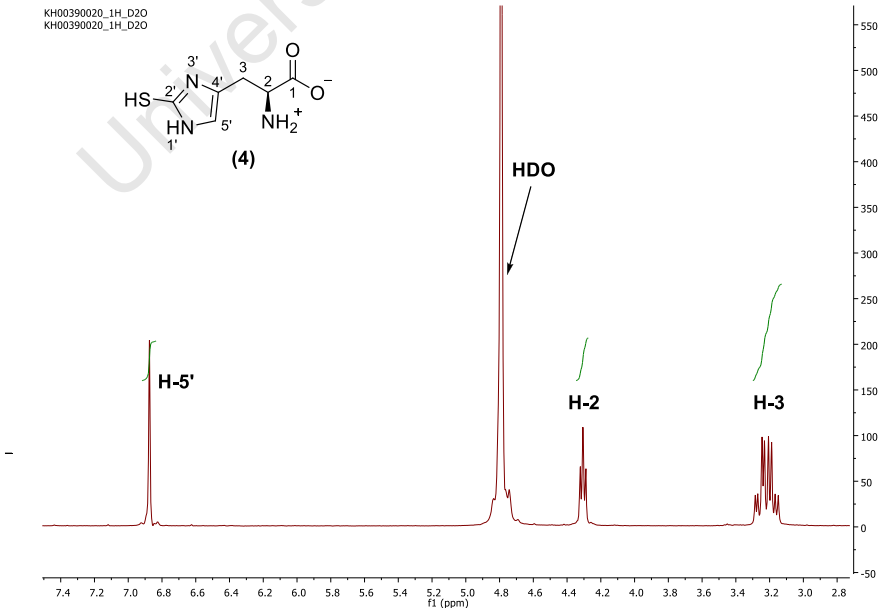

Figure 2.3 ^{1}H NMR spectrum of (**4)** in D_2O + DCl at 400 MHz

University of Cape Town

The ^{13}C NMR spectrum of compound **(4)** (Figure 2.4) displayed six carbon resonances, supporting the carbon skeleton of *L*-mercaptohistidine **(4)**. In addition, the melting point was recorded as 206-208°C (with decomposition) which was in agreement with that which was reported by *Harington et al.*[14]

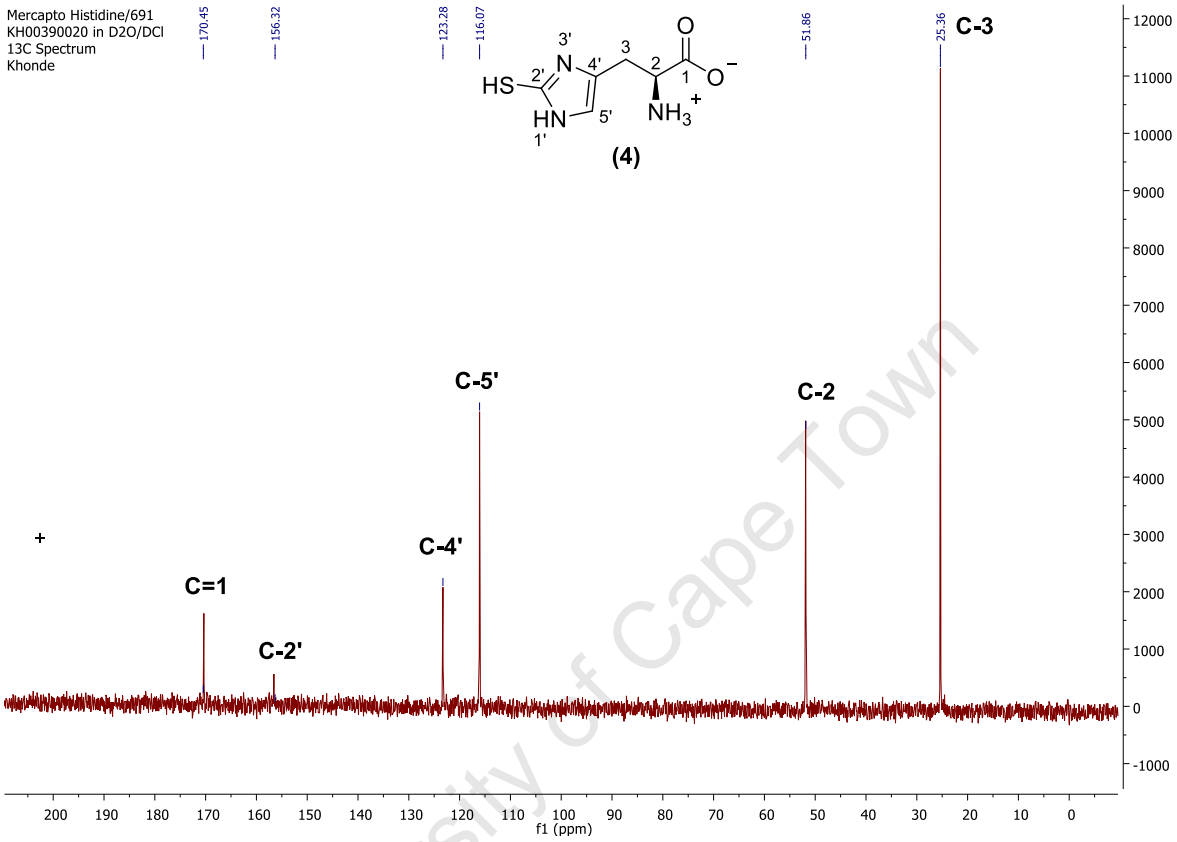

Figure 2.4 ^{13}C NMR spectrum of **(4)** in D_2O + DCl at 400 MHz

The FTIR spectrum in KBr showed a strong absorption at 2073 cm^{-1}, characteristic of a mercapto band (N=C-SH) proving successful thiation. Strong absorption at 3465, 1634 and 1129 cm^{-1} indicated the presence of a free amine, while a medium absorption at 1383 cm^{-1} indicated the presence of a carboxylate ion which strongly supported the assigned structure of **(4)**. Finally the EI^+ mass spectrum didn't display the molecular ion peak, instead it revealed the sodium adduct at *m/z* 209.0 confirming the assigned structure of **(4).**

2.4.4. Synthesis of (*S*)-2-amino-3-(2-(*tert*-butylthio)-1*H*-imidazol-4-yl) propanoic acid (5)

In order to protect the integrity of the mercapto imidazole ring and to proceed to a regio selective *N*-alkylation, the sulfur atom was protected by a *tert*-butyl group prior to the reductive amination.

University of Cape Town

Compound (**5)** was obtained by refluxing 2.6 mol equivalents of *t*-butanol and *(2S)*-2-amino-3-(2-mercapto-1*H*-imidazol-4-yl) propanoic acid (**4)** in distilled H_2O containing HCl as a catalyst (to limit by product formation) for 4 hours. The protected thiohistidine (**5)** was isolated in a moderate yield of 62.7 % after buffering with aqueous sodium acetate to pH 5 in order to liberate the free base which allowed extraction in warm 2-propanol (Scheme 2.9).

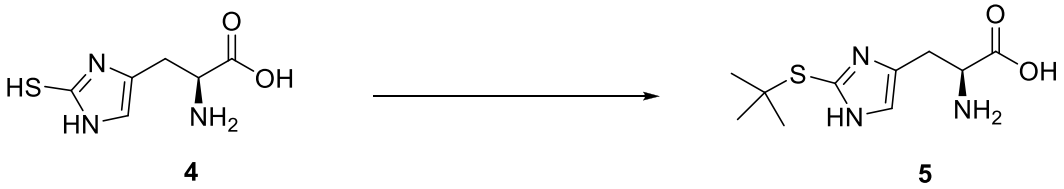

4 **5**

Scheme 2.9 Synthesis of (5).reagent and conditions: *t*-BuOH / HCl reflux for 3-4 hrs (62.7 %)

The *S-butyl* protection proceeded through a S_N1 reaction involving the formation of the *t-butyl* cation as the rate determining step of the reaction (Scheme 2. 10).[15]

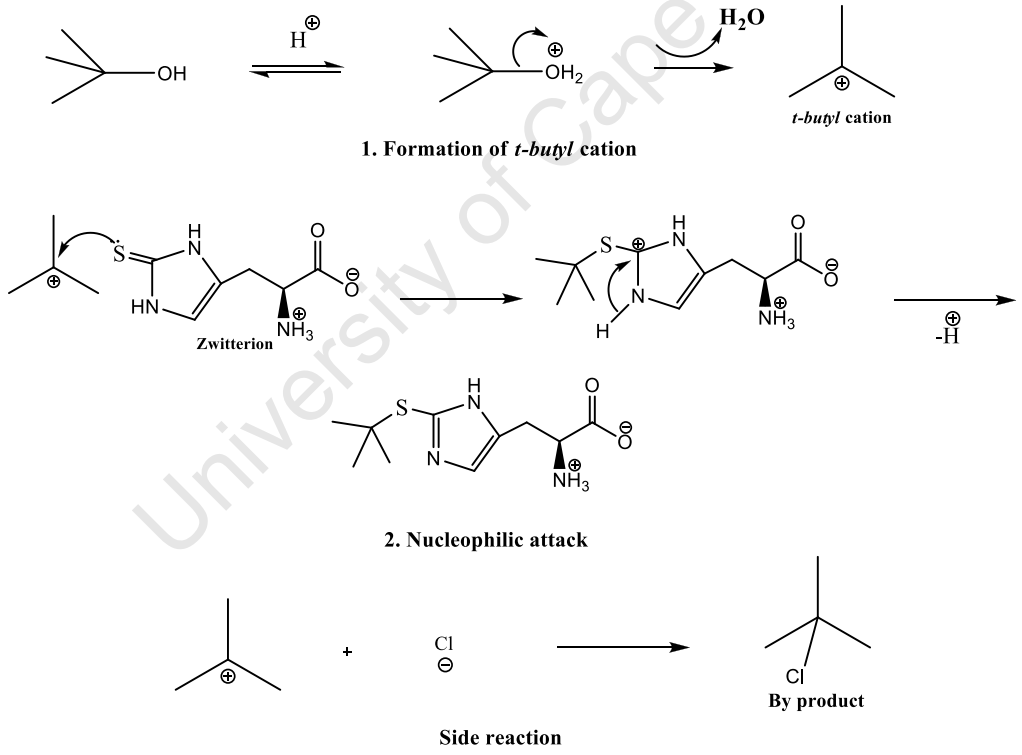

Scheme 2. 10. Proposed mechanism of *S*-butylation.[15]

A key diagnostic signal in the ^{1}H NMR spectrum of *(2S)*-2-amino-3-(2-(*tert*-butylthio)-1*H*-imidazol-4-yl) propanoic acid **(5)** was the appearance of a new up field resonance appearing as a singlet at δ_H 1.44 ppm integrating for 9 protons confirming that the sulfur protection had occurred. The α-amino acid proton signal resonating as a triplet at δ_H 4.18 ppm instead of a

University of Cape Town

multiplet as observed in (**4)** (from δ_H 4.20 to 4.07 ppm) suggests a different environment. A slight down field shift of the methylene signal, resonating from two doublet of doublets at δ_H 3.28 and δ_H 3.17 ppm in (**4)** to two doublet of doublets at δ_H 3.39 and δ_H 3.30 ppm in **(5)** that was due to the introduction of *t-butyl* group that donates electron density into the mercapto imidazole ring in the near proximity.

The optical rotation was $[\alpha]^{20}_D$ = +14.1 ° (*c* = 0.7, H_2O) which was in full agreement with that reported by *Trampota et al.*[6]

Finally the EI^+ mass spectrum displayed a molecular ion at *m/z* 243.1 calculated for $C_{10}H_{17}N_3O_2S$: 243.1 supporting the assigned structure of (**5).**

2.4.5. Synthesis and characterisation of (2*S*)-3-(2-(*tert*-butylthio)-1*H*-imidazol-4-yl)-2-(dimethylamino) propanoic acid (6).

With the protected thiohistidine in our hand, the *N*-methylation could be performed. The synthesis starts with the preparation of sodium triacetoxyborohydride *in situ* by reacting sodium borohydride with three mol equivalents of glacial acetic acid in ethyl acetate which was used as solvent.

The synthesis of (**6)** was achieved by reacting 3.8 mol equivalents of formalin (37%) with (**5)** in THF, followed by the addition of a concentrated solution of previously prepared sodium triacetoxyborohydride. After allowing the reaction to stir at 10°C for 8 hours, TLC showed completion. Compound (**6)** was isolated after crystallization as the free base in poor yield (33.7 %) (Scheme 2.11).

5 **6**

Scheme 2.11 Synthesis of (6), reagent and conditions: Formalin, sodium triacetoxyborohydride / THF , 6-8 h at 10°C (33.7 %)

A key diagnostic signal in the ^{1}H NMR spectrum was the down field resonance of a singlet at δ_H 3.01 ppm integrating for 6 protons, indicating that reductive *N*-alkylation occurred.

University of Cape Town

2.4.6. Final stage of *L*-ergothioneine (8) synthesis.

The synthesis of ergothioneine (**8)** was achieved in a two step reaction from the intermediate **(6)**. The dimethylated product (**6)** was allowed to react with 1.5 mol equivalents of iodomethane at room temperature for 24 hours. After simple filtration and removal of the solvent under high vacuum, the crude quaternary amine **(7)** was deprotected by refluxing in acid (conc HCl) for 21 hours, using 2-mercaptopropionic acid as *tert-butyl* ion scavenger. Ergothioneine (**8)** was isolated as the chloride salt after work up and crystallization in a mixture of EtOH/H_2O (10:1) in 27.3% yield over 2 steps (Scheme 2.12).

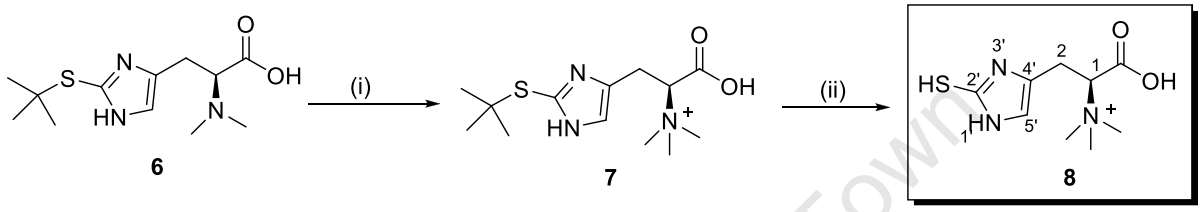

Scheme 2.12 Synthesis of (8).reagent and conditions: (i) NH_4OH, CH_3I / MeOH 24 h at rt; (ii) HCl, 2-mercaptoprionic acid refluxed for 21h (27.3 % over 2 steps).

The ^{1}H NMR spectrum displayed the right amount of signals and was in full agreement with that reported by *Trampota et al.*[6]

The ^{13}C NMR spectrum of ergothioneine (**8)** displayed a carbonyl signal at δ_C 177.0 ppm, three aromatics carbons resonated respectively at δ_C 161. 2 ppm (deshielded for C-2'), 128.9 ppm (for C-4'), 103.4 ppm (for C-5') and finally three sets of shielded aliphatic carbons, with C-2 resonating at δ_C 60.6 ppm, the characteristic NMe_3 signal at δ_C 55.6 ppm and the methylene carbon (C-3) at 24.9 ppm, all in accordance with data recently reported by *Erdelmeier et al.*[16, 17]

In addition, the melting point was recorded as 276-279 °C which was in agreement with that reported by Sigma-Aldrich (275-277°C).[18]

The optical rotation was $[\alpha]^{20}_D$ = +138.21° (*c* = 1; H_2O) which was in agreement with that reported by *Trampota et al* $[\alpha]^{25}_D$ = +125°(*c* = 1; H_2O).[6]

The HRMS evaluation (ESI^+) (*m/z* 230.0958 [M^+]) corresponding to $C_9H_{16}N_3O_2S^+$ (*m/z* 230.0963 [M^+]) supported the structure of *L*-ergothioneine **(8)** (Figure 2.5).

University of Cape Town

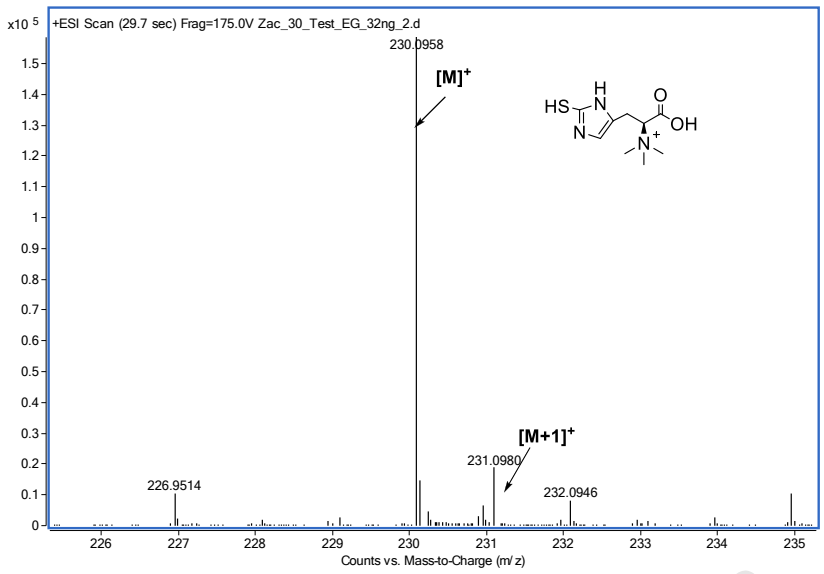

Figure 2.5 HRMS (ESI$^+$) of *L*-ergothioneine (**8.**)

In this research effort, *L*-ergothioneine was successfully synthesized with many process improvements. A key modification of the method was the use of reverse phase C18 chromatography, thus significantly reducing the amount of salts allowing the crystallization of ergorthioneine. However, several attempts to improve the overall yield (21.4 %) were unsuccessful.[7]

Recently, *Erdelmeier et al*[16, 17] published a new ergothioneine synthesis, completely different from that which was reported in two previous patents, whereby cysteine was used as the source of sulfur. The author claimed to have developed a biomimetic, environmentally friendly method with fewer reaction steps.

Synthesis of *L*-ergothioneine in a one pot synthesis sequence using *Erdelmeier's* method was also investigated; unfortunately even after several attempts we were not been able to isolate a pure (*L)*-ergothioneine from the reaction mixture, cysteine was rather isolated as it was utilized in the process as a reactant in large excess (5 mol equivalents).[16, 17]

University of Cape Town

2.5. References

1. http://www.oxisresearch.com/ergo/l-ergothioneine_monograph.pdf
2. Briggs, I., *J. Neurochem.*, **1972**, 19, 27.
3. Paul, B.D.; and Snyder, S.H., *Cell Death Differ*, **2009**, 17, 1134.
4. http://www.sigmaaldrich.com/catalog/product/sigma/e7521?lang=en&region=ZA
5. Xu, J.; and Yadan, J.C., *J. Org. Chem.*, **1995**, 60, 6296.
6. Trampota, M., *United States Patent*, **2010**, US 7, 767, 826, B2.
7. Bamberger, E., *Liebigs. Ann. Chem.*, **1893**, 273, 342.
8. Grace, M.E.; Loosemore, M.J.; Semmel, M.L.; and Pratt, R.F., *J. Am. Chem. Soc.*, **1980**, 102, 6784.
9. Avaera, S.N.; Krasnova, V.T., *Biorg. Khim.*, **1975**, 1, 1600.
10. Vliegenthart, J.F.G.; Dorland, L., *J. Biochem.*, **1970**, 117, 319.
11. Health, H.; Lawson, A.; Rimington, C., *J. Chem. Soc.*, **1951,** 2215.
12. Witrop, B.; Beiler, T., *J. Chem. Soc.*, **1955**, 74, 2882.
13. Shinkwin, A.E.; Whish, W.J.D. and Threadgill, M.D., *Biorg. Med. Chem.*, **1999**, 7, 297.
14. Harington, C.R.; Overhoff J., *J. Chem. Soc.*, **1933**, 388.
15. Clayden, J.; Greeves, N.; Warren, S.; Wother, P., *Organic. Chemistry*, **2001**, Oxford University Press, Oxford, ISBN 9780-0-19-850346-0.
16. Erdelmeier, I.; Daunay, S.; Lebel, R.; Farescour, L. and Yadan, J.C.; *Green Chem.*, **2012**, 14, 2256.
17. Erdelmeier, I., *Patent WO2011/042480 A1*, **2011.**
18. http://www.sigmaaldrich.com/MSDS/MSDS/DisplayMSDSPage.do?country=ZA&language=en&productNumber=E7521&brand=SIGMA&PageToGoToURL=http%3A%2F%2Fwww.sigmaaldrich.com%2Fcatalog%2Fproduct%2Fsigma%2Fe7521%3Flang%3Den

University of Cape Town

Chapter 3 Synthesis of ergothioneine biosynthetic enzyme substrates

The ultimate aim of this study is to unravel the biosynthesis of ergothioneine in *M. tb* and in the broader sense to better understand its implication for survival of *Mycobacteria*. While all steps in the pathway are interesting, our focus is on the last step of the biosynthesis, i.e. the step catalysed by the PLP-dependent lyase, EgtE. EgtE is involved in the cleavage of the intermediate, ***R/S*-(*β*-amino-*β*-carboxyethyl) ergothioneine sulfoxide,** to *L*-ergothioneine and pyruvate.[1] The EgtE enzyme of *M. tb* is the only enzyme in the pathway that has not yet been solubly expressed and none of the pathway enzymes have been thoroughly studied due to substrate unavailability. In the absence of expressed and purified EgtE, a classical purification of this enzyme is planned, using *M. smeg.* as the source. However, the latter is outside the scope of this effort and only crude cell free lysate was considered for the transformation of substrates at this time. In order to perform a classical isolation and purification of EgtE for kinetic studies, sufficient quantities of its substrate is required.

3.1. Synthesis and characterization of EgtE substrate, *R/S*-(*β*-amino-*β*-carboxyethyl) ergothioneine sulfoxide.

3. 1. 1. Retrosynthetic Analysis (Method 1)

In this approach, the proposed retrosynthesis consider cleavage on the distal side of the histidine moiety (left of the sulphur atom) of the substrate as depicted in Scheme 3.1, leading to a *β*-chloro-alanine methyl ester and ergothioneine. Thus, *S*-alkylation with a protected chloromethyl alanine ester, derived from serine, would provide the core structure. The resulting thioether can be oxidised under controlled conditions using either *m*CPBA or H_2O_2 depending on the solubility of the substrate. Therefore it is required that ergothioneine be synthesized in sufficient quantities and protected appropriately.

Chlorination of the serine hydroxymethyl side chain would lead to the second major component of our retrosynthons.

University of Cape Town

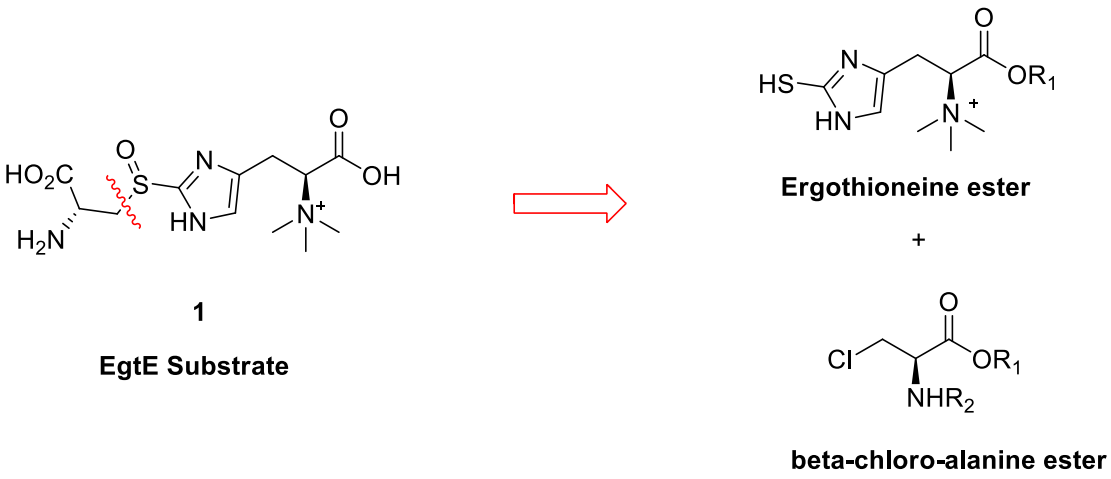

Scheme 3.1 Retrosynthesis of EgtE substrate.

3. 1. 2. Synthesis of the *N*-Boc protected-*β*-chloroalanine methyl ester.

With *L*-ergothioneine in our hand, attention was focused on the synthesis of the chloromethylserine synthon. Commercially available *L*-serine (**9)** was protected as the *N*-Boc- *L*-serine methyl ester (**10**).[2] Although the latter intermediate is commercially available, we needed large quantities which were beyond our budget. The challenge was to synthesize the protected *N*-Boc-*β*-chloro-*L*-alanine methyl ester **(12)** without any racemisation or inversion of configuration of the chiral centre. The *tert*-butyloxy carbonyl (Boc) group was considered a suitable amine protecting group because of its facile removal by acid treatment.[3]

The synthesis of the ester involved acid catalysed esterification steps as outlined by *McKillop et al*,[2] whereby methanolic HCl was produced *in situ* by reacting acetyl chloride with methanol in an ice bath. The serine methyl ester was synthesized on a 5 g scale in quantitative yield and high purity. The Boc protection was achieved under standard conditions giving access to multigram quantities of the *N*-Boc-*L*-serine methyl ester **(10)** in 72.7% yield (Scheme 3.2).

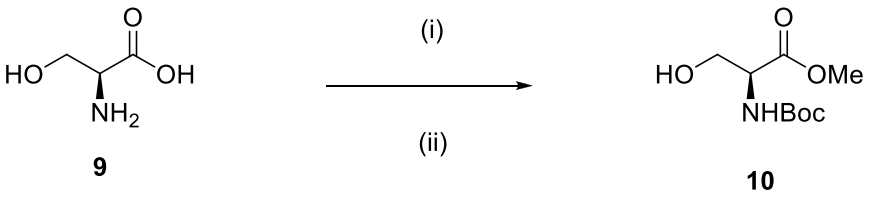

Scheme 3.2 Synthesis of (10) reagent and conditions: (i) MeOH / CH_3COCl reflux 2 h; ii) $(Boc)_2O$, Et_3N / THF, 6 h at rt (72.7 %).

University of Cape Town

The optical rotation, $[\alpha]^{20}_{D}$ = -25.7 °(*c* = 5, MeOH), was considered to be sufficient by comparison with commercially (Aldrich) available *L*-enantiomer ($[\alpha]^{20}_{D}$ = -18 °(*c* = 5, MeOH) (Aldrich), and with that which was reported by *McKillop et al*[5] $[\alpha]^{20}_{D}$ = -18.9°(*c* = 5, MeOH).[5] Based on optical rotation, it can be claimed that the synthesis was completed without significant racemization, if any.

3. 1. 3. Chlorination of the protected serine methyl ester.

The chlorination of alcohols is an industrially important transformation in organic synthesis having a wide range of applications in fine chemical production.[4, 5] Thus, the mildest conditions for the conversion of the primary alcohol of protected serine to the chloromethyl group was sought. Many methodologies have been published to date and more commonly utilize Ph_3P-CCl_4, PCl_5, thionyl chloride, phenylmethyleniminium, benzoxazolium, Vilsmier-Haack and Viehe salts as chlorinating agents.[5] As such, *Lidia et al* [6] reported a simple and efficient chlorination method involving the reaction of TCT and DMF. The mechanism involves a S_N2 nucleophilic substitution via the formation of a Vilsmeier-Haack intermediate **(I)** (Figure 3.1). The Vilsmeier-Haack complex adds to the hydroxyl group to form a labile vinyl ether derivative. Upon substitution with the chloride ion, the corresponding alkylhalide is obtained with the concomitant formation of DMF as a side product.

University of Cape Town

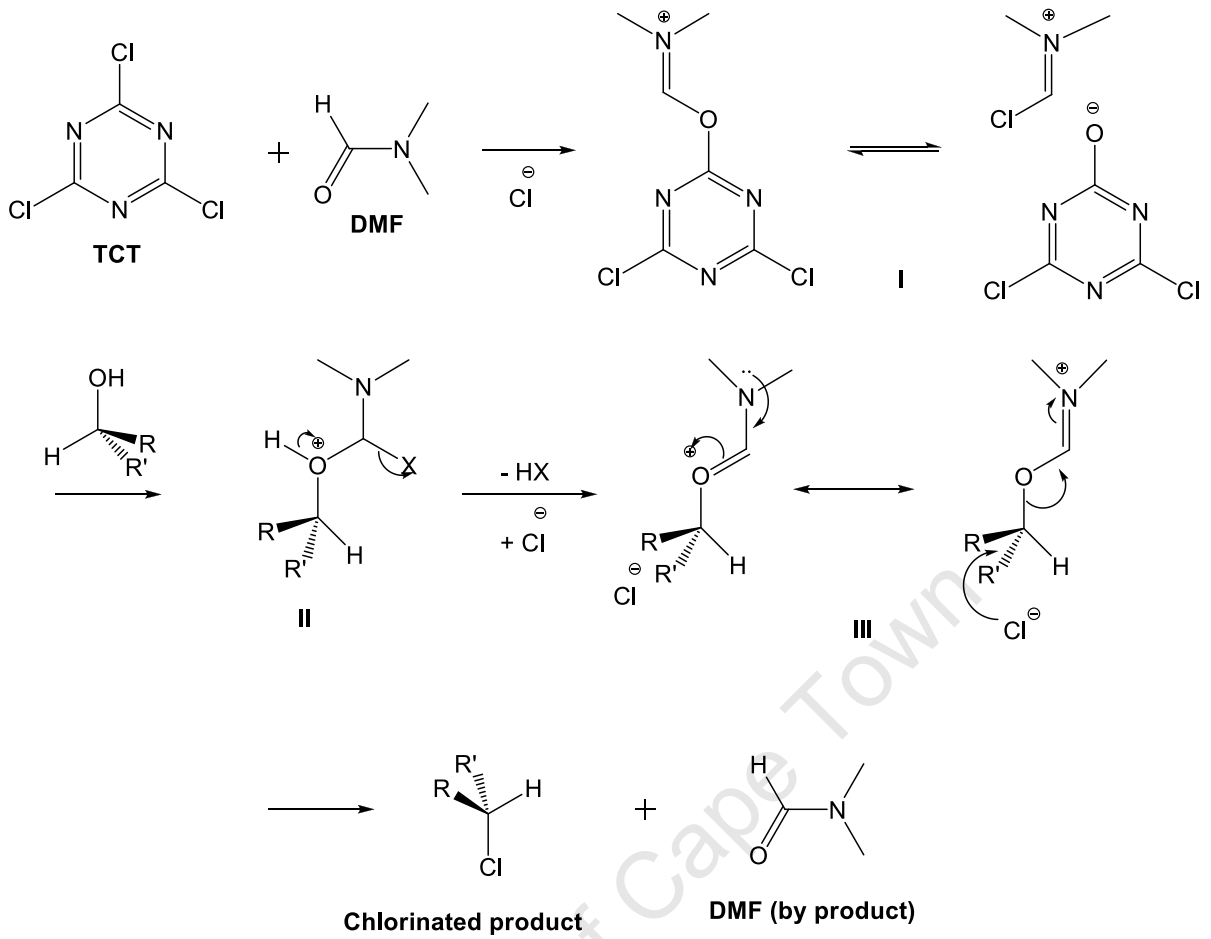

Figure 3.1 Proposed mechanism of chlorination of alcohol using Vilsmeier-Haack type complex as a chlorinating agent.[6]

With sufficient (7.5 g) *N*-Boc-*L*-serine methyl ester **(10)**, chlorination of the hydroxymethyl side chain could be attempted.[7] The chlorination was accomplished by reacting one molar equivalent of *N*-Boc-*L*-serine methyl ester **(10)** with the TCT/DMF complex. TLC indicated the formation of *N*-Boc-*β*-chloro-*L*-alanine methyl ester **(12)** after 4 hours at room temperature (Scheme 3.3).

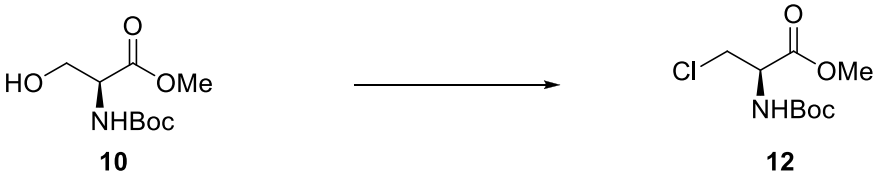

Scheme 3.3 Synthesis of (12) reagent and conditions: TCT / DMF in CH_2Cl_2 , 4 h at rt (30.5 %).

The compound was isolated in 30.5% yield after flash column chromatography and crystallization from a mixture of petroleum ether and ethyl acetate. The *N*-Boc-*β*-chloro-*L*-alanine methyl ester **(12)** was unstable in the presence of SiO_2 and degraded upon long

University of Cape Town

exposure time on the column and therefore was used immediately after chlorination and flash chromatography.

A key diagnostic signal in the ^{1}H NMR spectrum of *N*-Boc-*β*-chloro-*L*-alanine methyl ester **(12)** was the slight upfield shift of the methylene proton signal where the substitution occurred (Figure 3.2). Thus, the resonance of methylene proton H-3 shifted from δ_H 3.90 ppm in (**10)** to 3.84 ppm in (**12)** due to the substitution of hydroxyl by chloride, which is attributed to the shielding effect of an adjacent electronegative atom.

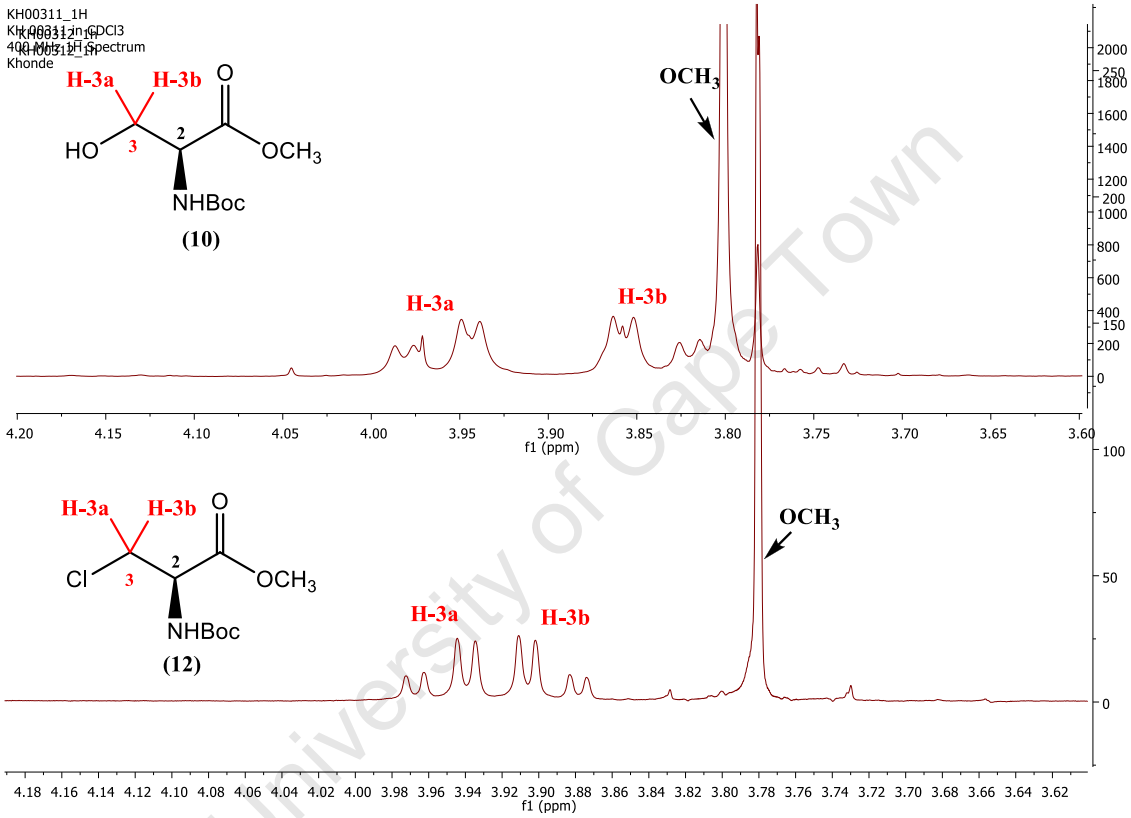

Figure 3.2 Methylene proton (H-3) shift in ^{1}H NMR spectrum of *N*-Boc-*β*-chloro-*L*-alanine methyl ester **(12)** compare to *N*-Boc-*L*-serine methyl ester **(10)** in $CDCl_3$ at 400 MHz.

The chlorination was further confirmed by respectively medium and strong absorption bands in the FTIR Infrared spectrum at 809 and 852 cm^{-1} for the C-Cl stretch.

The optical rotation was $[\alpha]^{20}_D$ = +32.5° (*c* = 0.15; $CHCl_3$), which was in accordance with that which was reported by *Kenworthy et al* [7] ($[\alpha]^{21}_D$ = +37.8° (*c* = 0.15; $CHCl_3$), suggesting that the chlorination was achieved without significant racemisation, if any.

The melting point obtained was 59-61 °C which was in accordance with that reported by *Kenworthy et al* [8] (62-64 °C) and *Tao et al* [9] (59-60°C).

University of Cape Town

Finally, the EI^+ mass spectrum displayed a molecular ion at *m/z* 235.8 $[^{35}M\text{-}H]^+$ calculated for $C_9H_{15}{}^{35}ClNO_4$: 236.1 $[^{35}M\text{-}H]^+$, 238.1 $[^{37}M\text{-}H]^+$, The fragment corresponding to the loss of Boc has been also detected at *m/z* 138.0 ($[^{35}M^+$- Boc]; 11 %) and 140.0 ($[^{37}M^+$- Boc]; 2.6 %), supporting the assigned structure of *N*-Boc-*β*-chloro-*L*-alanine methyl ester (**12).**

3. 1. 4. The synthesis of *N*-Boc-*β*-chloro-*D*-alanine methyl ester (13).

The *N*-Boc-*β*-chloro-*D*-alanine methyl ester **(13)** was synthesized as an intermediate toward the synthesis of the non-natural diastereoisomeric EgtE substrate analogue, hercynyl-*D*-cysteine sulfoxide, which may act as an EgtE enzyme inhibitor. This stems from the fact that the amine functional group is essential for the PLP mediated lyase initiation and the *D*-enantiomer may not be able to undergo normal lyase activity, but result in inhibition instead.

The same chlorination procedure as described above was applied to Aldrich commercially available *N*-Boc-*D*-serine methyl ester.

The *N*-Boc-*β*-chloro-*D*-alanine methyl ester **(13)** was isolated in low yield of 14.14 % after recrystallization in a mixture of petroleum ether and ethyl acetate (Scheme 3.4).

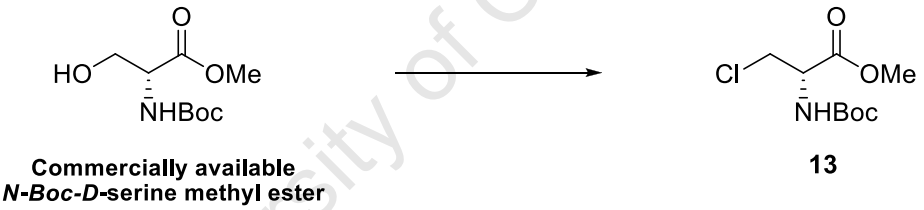

Scheme 3.4 Synthesis of (13), reagent and conditions**:** TCT / DMF in CH_2Cl_2, 4 h at rt (14,14 %).

The *N*-Boc-*β*-chloro-*D*-alanine methyl ester **(13)** was fully characterized as a novel product. The ^1H NMR spectrum as well as ^{13}C NMR were identical to the *L*-enantiomer analogue **(12)** as expected (Figure 3.3).

University of Cape Town

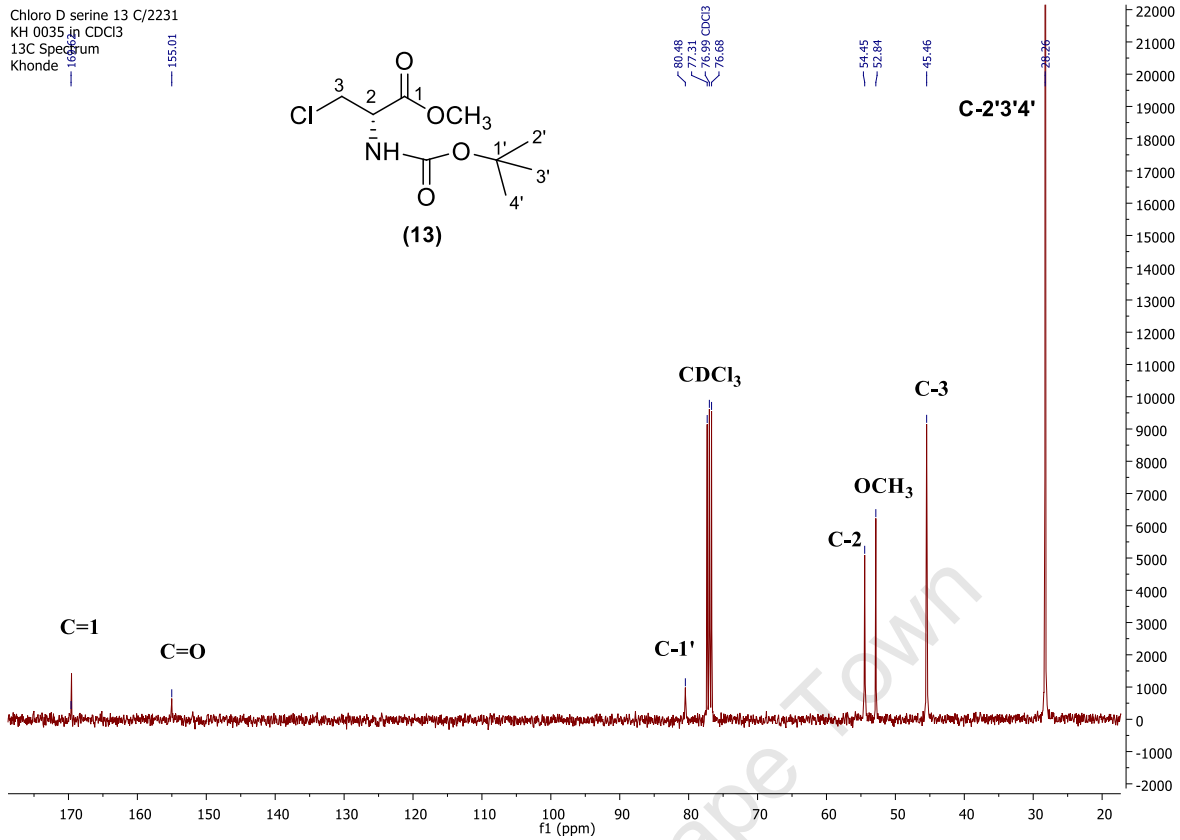

Figure 3.3 ^{13}C NMR spectrum of *N*-Boc-*β*-chloro-*D*-alanine methyl ester **(13)** in $CDCl_3$ at 100 MHz.

The optical rotation measured for the *D*-enantiomer was $[\alpha]^{20}_{D}$ = -35.7° (*c* = 1, $CHCl_3$) which compared well in sign and magnitude to its *L*-enantiomer at approximately the same concentration. Thus, the reactions did not cause any significant racemisation.

Finally the EI^+ spectrum showed the molecular ion at *m/z* 236.1 $[^{35}M\text{-}H]^+$ and 238.1 $[^{37}M\text{-}H]^+$, probably due to the loss of a proton from NH which is required for $C_9H_{15}{}^{35}ClNO_4$:236.1 $[^{35}M\text{-}H]^+$ and $C_9H_{15}{}^{37}ClNO_4$:238.1 $[^{37}M\text{-}H]^+$, thus supporting the assigned structure of *N*-Boc-*β*-chloro-*D*-alanine methyl ester **(13).**

The chlorination reaction gave the crude products in good yield as TLC indicated complete disappearance of starting material and the formation of a relatively clean product. However, after silica gel column chromatography a very poor yield was obtained, suggesting that the *N*-Boc-*β*-chloro-alanine methyl ester (*D* or *L* enantiomer) were indeed unstable on SiO_2, with *N*-Boc-*β*-chloro-*D*-alanine methyl ester **(13)** the more unstable enantiomer (14.1 %). Thus, flash column chromatography purification was required in order to reduce the silica exposure time (Scheme 3.5).

University of Cape Town

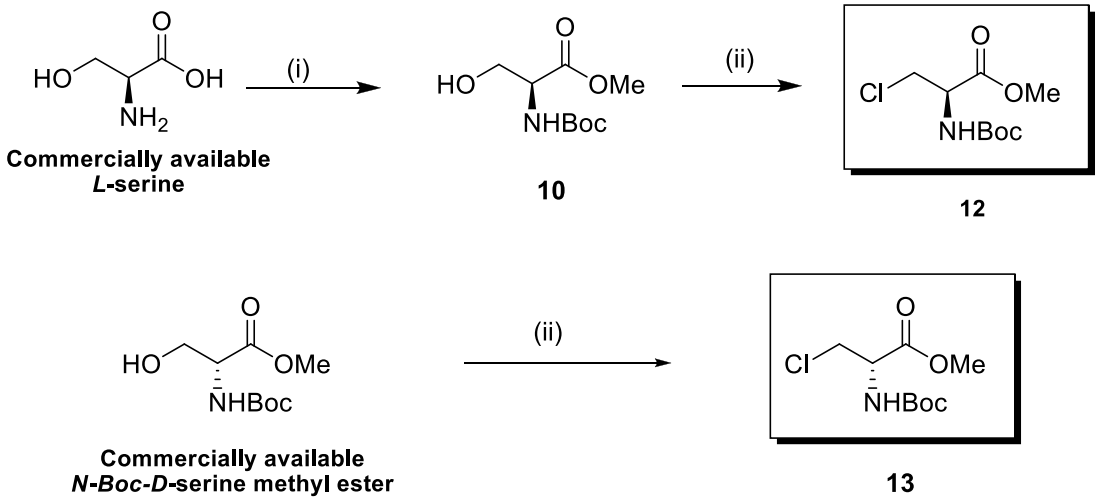

Scheme 3.5 Synthesis of (12) and (13), reagent and conditions**:** (i) a) MeOH / HCl; b) $(Boc)_2O$, Et_3N / THF 6 h at rt (72.7 % over 2 steps); (ii) TCT / DMF in CH_2Cl_2 4 h at rt. **12** (30.5 %), **13** (14.1 %)

3. 1. 5. The synthesis of *R/S*-(*β*-amino-*β*-carboxyethyl) ergothioneine sulfoxide, the EgtE substrate.

With both retrosynthons in hand the next challenge was to synthesize the EgtE substrate, (*R/S*)-*β*-amino-*β*-carboxyethyl)ergothioneine sulfoxide. To this end, unprotected ergothioneine (**8)** was directly *S*-alkylated under basic conditions with the *N*-Boc-*β*-chloro-*L*-alanine methyl ester **(12),** and *N*-Boc-*β*-chloro-*D*-alanine methyl ester **(13)** respectively to give hercynyl *N*-Boc-*L*-cysteine methyl ester thioether **(19)**, and hercynyl *N*-Boc-*D*-cysteine methyl ester thioether **(20)** (Scheme 3.6).

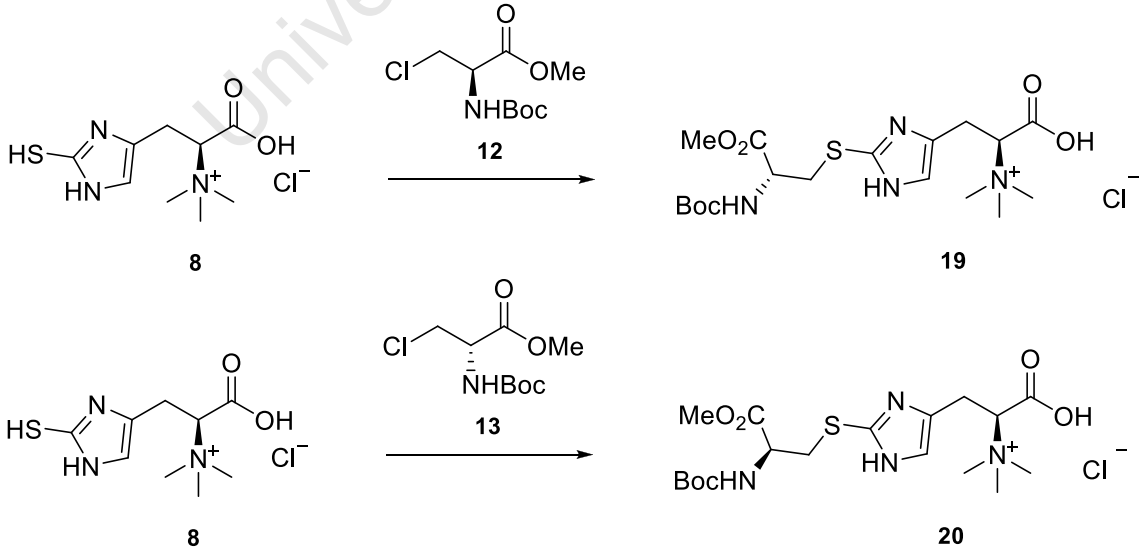

Scheme 3.6 Outlined Synthesis of 19 – 20, reagent and conditions: Et_3N / H_2O 5 h at 30°C, **19** (50.5 %), **20** (33. 3%).

University of Cape Town

The two thioether coupled products **(19** and **20)** were subjected to *S*-oxidation using one equivalent each of *m*CPBA to afford the hercynyl *N*-Boc-*L*-cysteine methyl ester sulfoxide **(24),** and hercynyl *N*-Boc-*D*-cysteine methyl ester sulfoxide **(25)** (Scheme 3.7).

Finally, deprotection of the Boc group under acid conditions gave the target compounds hercynyl *L*-cysteine methyl ester sulfoxide **(26)** and hercynyl *D*-cysteine methyl ester sulfoxide **(27)** (Scheme 3.7).

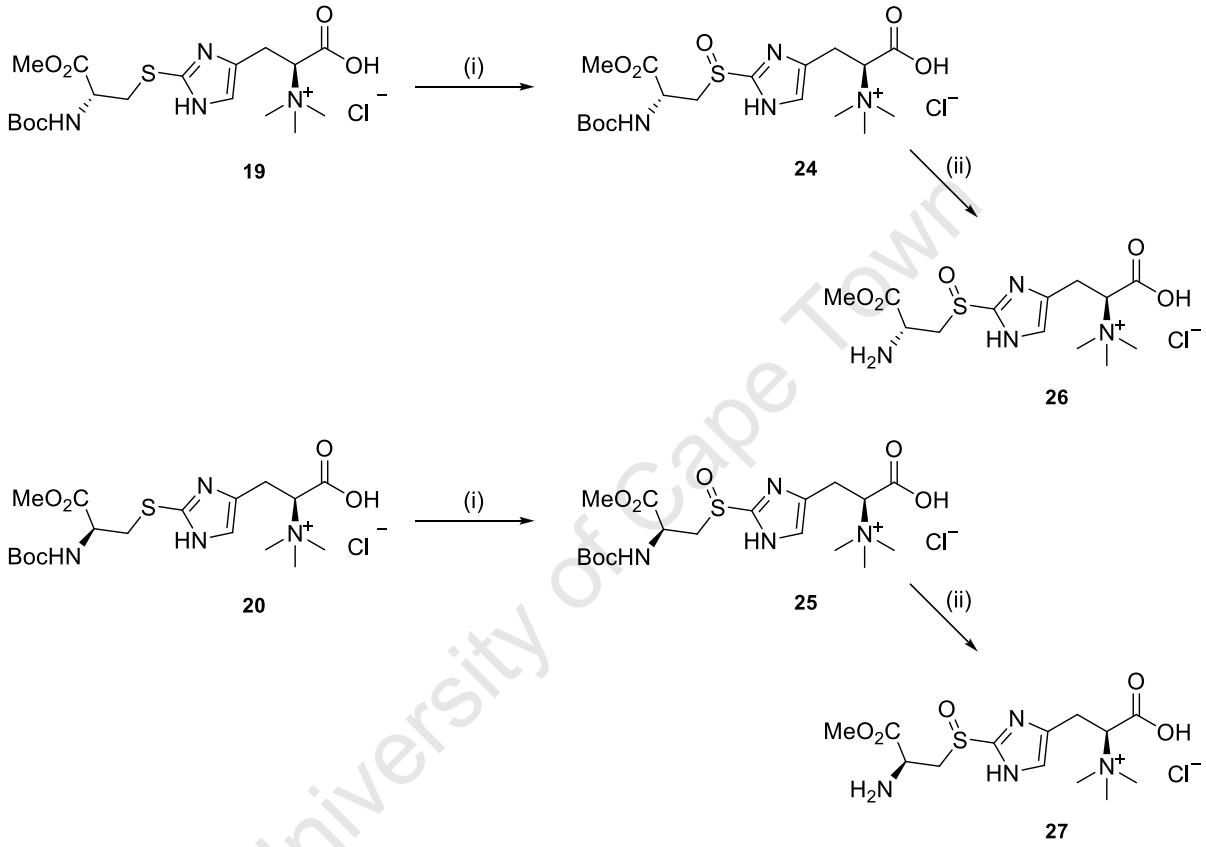

Scheme 3.7 Outlined Synthesis of 26-27 reagent and conditions (i) *m*CPBA, H_2O / DCM 1:1, 5 hr at 25°C, **24** (96.3%), **25** (73.2%) (ii) TFA, DCM / H_2O, **26** (70.2%), **27** (73.2%).

3. 1. 6. Coupling of *N*-Boc protected *β*-chloro-*L* and *D*-alanine with ergothioneine.

The coupling was performed by improving the method outlined by *Ishikawa et al*[10] especially in terms of the purification technique, reverse phase (C18) was introduced instead of tedious biogel chromatography.

A small-scale coupling reaction was performed using 1 mole equivalent of ergothioneine (**8)** with 1.1 equivalent of *N*-Boc-*β*-chloro-*L*-alanine methyl ester (**12)** in presence of triethylamine (pH 9-10) at 30°C. The reaction progress was monitored by TLC, which

University of Cape Town

indicated completion after 5 hours. The hercynyl *N*-Boc-*L*-cysteine methyl ester (**19)** was isolated in a moderate yield of 51 % after reverse phase (C18) purification.

Likewise as described above *L*-ergothioneine **(8)** was coupled to *N*-Boc-*β*-chloro-*D*-alanine methyl ester (**13)** and purified by reverse phase (C18) chromatography to yield hercynyl *N*-Boc-*L*-cysteine methyl ester (**20)** in a low yield of 33.3%.

The mechanism followed by the reaction is still not well known to date, however *Ishikawa et al.*[10] suggested that the reaction may possibly occur via the formation of the cyclic ethylenimine-2 carboxylic acid intermediate **(I)** produced by the dehydrohalogenation of the *β*-chloroalanine (Scheme 3.8), followed by the ring opening induced by nucleophilic attack of the sulfur atom of ergothioneine, giving products majors **(19** and **20)** and minor products **(II a** and **II b)** depending on the orientation of the ring opening, (in this case only the major products, hercynyl *N*-Boc-*L*-cysteine methyl ester **(19)** and hercynyl *N*-Boc-*D*-cysteine methyl ester **(20)** were isolated in a moderate yield.

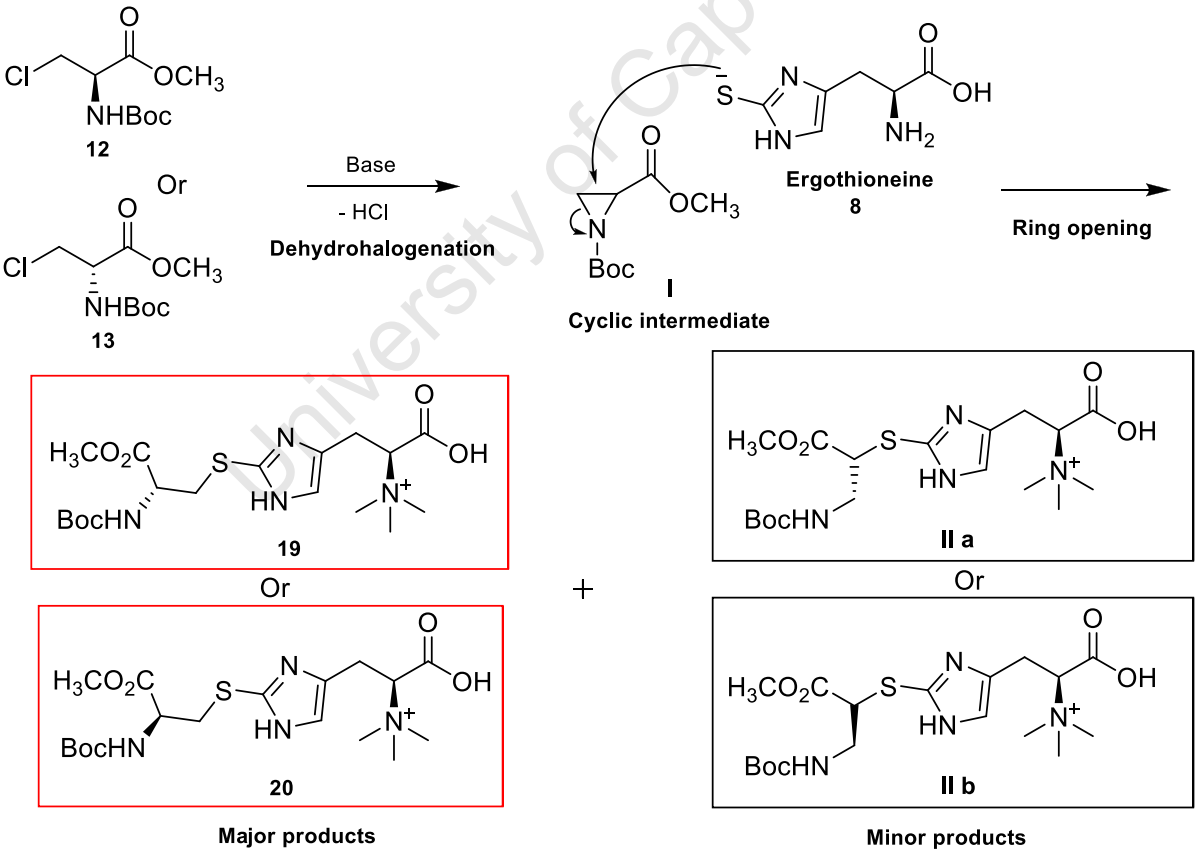

Scheme 3.8 Proposed mechanism of ergothioneine coupled to *N*-Boc protected *β*-chloro-*L* and *D*-alanine.[10]

University of Cape Town

3. 1. 7. Oxidation of the sulfide intermediate, the *(R/S)* hercynyl cysteine methyl ester sulfide.

In order to prevent or to minimise racemisation of the sulfoxide, *m*CPBA was preferably used because of its milder nature and potential for controlled sulfoxidation compare to hydrogen peroxide.[11] *Fernandez* and *Khiari* [12] highlighted that *m*CPBA could provide high diastereoselectivity under mild reaction conditions for the synthesis of (S_S)-*β*-sulfinyl thioglycosides **(32)**, and (R_S)-*β*-sulfinyl thioglycosides **(34)**, which was isolated as a single isomer (up to 100 % diastereoselectivity) (Scheme 3.9).[12]

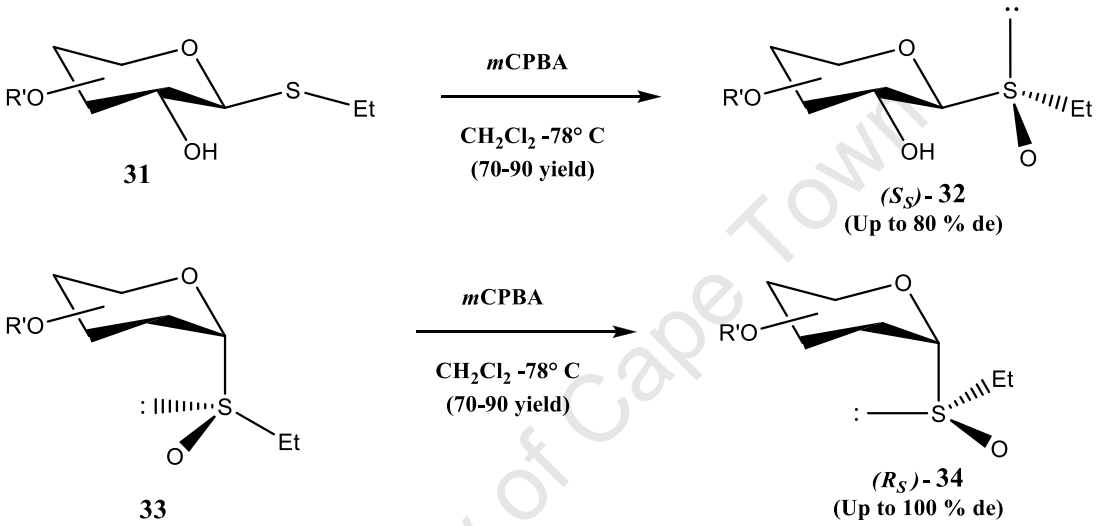

Scheme 3.9 Diastereoselective sulfoxidation of **(32)** and **(34)** using *m*CPBA as an oxidating agent.

The oxidation was performed using 1 mole equivalent of *m*CPBA in an ice bath to avoid any over oxidation to the sulfone (Scheme 3.10)

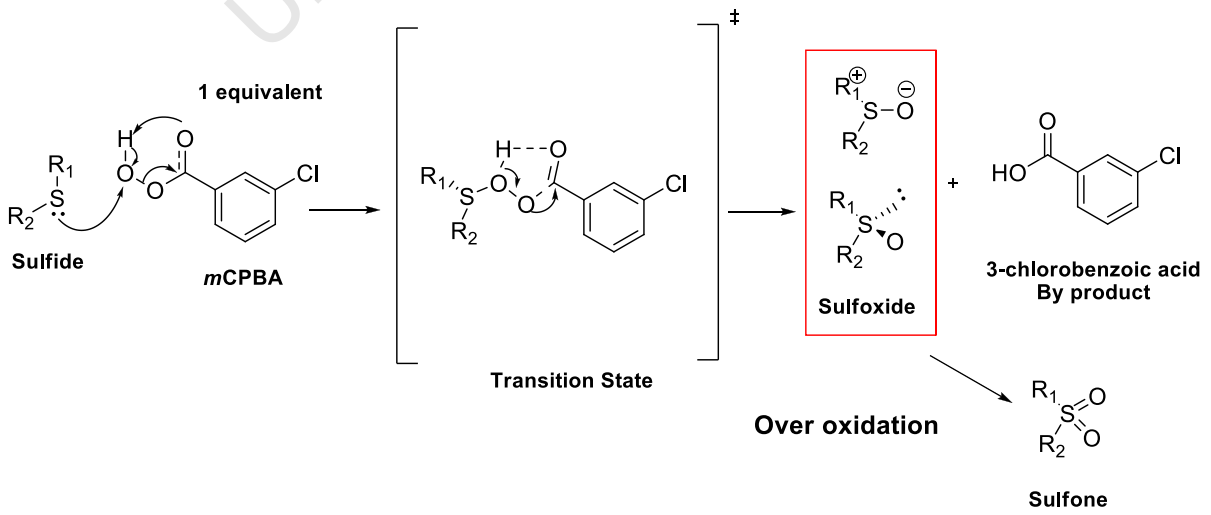

Scheme 3.10 Proposed mechanism of sulfoxidation using *m*CPBA as an oxidating agent.

University of Cape Town

The three dimensional lowest steric energy conformations (total energy 34.3722 Kcal/mol) of the *L*-hercynyl *N*-Boc-*L*-cysteine methyl ester **(19)** indicates the potential face selectivity toward sulfoxidation, that could lead to the S_R diastereoisomer sulfoxide derivative, even the proton NMR of hercynyl *L*-cysteine methyl ester **(26)** displayed some kind of diastereoselectivity (3:1 ratio), although the elucidation of crystal structure is still need to be established in the future that will determine the absolute configuration of the chiral sulfoxide (Figure 3.4).

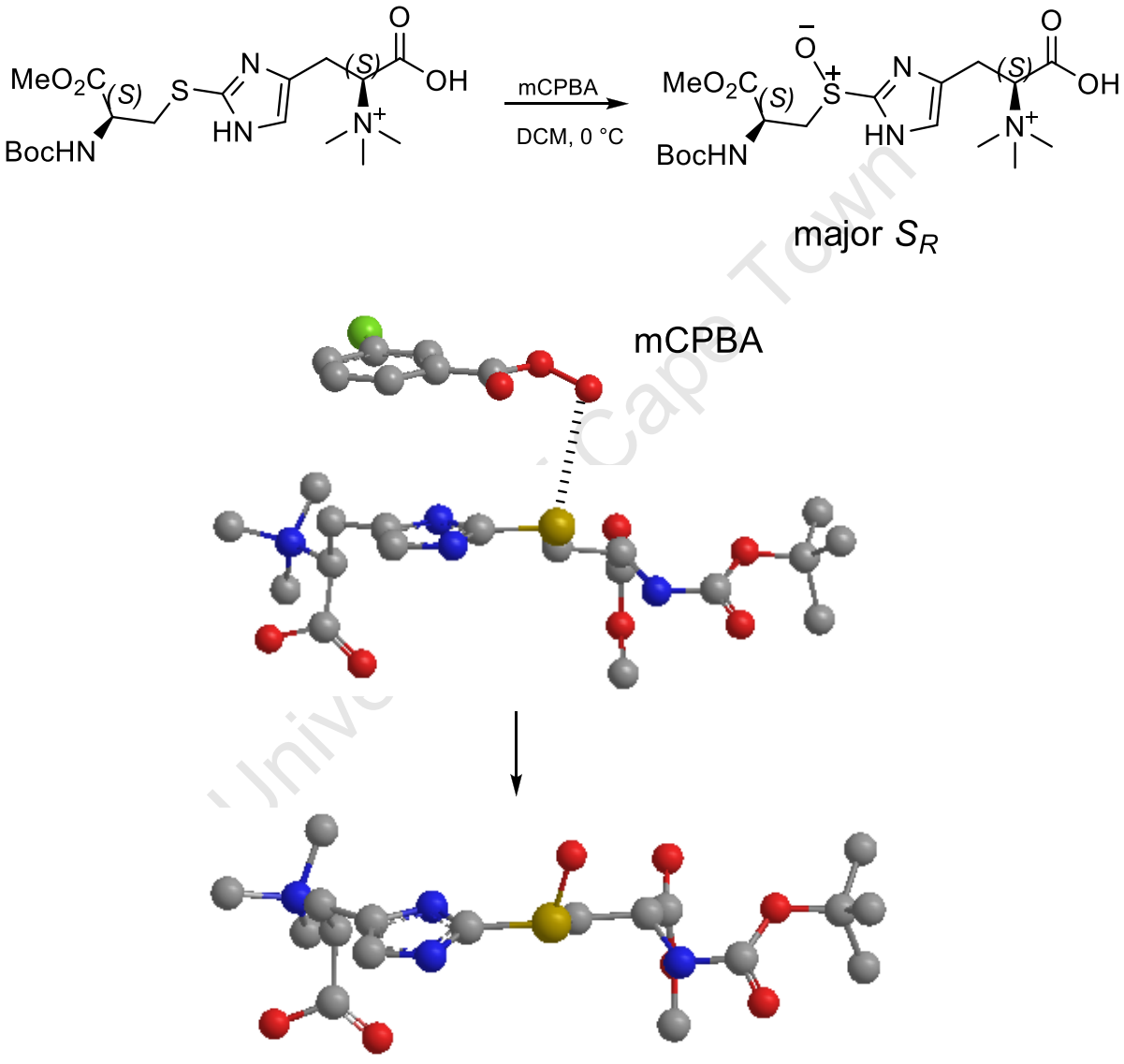

Figure 3.4 3D possible conformation of the sulfide **(19)** indicates potential face selectivity (3D ChemBioDraw Ultra 11.0, Total energy 34.3722 Kcal/mol, Dipole/Dipole 3.0912, Steric minimise energy)

The reaction was completed after 5 hours as monitored by TLC. The products (**23)** and (**24)** were isolated after reverse phase chromatography (C18) in good yield 96.3 % and 73.2% respectively (Scheme 3.11)

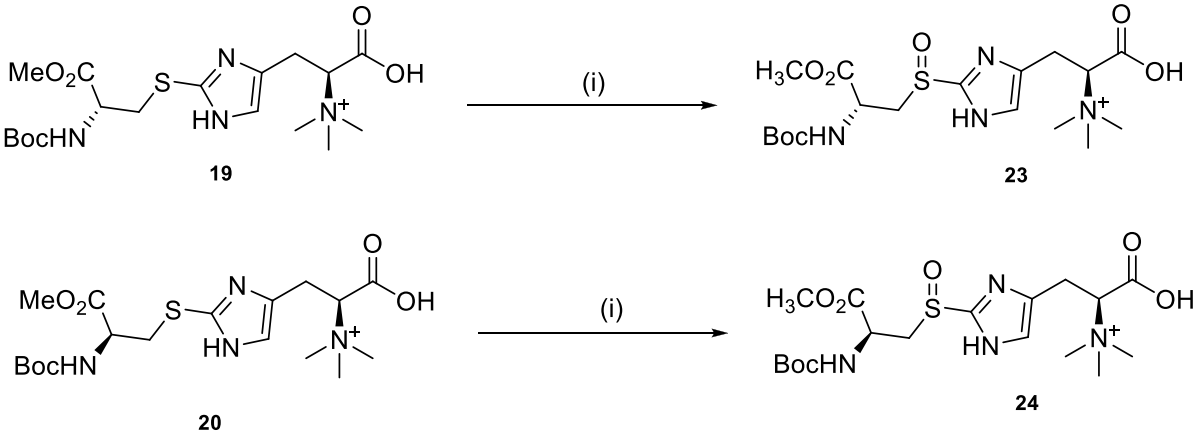

Scheme 3.11 Outlined Synthesis of 24-25. reagent and conditions (i) *m*CPBA, H_2O / DCM 1:1, 5 hr at 25°C, **24** (96.3%), **25** (73.2%).

The ^{1}H NMR spectrum of hercynyl *N*-Boc-*L*-cysteine methyl ester sulfoxide **(24)** displayed all the signals. Keys diagnostic signals were one aromatic proton which was slightly shifted up field, resonating as a singlet at δ_H 6.10 ppm, confirming the presence of the imidazole ring, two α- amino acid protons resonating as a broad singlet at δ_H 4.07 ppm and as a multiplet from δ_H 3.67 to 3.72 ppm respectively. The α-amino acid proton H-2" was shielded due to the close proximity of the methyl ester and secondary amine; a singlet resonated at δ_H 2.98 ppm integrating for 9 protons suggesting the presence of three equivalent methyl groups attached to a nitrogen atom and the Boc characteristic signal resonated at δ_H 1.49 ppm. The ^{1}H NMR spectrum of hercynyl *N*-Boc-*D*-cysteine methyl ester sulfoxide (**25)** was similar to that of hercynyl *N*-Boc-*L*-cysteine methyl ester sulfoxide (**24)** as expected.

The EI$^+$ mass spectrum did not reveal the molecular ion, but showed $[M+3H]^+$ at *m/z* 450.4 instead, which is probably due to the nitrogen hydrogen acceptor atoms, thus supporting the structure of hercynyl *N*-Boc-*L*-cysteine methyl ester sulfoxide **(24).**

3. 1. 8. Deprotection of hercynyl *N*-Boc-*L* and *D*-cysteine methyl ester sulfoxide.

With the hercynyl *N*-Boc-*L*-cysteine methyl ester sulfoxide (**23)** and hercynyl *N*-Boc-*D*-cysteine methyl ester sulfoxide (**24)** in our hand, the last challenge toward the synthesis of the target compounds was deprotection. Boc removal was successfully achieved in a mixture of DCM / H_2O with 1 ml of TFA. The products hercynyl *L*-cysteine methyl ester sulfoxide (**26)** and hercynyl *D*-cysteine methyl ester sulfoxide (**27)** was isolated in a good yield of 70.2 % and 73.2 % respectively after crystallization in a mixture of warm ethanol and distilled water. Subsequently methyl ester hydrolysis was attempted; unfortunately only the starting material

University of Cape Town

was recovered on all the amounts, even after several attempts using neutral base, or acid or conditions. The stability of amino acid methyl esters to hydrolysis is not new, previously it has been reported that the acid or base hydrolysis of its methyl ester is more often ineffective and only succeeded after resorting to enzyme mediate hydrolysis.[13, 14] *De la Rosa et al* unsuccessfully attempted to hydrolyze the methyl ester group of *S*-methyl *L*-*N*-Cbz-cysteine methyl ester sulfoxide. After using several reaction conditions, they were unable to isolate any identifiable reaction product.[14]

Amongst many authors *Bryan et al.*[15], *Yoshiaka et al.*[16] *and Wild et al.*[13] suggested the use of pig liver esterase (PLE), Lipase As Amano (LAS) or Porcine Pancreas Lipase (PPL) to enantioselectively cleave the methyl ester. *Sang-You et al*[17] suggested the immobilisation of the esterase in order to improve the activity and the recyclability of the enzyme. *Holland et al* [52] utilized substilisin calsberg enzyme instead, to hydrolyze enantioselectively the methyl ester group of *S*-methyl *N*-MOC methionine sulfoxide, the hydrolysis gave the acid and the unreacted ester product in moderate yield (41 %). In our case esterase from porcine liver was unsuccessful and the starting material was recovered unchanged.

The evidence of structure of hercynyl *L*-cysteine methyl ester sulfoxide (**26)** was furnished by spectroscopic techniques. Two dimensionsional NMR, HSBC and COSY (Figure 3.7) were utilized for a full structural assignment.

The ^{1}H NMR spectrum of hercynyl *L*-cysteine methyl ester sulfoxide **(26)** displayed the correct number of resonances as shown in the Figure 3.5. A key signal in the ^{1}H NMR spectrum of hercynyl *L*-cysteine methyl ester sulfoxide (**26)** was the disappearance of the Boc signal at δ_H 1.47 ppm, one aromatic proton resonating as a broad singlet at δ_H 7.38 ppm, confirming the presence of an imidazole ring. An upfield signal resonating as a singlet at δ_H 3.05 ppm integrating for 9 protons showed clearly the presence of the quaternary amine (three equivalent methyl groups), a characteristic methyl ester signal resonating as a singlet at δ_H 3.86 ppm, two α-proton amino acid signals resonating as a doublet of doublets at δ_H 3.89 for H-2 and as a multiplet upfield signal resonating at δ_H 3.45 – 3.40 ppm for H-2" respectively. The diastereotopicity of the methylene protons due to the presence of the sulfoxide was clearly revealed as a ratio of 3:1 whereby H-1" resonated at δ_H 4.08 ppm for the major diastereoisomer and δ_H 4.02 ppm for the minor diastereoisomer.

University of Cape Town

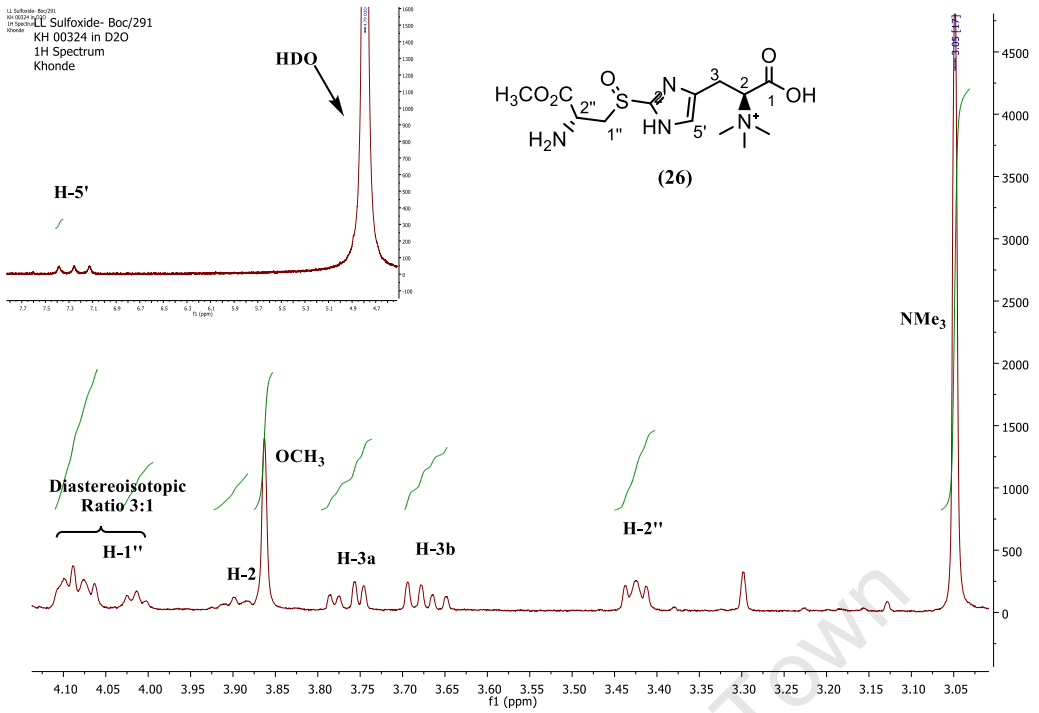

Figure 3.5 ^{1}H NMR spectrum of hercynyl *L*-cysteine methyl ester (**26)** in D_2O at 400 MHz,

The ^{13}C NMR spectrum of hercynyl *L*-cysteine methyl ester sulfoxide **(26)** displayed four carbonyl signals resonating at δ_C 162.6, 162.9, 163.3, and 163.6 ppm respectively confirming the presence of two carboxylic acid moieties and two enantiomers due to the sulfoxide chirality. Three aromatic signals resonating respectively at δ_C 120.9, 118.0, 115.1 ppm showing clearly the presence of an imidazole ring, also characteristically an α-amino acid carbon at δc 72.2 ppm for C-2 and 43.8 ppm for C-2" shielded due to the amino group (inductively withdrawing lesser than NMe_3^+ group) in its close proximity, four sets of aliphatic signals resonating at δc 66.0 ppm for methylene C-1" (major diastereoisomer), 62.9 ppm for methylene C-1" (minor diastereoisomer) showing clearly the diastereotopicity introduced by the vicinal sulfoxide; a characteristic methyl ester signal at δc 63.8 ppm and the trimethylamine signal at δc 43.4 ppm supporting the structure of hercynyl *L*-cysteine methyl ester sulfoxide **(26)** (Figure 3.6).

University of Cape Town

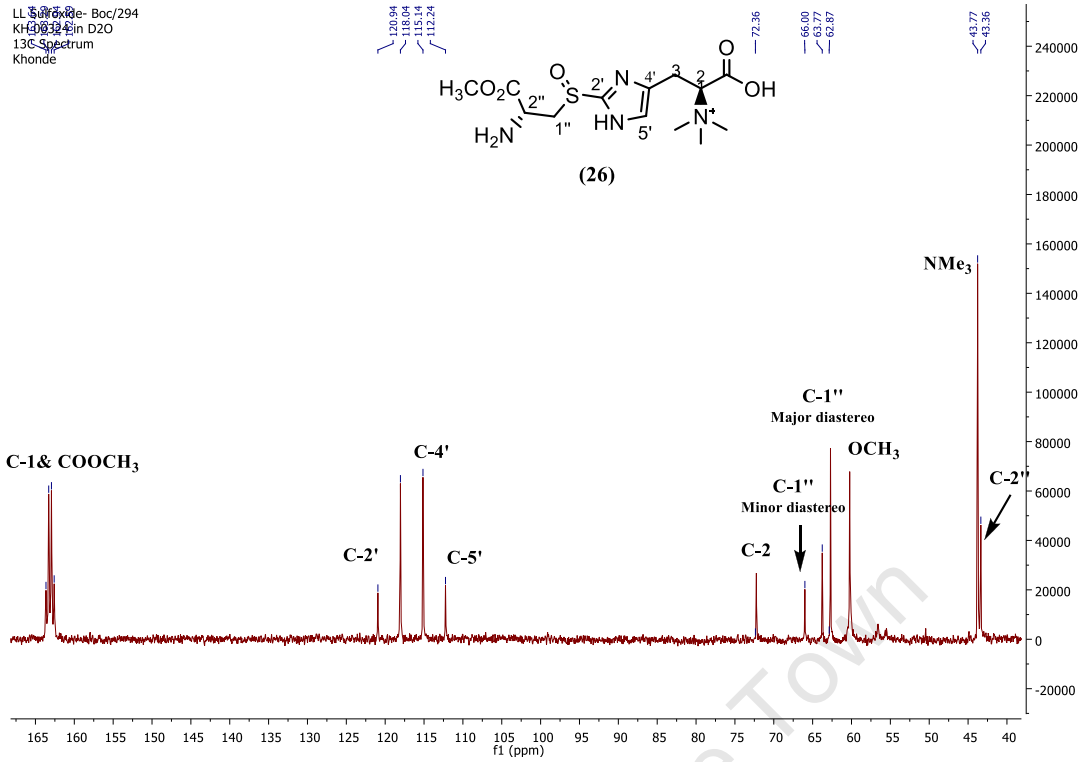

Figure 3.6 ^{13}C NMR spectrum of hercynyl *L*-cysteine methyl ester sulfoxide **(26)** in D_2O at 400 MHz.

The FTIR spectrum revealed a characteristic strong absorption band at 3409 cm^{-1} corresponding to the free amine, which supported Boc deprotection, while a diagnostic strong absorption band at 1142 cm^{-1} (S=O stretch bond) for the sulfoxide, suggested that the sulfur oxidation has successfully occurred.[18]

The optical rotation of hercynyl *L*-cysteine methyl ester sulfoxide (**26)** was $[\alpha]^{20}_D$ = -30.26° (*c* = 0.39, H_2O). Finally, a correct HRMS evaluation (ESI^+) (*m/z* 348.1465 $[M+H]^+$) corresponding to $C_{13}H_{24}N_4O_5S^+$ (*m/z* 348.1462 $[M+H]^+$) supported the structure of hercynyl *L*-cysteine methyl ester sulfoxide (**26).**

University of Cape Town

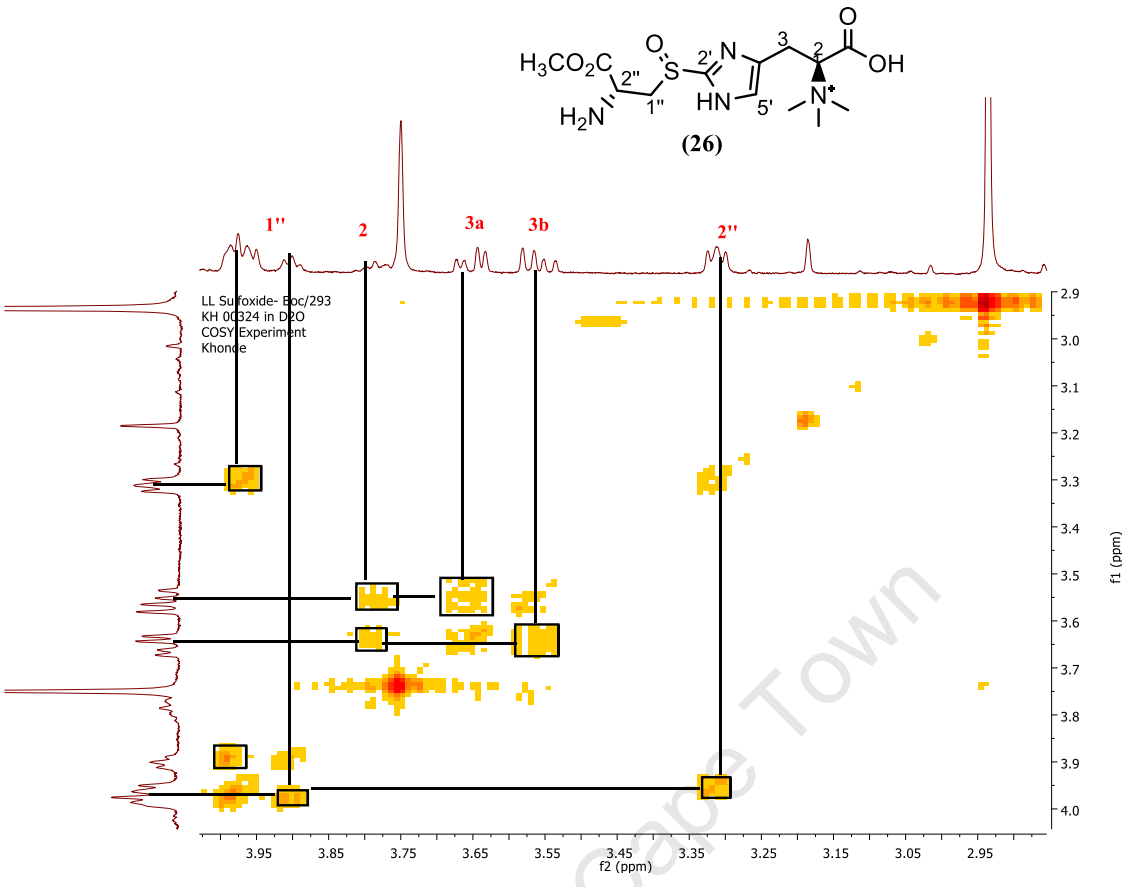

Figure 3.7 ^{1}H - ^{1}H COSY NMR spectrum of hercynyl *L*-cysteine methyl ester sulfoxide **(26)** in D_2O at 400 MHz.

The unsuccessful methyl ester hydrolysis to afford the EgtE substrate has led us to investigate an alternative synthetic route. The methyl ester has been used as a carboxylic protecting group, thinking that it could easily be deprotected in the final compound under aqueous basic conditions. Unfortunately the methyl ester removal was unsuccessful after trying: a) basic conditions using LiOH in THF/MeOH/H_2O gradually increasing the temperature from room temperature to 50°C, many reactions conditions were investigated including changing solvent and bases, but without success; b) acidic conditions using 6 N HCl refluxing for more than 24 hours and c) a porcine liver esterase enzyme at room temperature in a phosphate buffer (pH 7-8) was considered, but also without success[13] (Scheme 3.12). It has been reported that methyl esters of amino acids and polypeptides in some instances are difficult to remove.[13, 15]

University of Cape Town

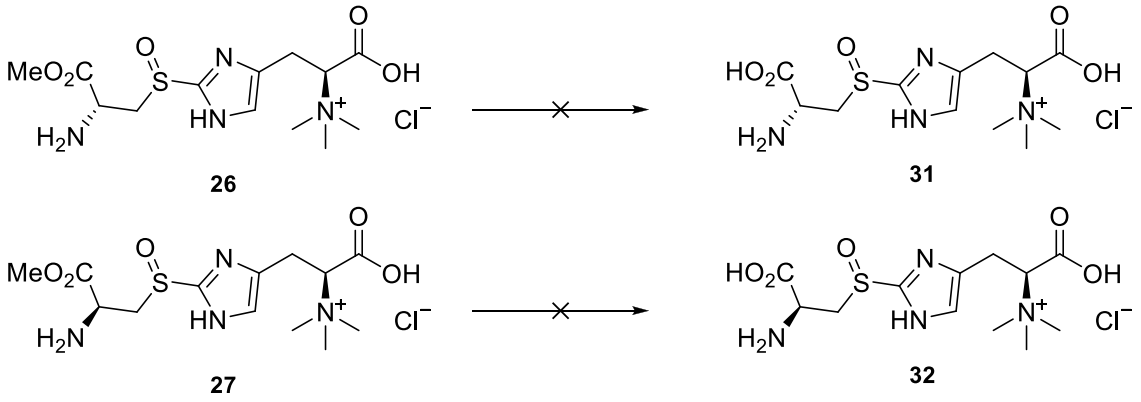

Scheme 3.12 method 1. LiOH/THF/MeOH/H_2O rt to 50°C 24 h; **method 2.** 6 N HCl reflux 24 h; **method 3.** H_2O reflux 48 h; **method 4.** esterase from porcine liver, pH 7-8 at rt 24 h.

The need for an alternative protecting group has led us to consider the preparation of an allyl ester which can be removed under neutral conditions using either $Pd(PPh_3)_3$ or $Rh(PPh_3)_3$ mediated homogenous catalysis.

3. 1. 9. Synthesis of *N*-Boc-*β*-chloro-*L*-alanine allyl ester (14).

Once again due to budgetary constraints and the need for gram quantities of the *N*-Boc protected *β*-chloro-*L*-alanine allyl ester **(14)**, a multigram-scale synthesis of the commercially available *N*-Boc protected *L*-serine allyl ester **(11)** was undertaken. The synthesis involved a two step reaction in one pot as described by *Navickas et al.*[19]

The cesium carbonate salt of *N*-Boc-*L*-serine was prepared, followed by the addition of one equivalent of allyl bromide using DMF as a solvent (Scheme 3.13). The *N*-Boc protected *L*-serine allyl ester **(11)** was isolated in 60 % overall yield after aqueous work up and silica gel flash column chromatographic purification.

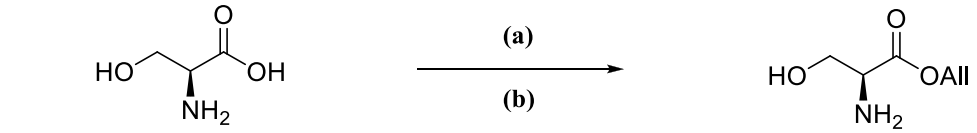

Commercially available *L*-serine

11

Scheme 3.13 Synthesis of (11), reagent and conditions: a) Cs_2CO_3 / MeOH; b) DMF / allylbromide 20 h at rt (60 % over 2 steps).

In the ^{1}H NMR spectrum of the *N*-Boc protected *L*-serine allyl ester **(11)** the downfield methylene signal resonated as doublet of quartets at δ_H 5.22 ppm, the vinyl proton resonated as multiplet from δ_H 5.91 to 5.76 ppm and the allylic signal resonated as a multiplet from δ_H

University of Cape Town

4.46 to 4.34 ppm, characteristic of an allyl ester. All other signals in the proton NMR were in full agreement with that which was reported by *J. Alsina et al.*[20]

The same chlorination procedure as described above was applied to *N*-Boc-*L*-serine allyester (**11)** synthesized previously. The compound *N*-Boc-*β*-chloro-*L*-alanine allyl ester (**14)** was isolated after flash silica gel column chromatography as yellow oil in very good yield of 88.5% (Scheme 3.14).

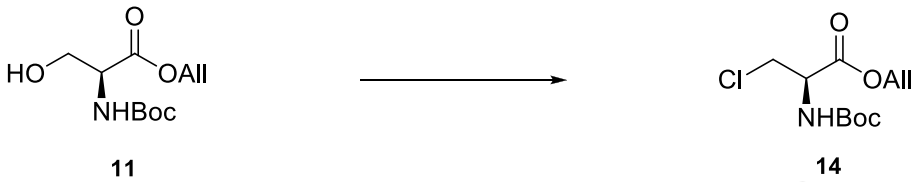

Scheme 3.14 Synthesis of (11), reagent and conditions**:** TCT / DMF in CH_2Cl_2 10 h at rt (88.5 %).

The compound was fully characterized as we couldn't find any data from the literature for direct comparison. The proton NMR as well as ^{13}C NMR displayed the right amount of signals but didn't show much difference with its alcohol **(11)** as expected, although all chemical shifts measured in the same deuterated solvent ($CDCl_3$) were slightly shifted compare to its alcohol which implies different compound.

The evidence of the chlorination was furnished by EI^+ mass spectrum, although the molecular ion wasn't shown, the mass corresponding to the loss of Boc, very labile group toward low mass spec technique, was shown in a high abundance of 30 % at *m/z* 160.1 $[MCl^{35}\text{-Boc - H}]^+$, *m/z* 162.1 ($[MCl^{37}\text{-Boc - H}]^+$, 10 %) and the base peak at *m/z* 133.0 fragment corresponding to the lost of subsequently Boc and an ethyl group characteristic of fragmentation of α-amino acid (scheme 3.15), as shown by *Schmidt et al* [36] in their work on a mass spectrum of conjugated amino acid, they proved that most α-amino acids could easily lose the carboxylic acid moiety, ethyl group, isopropyl group in their EI positive mass spectrum depending on the structure of the amino acid parent.

In addition TLC revealed a new less polar spot at R_f 0.75 (hexane/EtOAc 2: 1) compared to *N*-Boc-*L*-alanine allyl ester **(11)** at R_f 0.25 (hexane/EtOAc 2: 1), as expected, due to the substitution of an OH by a less polar chloro group. The FTIR infrared spectrum couldn't give us any useful information as the C-Cl absorption band interfered with the chloroform signal used as solvent.

University of Cape Town

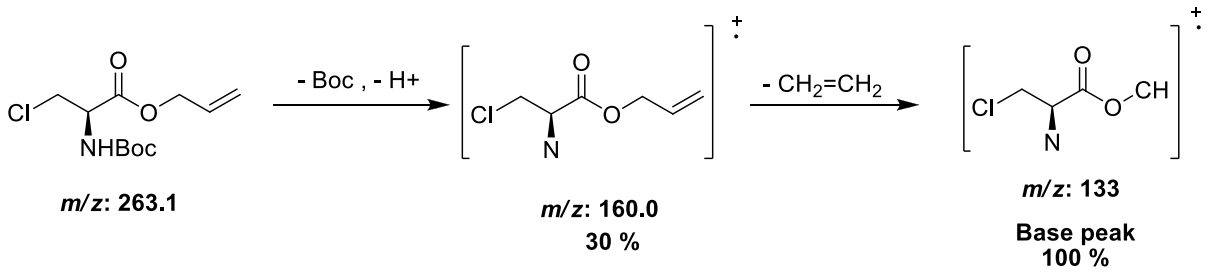

Scheme 3.15 Proposed fragmentation of *N*-Boc-*β*-chloro-*L*-alanine allyl ester **(14)** observed in the EI^+ mass spectrum

3. 1. 10. Deprotection of the allyl compounds.

The mechanism of allyl deprotection using $RhCl(PPh_3)_3$ (Wilkinson's catalyst) as homogenous catalyst is still not well known to date.

Based on the earlier proposed mechanism by *Lim et al* [21] and *Sato et al*,[22] the deprotection could proceed through catalytic cycle as shown in Figure 3.8. Subsequent $RhCl(PPh_3)_3$ (16 es) activation to the reactive form of the catalyst $RhCl(PPh_3)_2$ (14 es), the determinant interaction required for the catalytic process could be the coordinative interaction between the oxygen of the ally ester with the Rhodium of the catalyst (**iii** and **iv**), the last step could be the cleavage of the intermediate **(iv)** to carboxylic acid (**v)** (major product), volatile alkane (**vi)** and $RhCl(PPh_3)_3$ used again in the cycle.

The catalytic activation could proceed using heat, micro wave or ultra violet light, in our project the reaction mixture in EtOH / H_2O (80:20) was refluxed at 90 °C, reaction conditions reported recently by *Navickas et al*.[19]

University of Cape Town

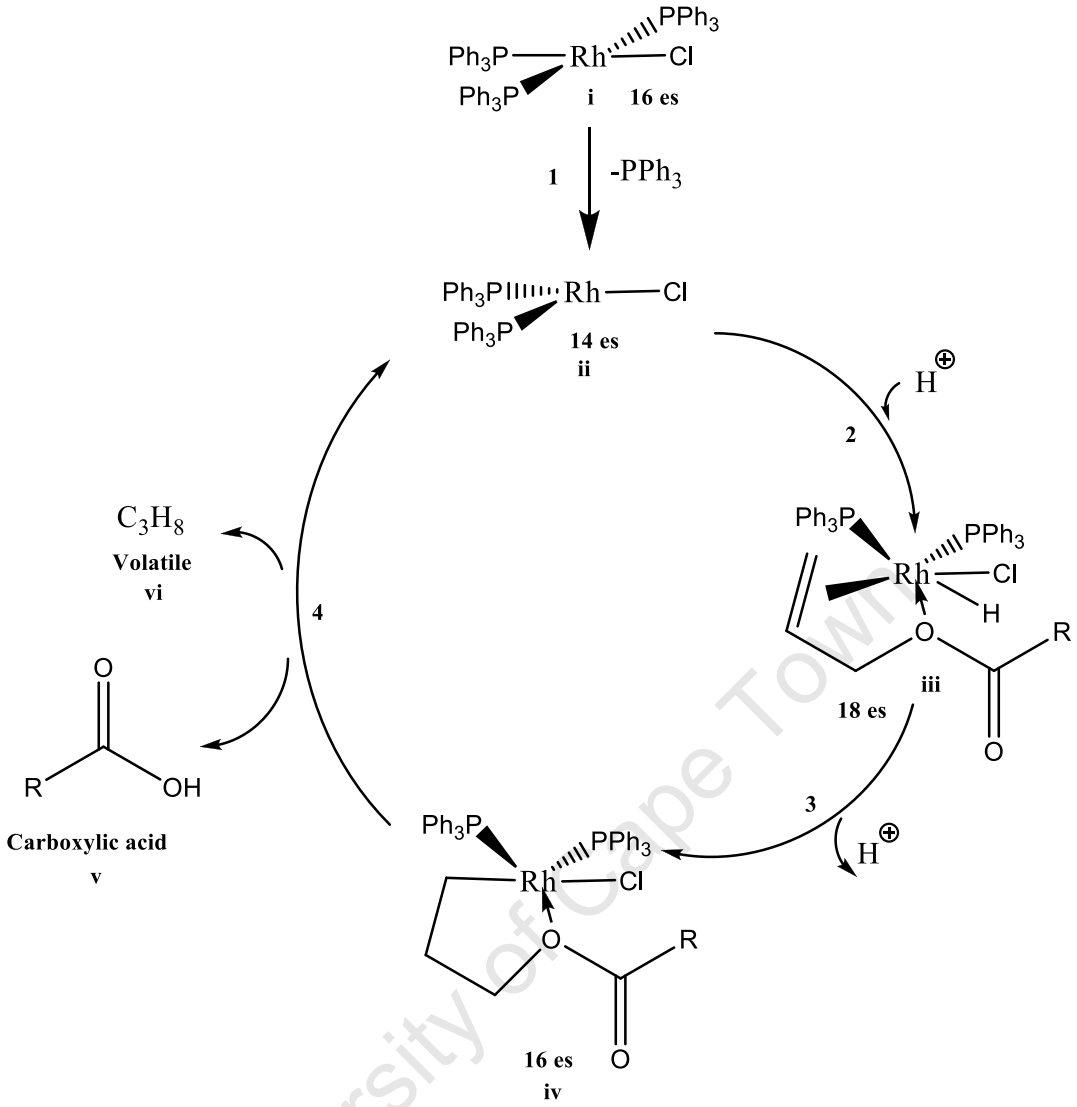

Figure 3.8 Proposed mechanism of allyl deprotection using $Rh(PPh_3)_3Cl$ as catalyst. [21, 22]

University of Cape Town

3.2 Biomimetic synthesis of EgtE, *R/S*-(*β*-amino-*β*-carboxyethyl) ergothioneine sulfoxide.

3. 2. 1. Retrosynthetic analysis (Method 2)

In this approach, the proposed retrosynthesis consider a biomimetically inspired cleavage on the right hand side of the sulfur atom of the substrate resulting in retrosynthons, 2-bromo hercynine and cysteine (Figure 3.10).

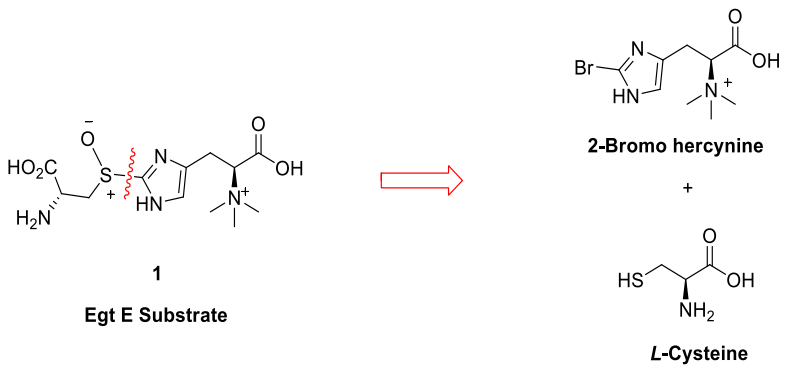

Figure 3.10. Retrosynthesis of EgtE**.**

A synthetic method originally inspired by *Ito et al.*[23] in 1985 was recently revised, reporting a protecting group-free green synthesis of ergothioneine using fewer steps.[24] Intriguingly, the reactivity of the histidine imidazole ring was utilized to synthesize (one pot) the thioether **(28)** in a moderate yield of 58 % (Scheme 3.16).

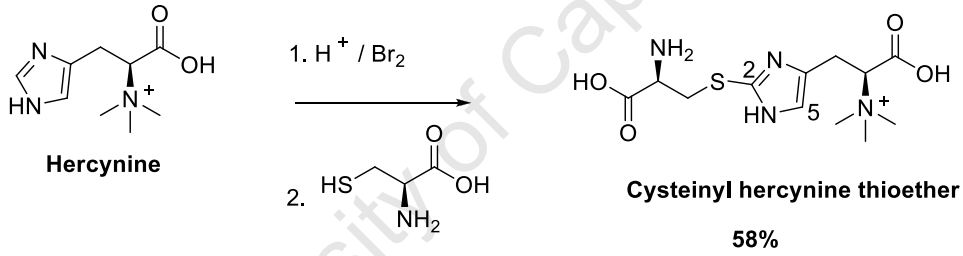

Scheme 3.16 Cysteinyl hercynine synthesis.[24]

This approach is attractive because it was a biomimetic synthesis and the EgtE substrate could also be synthesized from hercynine as precursor.[1] The EgtE substrate precursor was synthesized in fewer steps compared to the natural pathway.

The synthesis of hercynine was then embarked upon for multiple reasons. This synthetic approach will provide us a short, cheap, protecting group free synthesis in water (green chemistry) of the hercynyl cysteine thioether, hercynyl cysteine sulfoxide (EgtE enzyme substrate) and *L*-ergothioneine in fewer steps.

Hercynine (EgtB enzyme substrate) was the first intermediate toward EgtE enzyme substrate synthesis, even though commercially available the need of multi gram quantity which was beyond our budget has led us to it synthesis. In order to improve the *L*-hercynine synthesis two alternative routes were also investigated.

University of Cape Town

3. 2. 2. Synthesis of *L*-hercynine

The synthesis of *L*-hercynine was inspired by method developed by *Ishikawa et al.* [25] with some few modifications such as reductive amination and was performed under milder reaction conditions (Scheme 3.17). Methyl ester histidine **(1)** was preferred as starting material to *N*-benzyl histidine which needed to be deprotected under catalytic hydrogenation (Pd/C) conditions.

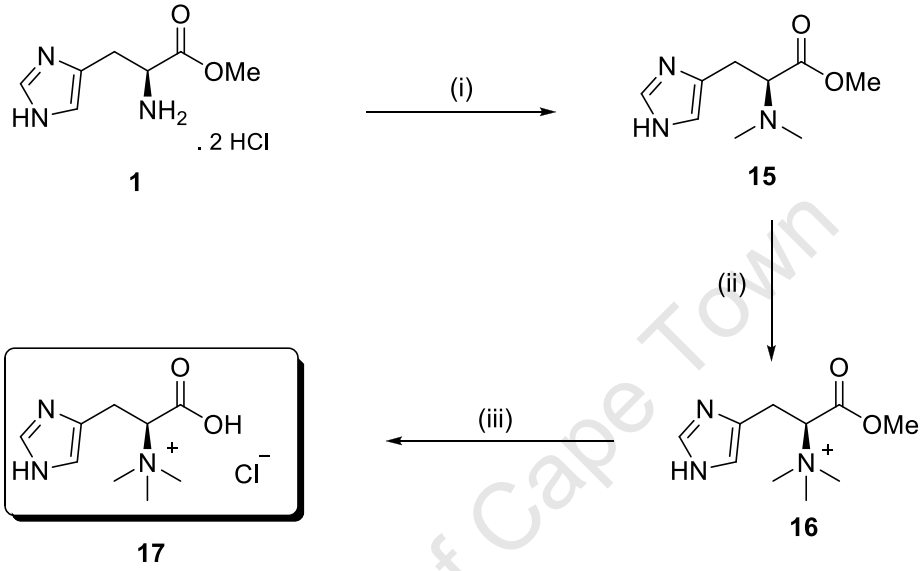

Scheme 3.17 Synthesis of *L*-hercynine (17), reagent and conditions: (i) CH_2O, $NaBH(OAc)_3$ / CH_3OH 24 h at rt (83.6 %); (ii) CH_3I / THF overnight at rt (37 %); (iii) 6 N HCl reflux 16 -20 h (60 %).

The synthesis of *L*-hercynine was initiated with the reductive amination of commercially available *L*-histidine methyl ester dihydrochloride **(1)** using 3.5 equivalents of formaldehyde (37 %) and 2 equivalents of sodium triacetoxyborohydride in THF. The resulting *N*,*N*-dimethyl *L*-histidine methyl ester (**15)** was isolated in a good yield (84 %) after aqueous work up and purification by silica gel chromatography.

The ^{1}H NMR spectrum of *N*,*N*-dimethyl *L*-histidine methyl ester (**15)** revealed the appearance of a downfield singlet, resonating at δ_H 2.39 ppm and integrating for 6 protons, thus proving that the *N*,*N*-dimethylation was successful. Another key diagnostic signal was the α-proton which resonated as a triplet that was shifted slightly up field at δ_H 3.73 ppm as result of the shielding effect of $-N(CH_3)_2$ in close proximity and characteristic methyl ester signal resonated as a singlet at δ_H 3.69 ppm. Two aromatic signals resonated as singlet respectively at δ_H 6.90 for H-5', δ_H 7.85 ppm for H-2' and a NH resonance as a broad singlet at δ_H 6.99 ppm confirming the presence of the imidazole moiety (Figure 3.9).

University of Cape Town

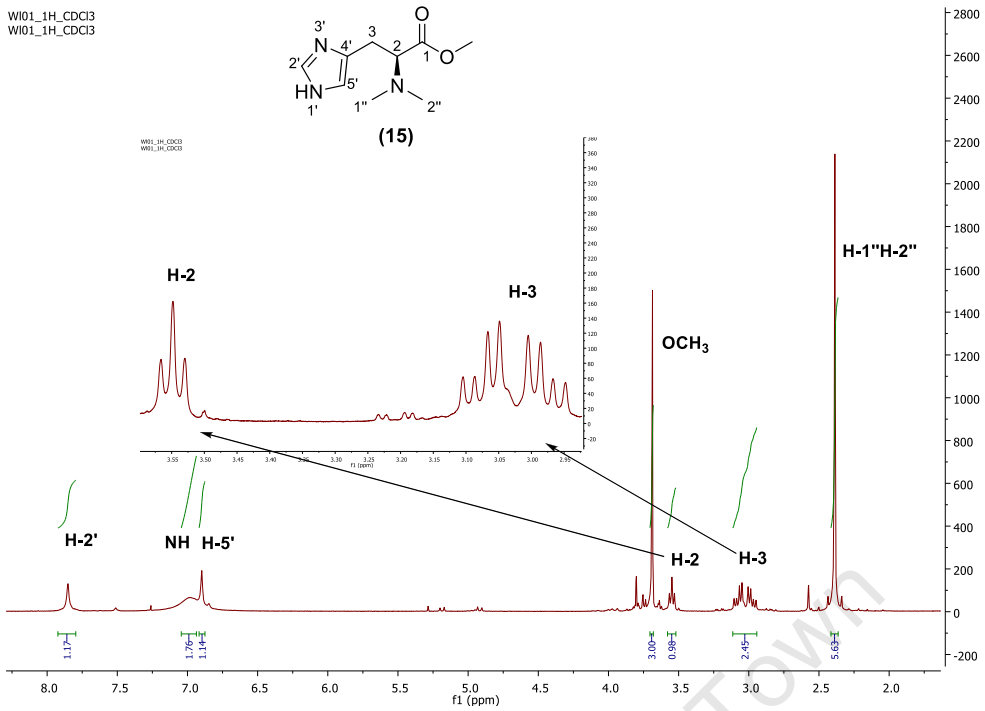

Figure 3.9 ^{1}H NMR spectrum of *N*,*N*-dimethyl *L*-histidine methyl ester **(15)** in $CDCl_3$ at 400 MHz

The ^{13}C NMR spectrum of *N*,*N*-dimethyl *L*-histidine methyl ester (**15)** revealed the characteristic downfield carbon signal resonating at δ_C 41.6 ppm, assigned to the *N*,*N*-dimethyl group displaying the required number of ^{13}C resonances, thus confirming the carbon skeleton of the *N*,*N*-dimethyl *L*-histidine methyl ester (**15).**

Quaternarization of *N*,*N*-dimethyl *L*-histidine methyl ester (**15)** was accomplished using 1.5 molar equivalents of methyl iodide in methanol at room temperature. TLC indicated the formation of the product after 24 hours. The *L*-hercynine methyl ester (**16)** was isolated in 37.2 % yield after crystallization from a mixture of warm methanol and diethyl ether. The ^{1}H NMR spectrum of *L*-hercynine methyl ester (**16)** revealed a characteristic downfield singlet resonating at δ_H 3.32 ppm and integrating for 9 protons. The signal belonging to the NMe_3 in the ^{13}C NMR spectrum of *L*-hercynine methyl ester (**16)** was overlapped by the DMSO-d_6 resonance from δ_C 40.6 to 39.4 ppm as indicated in the ^{13}C APT NMR. Finally the EI^+ mass spectrum displayed a molecular ion at *m/z* 213.0 $[M+H]^+$ calculated for $C_{10}H_{19}N_3O_2^+$: 212.1 supporting the assigned structure of *L*-hercynine methyl ester **(16).**

With *L*-hercynine methyl ester (**16)** in hand, the final step toward *L*-hercynine **(17)** was the hydrolysis of the methyl ester. At first attempt, normal basic hydrolysis was applied. However, the methyl ester hydrolysis was unsuccessful even though many different reaction conditions were investigated. The methoxide group is known to be a poor leaving group and

University of Cape Town

may also be influenced by the steric hindrance effect of the bulky -$N(CH_3)_3$ group which is making the carbonyl inaccessible to any nucleophilic attack.

Due to the failure of base mediated ester hydrolysis, acid hydrolysis was attempted. Successful deprotection of hercynine methyl ester (**16)** was accomplished by refluxing the starting material *L*-hercynine methyl ester (**16)** in excess of 6 N HCl to afford *L*-hercynine **(17)**, which was isolated in a moderate yield of 60 %. (Scheme 3.18)

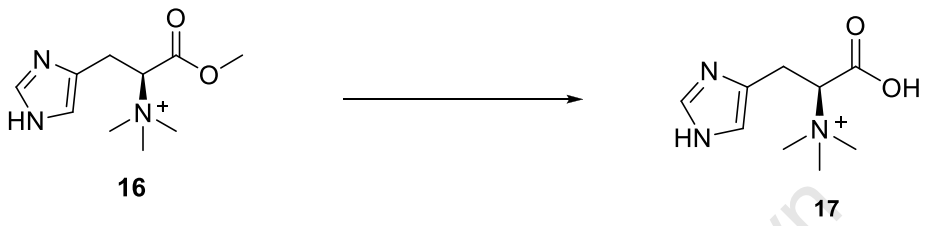

Scheme 3.18 Hydrolysis of *L*-hercynine methyl ester (16), reagent and conditions**:** 6 N HCl reflux overnight (60 %).

In the proton NMR spectrum of *L*-hercynine (**17)**, the absence of a methyl ester signal at δ_H 3.67 ppm in (**16)** indicated successful hydrolysis.

All ^{13}C NMR resonances were accounted for in the spectrum confirming the carbon skeleton of *L*-hercynine **(17).**

In addition the FTIR spectrum revealed a medium absorption band at 1632 cm^{-1} (C=O stretch) for carboxylic acid. The optical rotation was $[\alpha]^{20}_D$ = +48.7°(*c* = 0.9, 5N HCl) which was in accordance with that reported by *Reinhold et al* $[\alpha]^{20}_D$ = +44.5°(*c* = 1, 5N HCl).[25] Finally the EI^+ mass spectrum displayed the sodium adduct of *L*-hercynine **(17)** at *m/z* 223.6 which requires 223.11 for $C_9H_{18}N_3NaO_2^+$.

3. 2. 3. Alternative synthesis of *L*-hercynine.

Inspired by the method developed by *Fattori et al.*[26] hercynine was also synthesized in a one step reaction using exces of Me_2SO_4 (2.6 mol equivalents) as methylating agent under basic conditions (NaOH 10 %) (Scheme 3.19). The proton NMR displayed a reasonably pure product which was used in the next reaction without further purification.

University of Cape Town

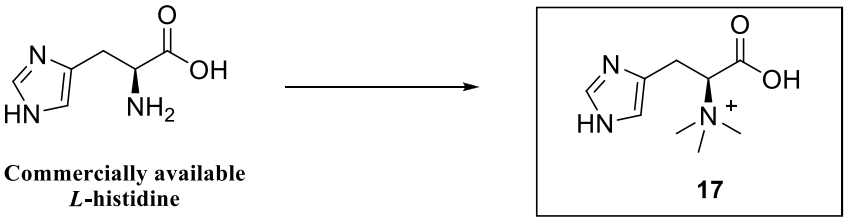

Scheme 3.19 One step Synthesis of *L*-hercynine (17), reagent and conditions: NaOH (10 %) / Me_2SO_4 (2.6 mol equivalents), 30 min at 0° C and 30 min at rt.[26]

3.2.4. Synthesis of *(R/S)*-hercynyl cysteine thioether.

With the *L*-hercynine in hand, our next challenge was to couple it to cysteine via the 2-bromo hercynine intermediate. This reaction required many attempts in order to improve the yield and purity. Only an excess of *L*-hercynine (3 to 5 equivalents) could afford the desired product, thus complicating the purification process. Similar observations were pointed out by *Erdelmeier et al* [27] that very recently published the new synthesis of *L*-ergothioneine.

3.2.4.1. Bromination of *L*-hercynine.

Bromination (aromatic electrophile substitution) at the C-5 position of the imidazole ring to form the reactive intermediate (bromo lactone), reacts with cysteine (nucleophile) to give the desired thioether driven by aromatization (Figure 3.10).[27]

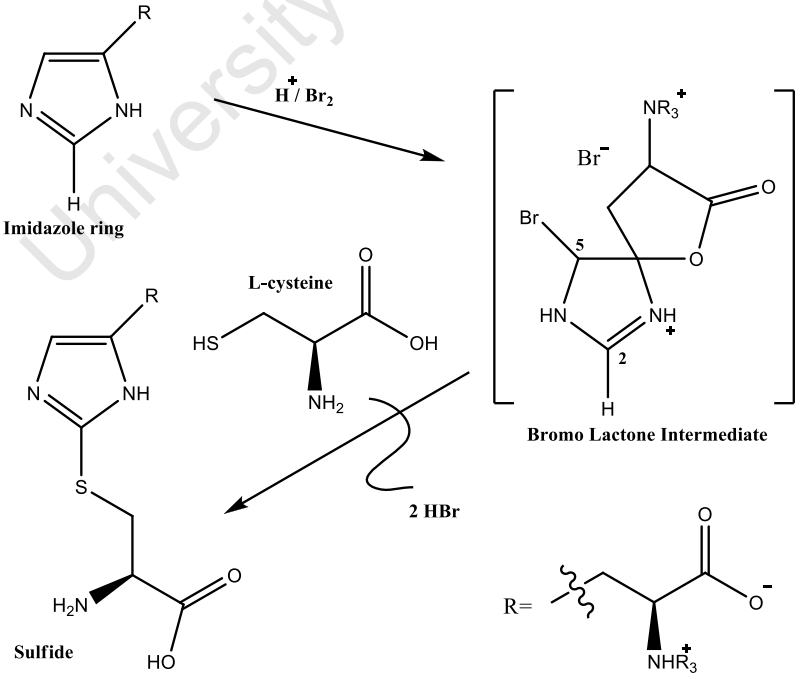

Figure 3.10 Proposed mechanism of synthesis of the hercynyl cysteine thioether.[27]

University of Cape Town

The author established the position of bromination on the basis of the proton NMR spectrum, which revealed only the H-2 resonance.[46]

The bromination was performed using a slight excess of bromine (1.3 molar equivalent) added drop wise in an ice water bath (0 - 5°C) for preventing the formation of much possible by products, noteworthy the labile bromo intermediate was not isolated even after several tentatives.[23, 27]

In order to prove that bromo lactone is indeed the reactive intermediate, *N* acetyl *L*-histidine and *L*-histidine methyl ester derivatives were treated with bromine respectively, followed by treatment with cysteine. Only the derivatives with the free carboxylic acid (*N*-acetyl *L*-histidine) led to a reasonable amount of the desired product. Thus, the free carboxylic acid is a prerequisite feature for this proposed mechanism.

3.2.4.2. Synthesis and characterisation of *(R/S)*-hercynyl cysteine thioether (28).

L-hercynine **(17)** was rapidly brominated using Br_2 in HCl at 0 °C. Five equivalents of *L*-cysteine was added after the formation of an orange yellow solid and the reaction mixture was allowed to stir for 1 h at 0 °C. TLC indicated the disappearance of hercynine after 90 min. The hercynyl cysteine thioether **(28)** was isolated as a yellow solid (47%) as the trihydrochloride hydrate salt after Dowex ion exchange chromatography, followed by reverse phase chromatography (C18).

The proton NMR spectrum of hercynyl *L*-cysteine thioether (**28**) displayed two characteristic signals for the α-amino acid protons, the first resonating at δ_H 4.53 ppm as doublet of doublets suggesting a coupling with the non-equivalent neighbouring methylene protons. The second characteristic signal resonated at δ_H 4.42 ppm as a triplet, suggesting a coupling with methylene protons, slightly deshielded as an effect exerted by the amino group of the neighbouring cysteine moiety (lesser electrowidrawing group than NMe_3^+). This was indicative that the coupling had successfully occurred. The characteristic three *N*-methyl resonances appeared between δ_H 3.31 and 3.16 ppm as a multiplet integrating for 9 protons. Surprisingly, the aromatic proton H-5' resonated as two signals integrating for one proton at δ_H 8.77 and 7.47 ppm. This is possibly due to the presence of two different tautomeric forms of the compound in the D_2O solution (Figure 3.11)

University of Cape Town

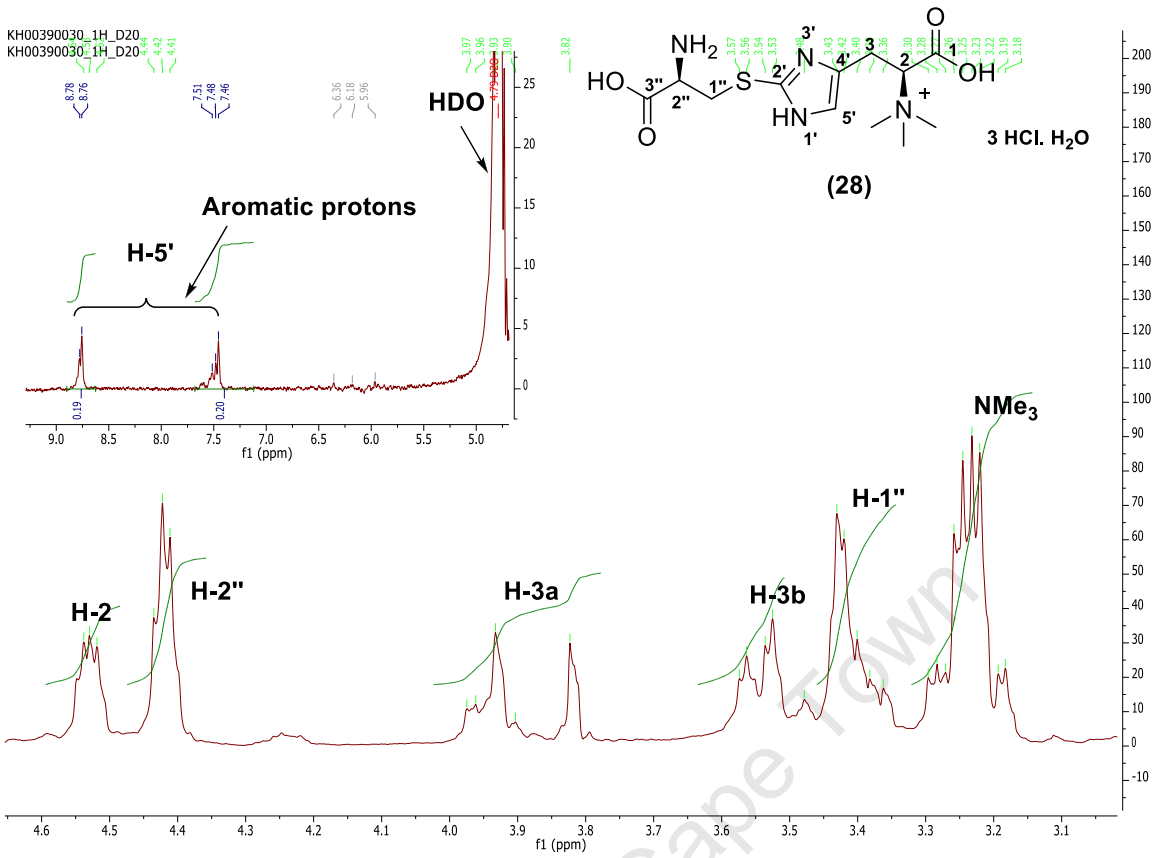

Figure 3.11 ^{1}H NMR of hercynyl cysteine thioether **(28)** in D_2O at 400 MHz

The ^{13}C NMR of hercynyl cysteine thioether **(28)** displayed the correct number of resonances supporting the carbon skeleton of the hercynyl cysteine thiother **(28)** and were strongly in agreement with the one reported by *Erdelmeier et al* [27](table 3.1)

University of Cape Town

Table 3.1. NMR Data of (28) in D_2O

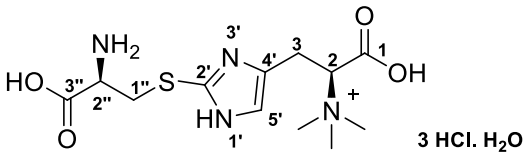

(28)

Positions	δ_H (*J* in Hz) 400 MHz, D_2O	δ_C (100 MHz, D_2O)
2	4.53 (dd, 7.6, 4.3, 1H)	67.7
3	4.02 – 3.88 (m, 1H) 3.55 (dt, 22.3, 7.6, 1H)	36.6
5'	8.77 (d, 7.6, 0.5H), 7.47 (d, 10.5, 0.5 H)	118.5
1"	3.41 (m, 2H)	24.0
2"	4.42 (t, 4.4, 1 H)	54.6
$N(CH_3)_3$	3.31 – 3.16 (m, 9H)	52.0 (3 C)
C-2'	-	134.6
C-4'	-	122.8
COOH	Exchange with D_2O	170.7 , 170.3

University of Cape Town

The melting point was 79 °C with decomposition, which agreed with that reported by *Erdelmeier et al* [41] (77 °C with decomposition).

Finally, a correct HRMS evaluation (ESI^+) (*m/z* 317.1277 $[M]^+$) corresponding to $C_{12}H_{21}N_4O_4S^+$ (*m/z* 317.1284 $[M]^+$) supported the structure of the hercynyl cysteine thioether (**28).**

3.2.4.3. A salt-free synthesis of *(R/S)*-hercynyl cysteine thioether (28)

It was difficult to separate the ammonium salts from the product during purification, which involved consecutively Dowex ion exchange and reverse phase (C18) chromatography.

Erdelmeier et al [27] utilized electrodialysis (ED) equipment for desalinisation. We did not have access to ED equipment and therefore it was useful to develop an alternative way of purifying the hercynyl cysteine intermediate.

A salt free synthesis of hercynyl cysteine thioether (**28)** was then investigated. The *in situ* protection of the amino group with Boc and the carboxylic groups as the benzyl esters gave a sufficiently hydrophobic product, ideal for organic extraction. Thus, after extraction and silica chromatography, the salt-free product was obtained.

The amino and the carboxylic acid groups of the crude hercynyl cysteine thioether (**28**) were protected in a one pot synthesis, affording the fully protected hercynyl *L*-cysteine thioether derivative (**29**) (Scheme 3.20).

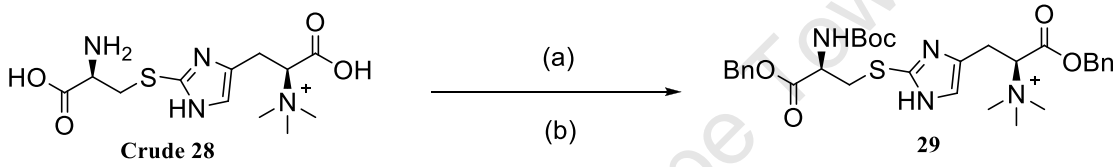

Scheme 3.20. One pot double protection of crude (28), reagent and conditions: a) Boc_2O / NaOH, H_2O / CH_3CN, rt overnight b) BnBr / DMF, rt overnight. 37.6 %.

Two dimensionnal NMR HSQC, COSY and ^{13}C-APT NMR were utilized for full structural assignment of hercynyl benzyl ester *N*-Boc-*L*-cysteine benzyl ester **(29).** The key resonance in the proton NMR of hercynyl benzyl ester *N*-Boc-*L*-cysteine benzyl ester **(29)** was a multiplet resonating from δ_H 8.63 to 8.24 ppm integrating for 10 protons due to the phenyl ester groups as well as the benzylic methylene protons resonating as a singlet at δ_H 4.72 for H-1", while H-1"" appeared at δ_H 4.44 ppm, clearly showing that the benzyl esterification had occurred successfully. The Boc signal resonated at δ_H 2.68 ppm due to the deshielding effect of the neighbouring benzyl ester, thus confirming that crude hercynyl cysteine thioether **(crude 28)** was indeed fully protected (table 3.2).

The ^{13}C NMR of hercynyl benzyl ester *N*-Boc-*L*-cysteine benzyl ester (**29)** displayed the right amount of resonances supporting its carbon skeleton.

University of Cape Town

Table 3.2. Characteristic NMR Data of (29) in DMSO-*d*$_6$

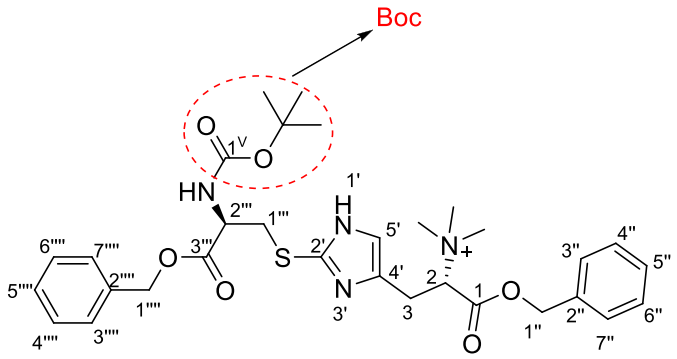

(29)

Positions	δ_H (400 MHz, DMSO-*d*$_6$)	δ_C (100 MHz, DMSO-*d*$_6$)
Boc	2.68 (s, 9H)	36.3 68.0 (C) 168.7 (C=O)
1"	4.72 (s, 2H)	70.4
1''''	4.44 (s, 2H)	69.5
2 X Phenyl	8.63 – 8.24 (m, 10H)	129.7, 129.1, 128.8, 128.5, 128.0, 127.8, 127.1, 126.9

University of Cape Town

Global deprotection of hercynyl benzyl ester *N*-Boc *L*-cysteine benzyl ester **(29)** was achieved by hydrogenation (Pd/C) in the presence of TFA under 50 psi pressure (Scheme 3.21).

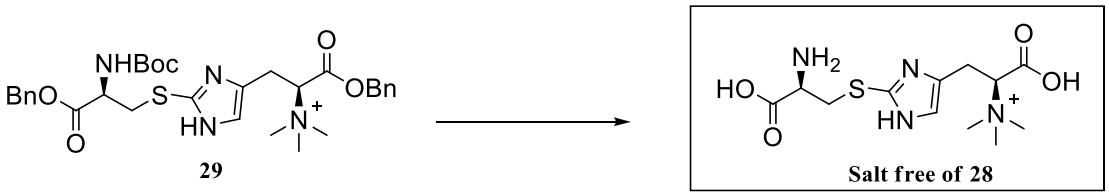

Scheme 3.21 Global deprotection of (29): (1-3 eq) TFA, H_2 Pd/C (50 psi), rt for 8-12 h.

The salt free hercynyl cysteine thioether **(28)** was fully characterized and the NMR data were strongly in agreement with that which was reported in the literature.[27]

3.2.5. Oxidation of hercynyl *L*-cysteine thioether (28) to *(R/S)*-(*β*-amino-*β*-carboxyethyl) ergothioneine sulfoxide (30), the EgtE substrate.

With the hercynyl *L*-cysteine thioether **(28)** in hand, our final challenge was to oxidize the thioether to the sulfoxide, the EgtE substrate. Despite the apparently simple transformation, the process chemistry proved to be very challenging. The oxidation reaction was complicated due to factors such aqueous solubility, choice of oxidant, reaction time and technique of reaction monitoring. The challenge was to find suitable oxidising conditions that would allow the synthesis of the sulfoxide without over oxidation to the sulfone.

Most reaction conditions previously investigated by *Ishikawa et al* [10] led to an over oxidation to the sulfone. However, literature [10] reports proposed the sulfoxide structure without any analytical evidence (Scheme 3.22). *Holland et al* [28] have utilized chloroperoxidase-hydrogen peroxide (CPO-catalyzed sulfoxidation) for the oxidation of sulfur to sulfoxide in a moderate to high diastereoisomeric excess, thus suggesting that the diastereoselective sulfoxidation is not a straightforward process.

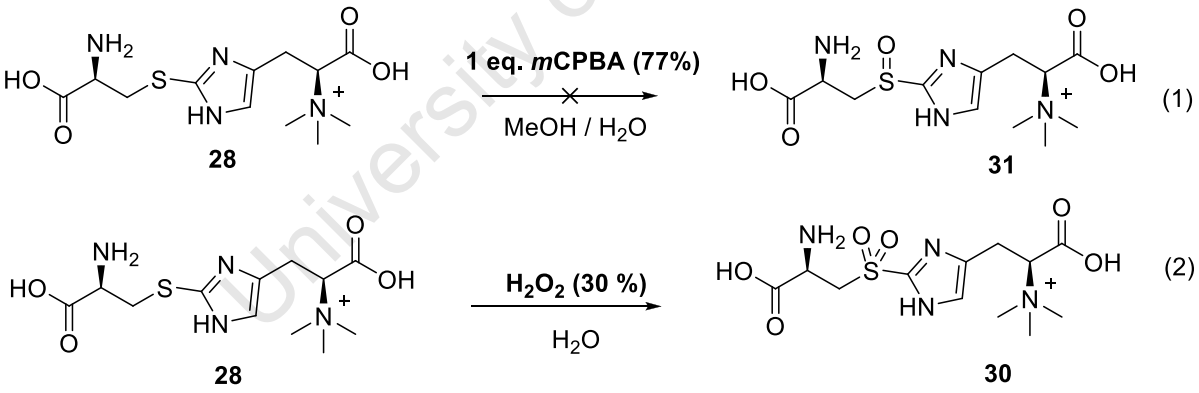

Scheme 3.22. Hercynyl *L*-cysteine thioether **(28)** sulfoxidation.

One equivalent of hercynyl *L*-cysteine thioether (**28)** was treated with slight excess of H_2O_2 (30 %) at room temperature for 4 hours. The hercynyl *L*-cysteine sulfone product (**30)** was isolated as white needles in quantitative yield of 93% after recrystallisation of the crude product in a mixture of warm EtOH/ H_2O.

The proton NMR spectrum, as expected, was similar to the hercynyl *L*-cysteine thioether (**28)** and displayed the correct number of protons resonances. The key diagnostic signal was the

University of Cape Town

methylene protons, H-1" which shifted downfield from δ_H 3.41 ppm in hercynyl *L*-cysteine thioether (**28)** to δ_H 3.80 ppm in hercynyl *L*-cysteine sulfone (**30)** due to the deshielding effect of the sulfone on its neighbouring protons.

A key diagnostic resonance in the ^{13}C NMR spectrum of hercynyl *L*-cysteine sulfone (**30)** was the C-1" signal, resonating at δ_C 21.2 ppm in hercynyl *L*-cysteine thioether **(28)**, shifting downfield to δ_C 49.0 ppm in hercynyl cysteine sulfone **(30)** due to the deshielding effect of the neighbouring sulfone (table 3.3).

Table 3.3. NMR Data of (30) in D_2O

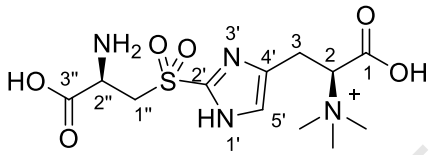

30

.

Positions	**δ_H (*J* in Hz) 400 MHz, D_2O**	**δ_C (100 MHz,D_2O)**
2	4.61 – 4.50 (m, 1H)	74.8
3	3.92 (m , 2H)	49.3
4'	-	136.0
5'	8.91 – 8.64 (m, 0.5H), 7.44 (dd, 27.3, 15.3, 0.5H) **Due to tautomers**	122.4
2'	-	137.5
1"	3.86 (dd, 11.3, 7.4, 1H) 3.75 (dd, 11.3, 7.4, 1H)	49.0
2"	3.34 (d, 7.4, 1H)	52.5
$N(CH_3)_3$	3.70 – 3.37 (m, 9H)	49.9 (3 C)
COOH	Exchange with D_2O	172.3, 169.8

University of Cape Town

In addition, the FTIR spectrum revealed a characteristic strong absorption band at 1204 cm^{-1} corresponding to the sulfone group, thus supported the over oxidation of the thioether **(28)** to the sulfone (**30)**.

Finally, the HRMS evaluation (ESI^+) (*m/z* 349.1182 $[M]^+$) corresponding to $C_{12}H_{21}N_4O_6S^+$ (*m/z* 349.1192 $[M]^+$) supported the structure of the hercynyl cysteine sulfone (**30).**

3. 3. Synthesis of deuterated ergothioneine and hercynine.

With one of the ergothioneine biosynthetic pathway enzyme substrates in our hand, our next challenge was to synthesize deuterated hercynine and ergothioneine. Since these compounds are commercially unavailable, their synthesis is of great value to ESH research.

LCMS was utilized as method to monitor the enzyme mediated conversion of the pathway substrates to ergothioneine. To this end, it was decided to synthesize deuterium labelled ergothioneine and hercynine as LCMS internal standards for quantitation. The stable deuterated isotopes are better internal standard as they display the same retention time and chromatographic characteristics compared to the natural isotope equivalent, thus making quantitation more accurate.

In addition, the deuterated hercynine was also used as an ergothioneine pathway enzyme substrate to follow the production of deuterated ergothioneine.

3. 3. 1. Synthesis of ergothioneine-d_3

The synthetic approach was inspired by the modified *Trampota* [29] method as described in chapter 2. Deuterated ergothioneine **(9)** was synthesized in two sequential reaction steps starting with the *S-t-butyl* protected 2-mercapto-histidine **(6),** derived from mercapto histidine **(5).** Selective *N*-methylation with methyl-d_3 iodide (for 24 hours), followed by *S-t-butyl* deprotection using 2-mercaptopropionic acid (*t-butyl* scavenger) in HCl gave product **(9)** which was isolated as a yellow solid after reverse phase (C18) chromatography. (Scheme 3.23).

University of Cape Town

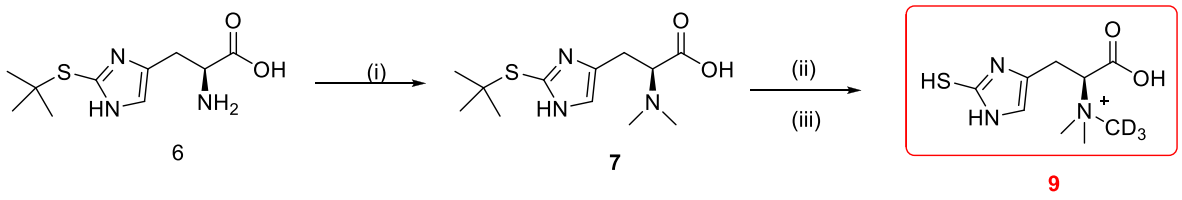

Scheme 2.23 Synthesis of (9).reagent and conditions: (i) Formalin, sodium triacetoxyborohydride / THF, 6-8 h at 10°C (33.7 %), (ii) NH_4OH, Cd_3I (methyl-d_3 iodide) / MeOH 24 h at rt; (iii) HCl, 2-mercaptoprionic acid refluxed for 21h (quantitative).

The proton NMR spectrum of ergothioneine-d_3 **(9)** displayed an aromatic proton at δ_H 6.95 ppm, a characteristic α-amino acid proton resonating as a multiplet from δ_H 4.34 to 4.13 ppm, while a multiplet signal from δ_H 3.73 to 3.43 ppm, integrating for 6 protons instead of 9, suggested the presence of a *N*,*N*-dimethyl group due to the introduction of the deuterated methyl group, and a methylene proton signal at δ_H 3.41 ppm resonating as a doublet of doublets (J = 11.3, 8.5 Hz) for H-3 (Figure 3.12).

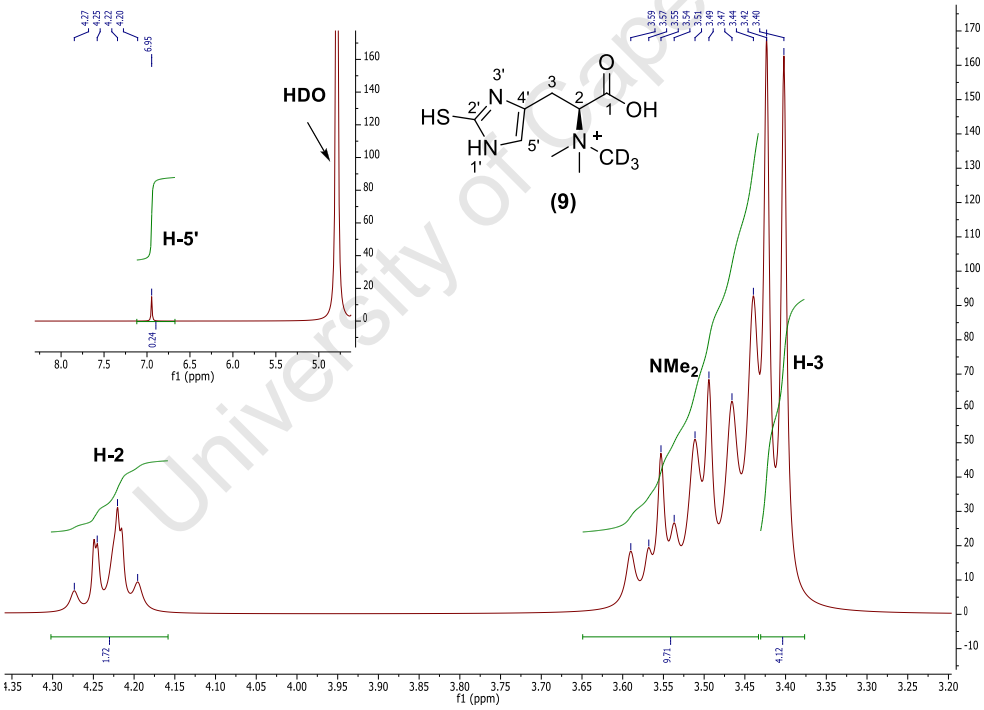

Figure 3.12 ^{1}HNMR of ergothioneine-d_3 **(9)** in D_2O at 400 MHz

The ^{13}C NMR spectrum of ergothioneine-d_3 **(9)** displayed a carbonyl signal at δ_C 180.34 ppm, three aromatic signals respectively at δ_C 134.9, 119.1 and 115.8 ppm for the imidazole ring; three aliphatic signals at δ_C 75.5 ppm for the α-carbon amino acid (C-2); a signal at 52.5 ppm integrating for two methyl groups due to NMe_2; and 22.7 ppm for C-3 confirming the carbon skeleton of ergothioneine-d_3 (**9**).

University of Cape Town

The HRMS evaluation (ESI$^+$) (*m/z* 233.1161 [M$^+$]) corresponding to $C_9H_{13}D_3N_3O_2S^+$ (*m/z* 233.1152 [M$^+$]) supported the structure of ergothioneine-d_3 **(9)** (Figure 3.13).

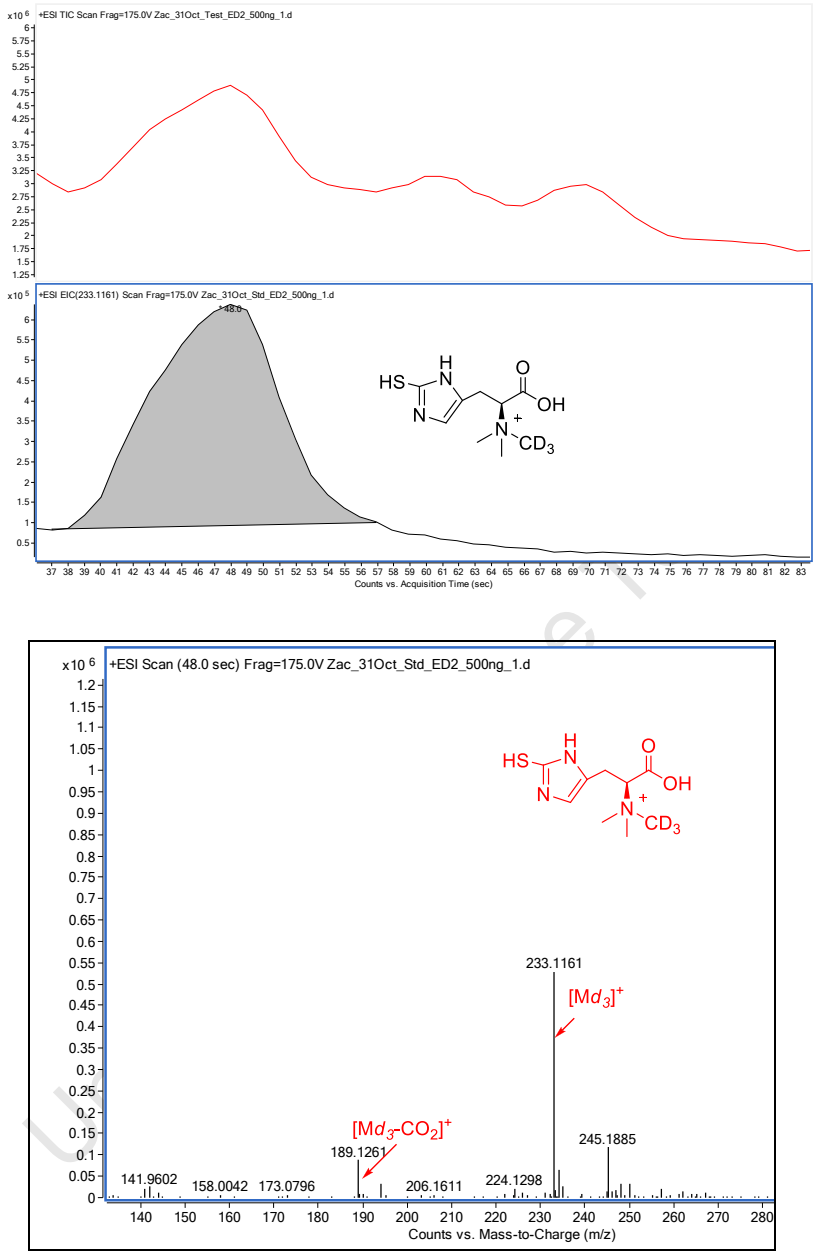

Figure 3.13 TIC extracted (top) and ESI HRMS spectrum (bottom) of ergothioneine-d_3 **(9).**

3. 3. 2. Synthesis of hercynine-d_3.

Deuterated hercynine (**18**) was synthesized in a two step reaction starting with the commercially available *L*-histidine. The first step involved reductive amination using aqueous formaldehyde (37%) and sodium triacetoxyborohydride. The second step involved the quaternaryzation of the crude *N*,*N*-dimethyl histidine using methyl-d_3 iodide under basic conditions (pH 9-10). The product (**18**) was isolated as a yellow solid in a moderate yield of

61 % after reverse phase chromatography (C18) and recrystallization from a mixture of warm EtOH/ H_2O.

The proton NMR spectrum of hercynine-d_3 (**18)** displayed two aromatic signals respectively at δ_C 8.70 ppm for H-2' and 7.45 ppm for H-5', three aliphatic resonances respectively at δ_H 4.44 ppm as a doublet (J = 7.7 Hz) for H-2, and two overlapped protons signals resonating as a multiplet from δ_H 3.74 to 3.30 ppm integrating for 8 protons due to NMe_2 and H-3.

The HRMS evaluation (ESI^+) (*m/z* 201.1414 [M^+]) corresponding to $C_9H_{13}D_3N_3O_2^+$ (*m/z* 201.1431 [M^+]) supported the structure of hercynine-d_3 **(18)** (Figure 3.14).

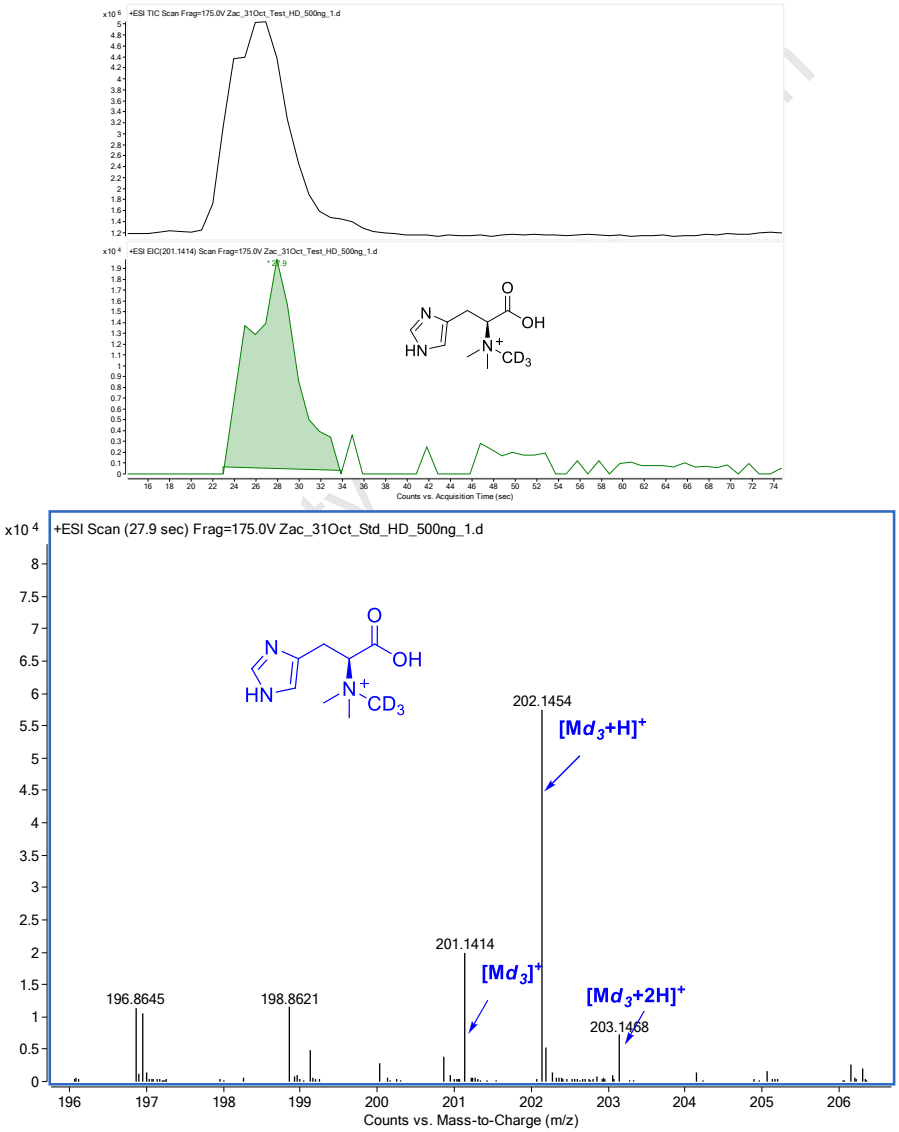

Figure 3.14 TIC extracted (top) and ESI HRMS spectrum (bottom) of hercynine-d_3 **(9)**

3.4. References

1. Seebeck, F.P., *J. Am. Chem. Soc*., **2010**, 132, 6632.
2. Mc Killop, A.; Taylor, R. J.K.; Watson R.J.; Lewis, N., *Synthesis*, **199**4, 31.
3. Isidro-llobet, A.; Alvares, M. and Albericio, F., *Chem. Rev.*, **2009**; 109, 2455.
4. Yasuda, M.; Onishi, Y.; Ueba, M.; Miyai, T. and Baba, A., *J. Org. Chem.*, **2001**, 66, 7741
5. Hengchng, M.; Zhikang, B.; Lianhua B. and Wei C., *Inter. J. Org. Chem*., **2012**, 2, 21.
6. Lidia, D. L.; Giampaolo, G. and Porcheddu A., *Org. Lett.*, **2002**, 4, 553.
7. Bregant, S.; and Tabor, A. B.; *J.Org. Chem*., **2005**, 70, 2430.
8. Kenworthy, M.N.; Kilburn, J.P.; Taylor R.J.K., *Org. Lett.*, **2004**, 6, 19.
9. Tao, F.; luo, Y.; Huang, Q.; Liu, Y.; Li, B.; Zhang, G.; *Amino acids* , **2009**, 37,603.
10. Ishikawa, Y.; Israel, S.E. and Melville, D.B., *J. Biol. Chem.*, **1974**, 279, 4420.
11. Clayden, J.; Greeves, N.; Warren, S.; Wother, P., *Organic Chemistry*, **2001**, Oxford University Press, Oxford, ISBN 9780-0-19-850346-0.
12. Inmaculuda, F. and Noureddine, N., *Chem. Rev*., **2003**, 103, 3651.
13. Wild, H., *J. Org. Chem.*, **1994**, 59, 2748.
14. De la Rosa, V.G.; Ordonez, M. and Liera, M.J., *Tetrahedron Asymmetry*, **2001**, 12, 1615.
15. Bryan, J.J., Hinks, R.S. and Hultin, P.G., *Can. J. Chem*., **1985**, 63, 452.
16. Baba, A. and Yoshioka, T., *Org. Biomol. Chem.*, **2006**, 4, 3303.
17. Sang-Yoon, L.; Byung-Hyuk, M.; Seong- Won, S.; Sun-Young, O.; Sang- Min, L.; Sang-lin, K. and Dong-II, K., *Biotechnol. Bioprocess Eng.*, **2001**, 6, 179.
18. Gordon, J. and Ford, R.A., *The chemist's companion*, **1972**, John Willey & sons, New-York, ISBN 0-471-31590-7.
19. Navickas, V.; Ushakov, D. B.; Maier M. E.; Stroebele, M. and Meyer, H-J., *Org. Lett*, **2010**, 12, 3418.
20. Alsina, J.; Rabanal, F.; Chiva, C.; Giralt, E. and Albericio, F., *Tetrahedron*, **1998**, 54, 10125.
21. Lim, Y.G.; Han, J.S.; Koo, B.T. and Kang, J.B., *Bull. Korean. Chem. Soc.*, **1999**, 20, 9, 1097.
22. Sato, K.; Omote, M.; Ando, A. and Kumadaki, I., *Org. Lett*., **2004**, 23, 6, 4359.
23. Ito, S., *J. Org. Chem*., **1995**, 50, 3636.

University of Cape Town

24. Erdelmeier, I.; Daunay, S.; Lebel; Farescour, L. and Yadan, J.C.; *Green Chem*, **2012**, 14, 2256.
25. Reinhold, V.N.; Ishikawa, Y. and Melville, D.B., *J. Med. Chem.*, **1968**, 11(2), 258.
26. Fattori, D.; Rossi, C.; Finscham, C.I.; Caciagli, V.; Catrambone, F.; D'andrea, P.; Felicetti, P.; Gensini, M.; Marastoni, E.; Paris, M.; Terracciano, R.; Bressan, A.; Guiliani, S.; Maggi, C.A.; Meini, S.; Valenti, C. and Quartara, *J. Med. Chem.*, **2007**, 50, 550.
27. Erdelmeier, I.; Daunay, S.; Lebel; Farescour, L. and Yadan, J.C.; *Green Chem*, **2012**, 14, 2256.
28. Holland, H.L.; Brown, F.M.; Lazada, D.; Mayne, B. ; Szerminski, W.R. and Van Vliet, A.J., *Can. J. Chem.* ; **2002**; 80; 633
29. Trampota, M., *United States Patent*, **2010,** US 7,767,826, B2.

University of Cape Town

Chapter 4 Cell free reconstitution of *Mycobacterium smegmatis* ergothioneine biosynthesis

4.1. Introduction

It has been demonstrated by *Seebeck* [1] that in mycobacteria, ESH is synthesized by sequential actions of four enzymes named EgtD, EgtB, EgtC and EgtE. Our focus was on the EgtE enzyme that catalyses the final step of the ergothioneine pathway, whereby the ($S_{R/S}$)-hercynyl cysteine sulfoxide intermediate was transformed to ergothioneine. EgtE of *M. tb* is the only enzyme in the pathway that has not yet been expressed and none of the pathway enzymes have been thoroughly studied due to substrate unavailability. The PLP-dependent EgtE enzyme could not be purified due to insolubility, which is a common problem with cloning and expression of proteins of slow growing organisms in fast growing vectors.[9] Thus, in the absence of soluble expressed EgtE, a classical purification of this enzyme was planned, using *M. smeg.* as the source. However, the latter is outside the scope of this effort and only crude cell free lysate was considered for the transformation of substrates at this time. In order to perform a classical isolation and purification of EgtE for kinetic studies, sufficient quantities of its substrate is required. The availability of pure EgtE for kinetic studies would ultimately allow multiwell plate assays for inhibition studies as required for early *M. tb* drug discovery.

While the role of ESH is not completely understood, one of the reasons could be due to the lack of a rapid, convenient and sensitive direct assay to detect ESH in biological compounds. Recent increased interest in ESH as a potential vitamin brought to light several analytical methods of detection including LCMS for low level detection.[2, 3, 4]

Nguyen et al. [2] developed a rapid HPLC quantification of ESH, based on the reaction of ESH with 2,2'–dipyridyl disulphide (2-Py-S-S-2-Py) under acidic conditions, prior to chromatographic purification (removing interference of co eluted biological material) followed by LCMS (ESI positive mode). The ESH concentration in mushrooms and in animal blood were analysed using this method.

Belo et al. [5] used fluorimetric detection coupled with LCMS (ESI positive mode) of ESH as a ESH-bimane adduct at very low level in *Neurospora crassa*, ranging between 5.2- 25.4 nmol

University of Cape Town

per mg protein (equivalent to 573 ± 44 ng of ESH per mg of dry weight). It has been reported that *cyanobacteria* produces a high level of ergothioneine (up to 0.8 10^6 ng /g dry mass).[12]

Having synthesized the ergothioneine biosynthetic precursors, our aim was to prove that the compounds are indeed pathway enzyme substrates. Deuterated metabolic intermediates can now be utilised as internal standards as well as probes for metabolism. Thus, the metabolic transformation was attempted by using fresh, cell free *M. smeg* lysate, capable of enzymatically converting the substrate precursors into ergothioneine.

4.2. LCMS analysis of the cell free reconstitution of *Mycobacterium smegmatis* ergothioneine biosynthesis assays.

4.2.1. Extraction of crude enzymes from *M. smegmatis.*

Mycobacterium smegmatis is a non pathogenic bacterium, easy to work with and shares significant genetic similarities with *Mycobacterium tuberculosis. M. smeg.* therefore serves as a suitable substitute for *M. tb* to be used as a model organism in our study.

Mc^2155 cultures of *Mycobacterium smegmatis* were grown and harvested at the exponential phase which is characterised by high enzymatic activity as reported by *Ashraf et al.*[6]. The cells were collected by centrifugation and lysed by sonication. A tablet of complete ultra tablets, EDTA-free, glass vials (Roche) containing a cocktail of protease inhibitors was added to preserve the enzymatic activities of the crude enzyme preparation after cell lysis.

In order to reproducibly prepare crude enzyme extracts with the same enzyme concentration, the total crude protein level was determined. A protein concentration of 0.17 µg/µl was obtained, using the protein Dc assay**,** whereby albumin was used as a standard for calibration (Figure 4.1).

University of Cape Town

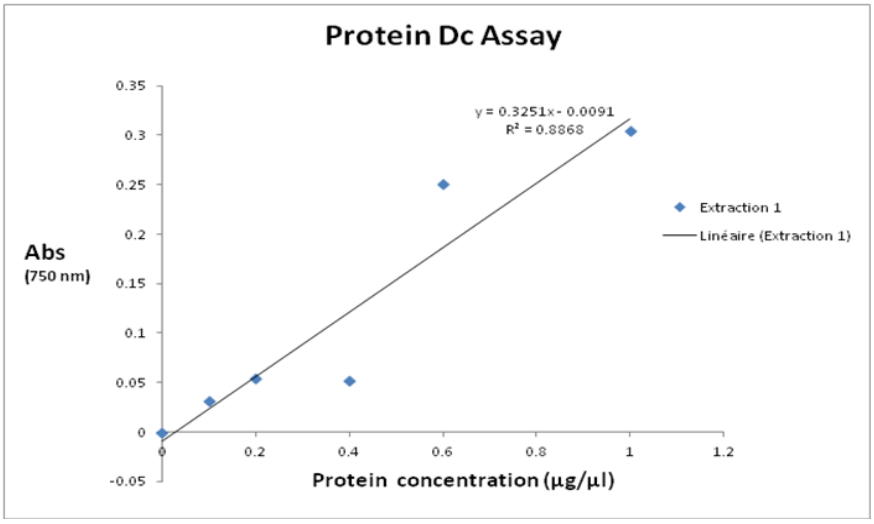

Figure 4.1 Albumin protein concentration calibration curve.

4.2.2. LCMS identification of ESH pathway metabolites.

Ultra high pressure liquid chromatography (UHPLC) was used for analyte separation, followed by MS analysis. This method demonstrated sufficient sensitivity and accuracy at low analyte concentrations. Due to the polarity and charge on the quaternary ammonium group present in all metabolites, poor retention on the UHPLC (Eclipse + C_{18} RRHD 1.8 µm.2.1 X 50) column was observed for ESH. Alternative columns were not considered at this time as the MS method of detection was sufficiently sensitive and unambiguous.

The ESI QTOF of the deuterated hercynine metabolites standard was determined prior the enzymatic reaction

4.2.2.1. Deuterated hercynine or [(2S)-*N,N,N*-2-trimethylamino-d_3-3-(1*H*-imidazol-4-yl) propanoic acid] (18)

The ESI QTOF of the deuterated hercynine metabolites standard **(18)** was determined prior to the crude enzymatic reaction. The ESI QTOF mass spectrum (positive mode) of deuterated hercynine (**18)** displayed a peak at *m/z* 201.1414 and *m/z* 202.1454 corresponding to $[Md_3]^+$ and $[Md_3 + H]^+$ ions respectively, the accurate mass for deuterated hercynine (**18)** requires *m/z* 201.1431 for $C_9H_{13}D_3N_3O_2^+[Md_3]^+$ (Figure 4.2).

University of Cape Town

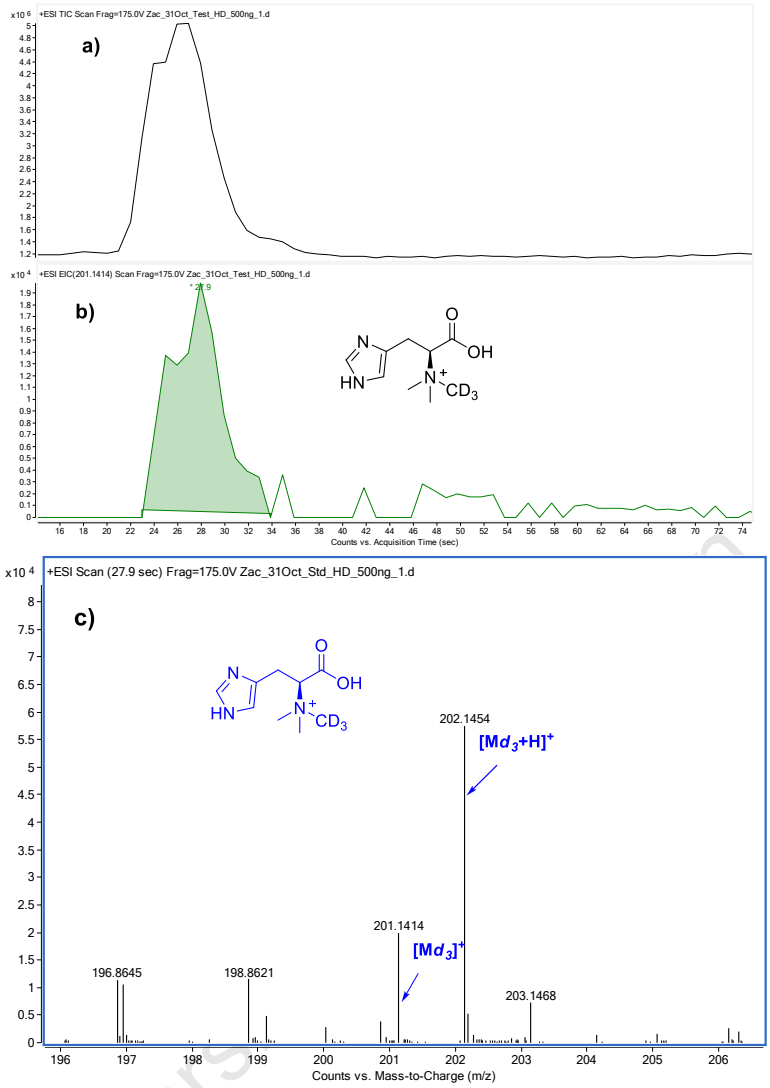

Figure 4.2 (a) TIC/QTOF trace of hercynine deuterated **(18)** (b) EIC/QTOF of hercynine deuterated **(18)** (c) ESI/QTOF mass spectra of deuterated hercynine **(18)** in positive ion mode. Data acquired by injection 10 µl solution in 3 % acetonitrile, 0.1 % formic acid in milli-Q water.

4.2.2.2. Hercynyl cysteine methyl ester sulfoxide or (2*S*)-*N*,*N*,*N*-2-trimethylammonium-3-[2- ((2*S*)-2-amino-2-methoxycarbonyl) ethylsulfinyl)- 1*H*-imidazol-4-yl] propanoic acid (26).

The ESI QTOF of the ($S_{R/S}$)-hercynyl cysteine methyl ester sulfoxide metabolites standard **(26)** was determined prior the crude enzymatic reaction. The ESI QTOF mass spectrum (positive mode) of ($S_{R/S}$)-hercynyl cysteine methyl ester sulfoxide (**26)** displayed peaks at *m/z* 348.1465 corresponding to $[M+H]^+$ ions, the accurate mass requires *m/z:* 348.1462 for $C_{13}H_{24}N_4O_5S^+$ $[M+H]^+$ (Figure 4.3).

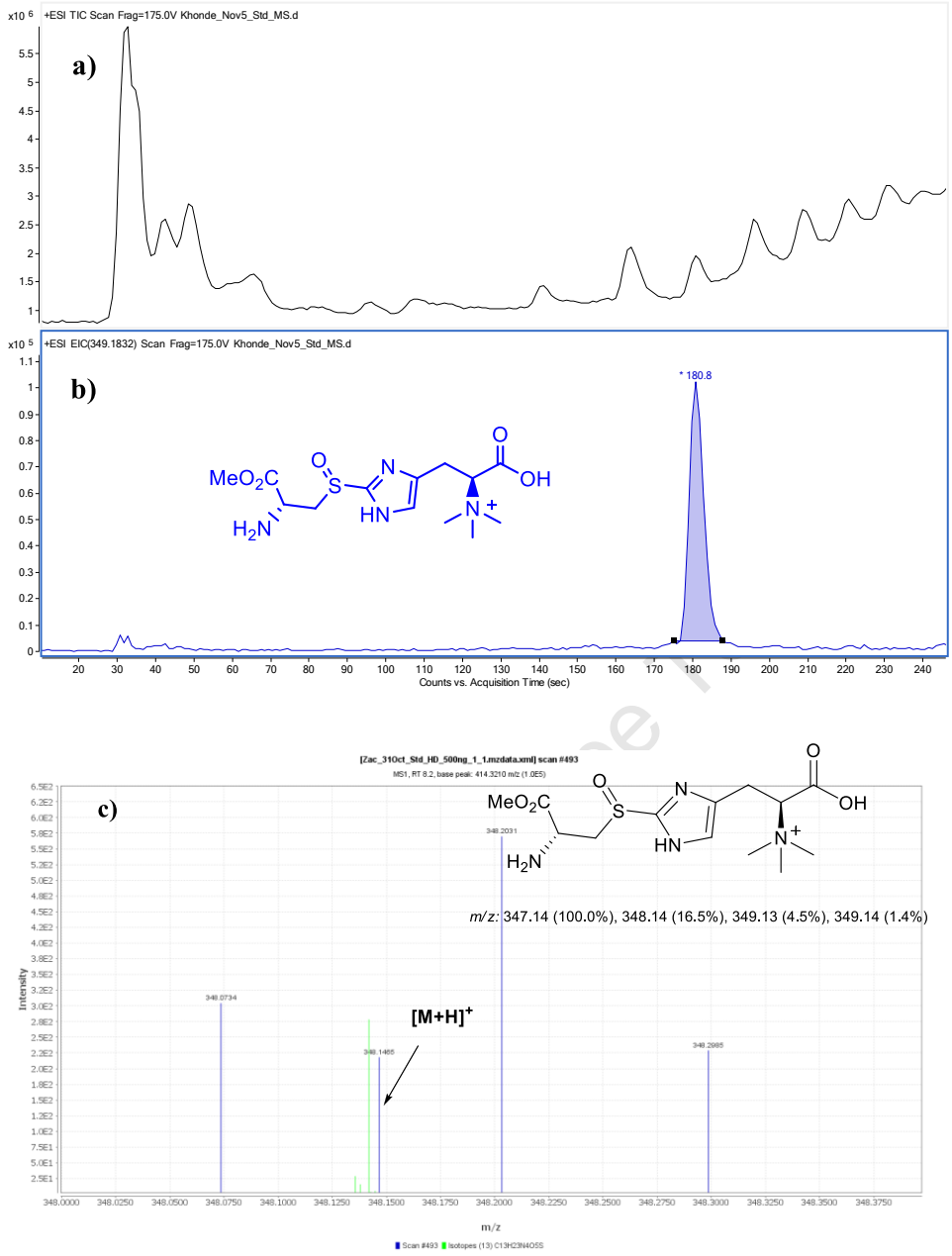

Figure 4.3 (a) TIC/QTOF trace of ($S_{R/S}$)-hercynyl cysteine methyl ester sulfoxide **(26)** (b) EIC/QTOF of ($S_{R/S}$)-hercynyl cysteine methyl ester sulfoxide **(26)** c) ESI/QTOF mass spectra of ($S_{R/S}$)-hercynyl cysteine methyl ester sulfoxide **(26)** in positive ion mode. Data acquired by injection 10 µl solution in 3 % acetonitrile, 0.1 % formic acid in milli-Q water

4.2.2.3. (*R/S*)-hercynyl cysteine or [*R/S*-(*β*-amino-*β*-carboxyethyl) ergothioneine sulfide (28) and the sulfone (30)]

The ESI QTOF of (*R/S*)-hercynyl cysteine or *R/S*-(*β*-amino-*β*-carboxyethyl) ergothioneine sulfide **(28)** and the sulfone **(30)** metabolites standards were determined prior to the crude enzymatic reaction.

The ESI QTOF mass spectrum (positive mode) of (*R/S*)-hercynyl cysteine thioether **(28)** showed peaks at *m/z* 317.1277, 318.1270 and 303.1484 corresponding to $[M]^+$, $[M+H]^+$ and $[M- CH_3]^+$ ions respectively.

The accurate mass determination gave a *m/z* 317.1277 which requires *m/z* 317.1284 for $C_{12}H_{21}N_4O_4S^+$ $[M]^+$ (Figure 4.4).

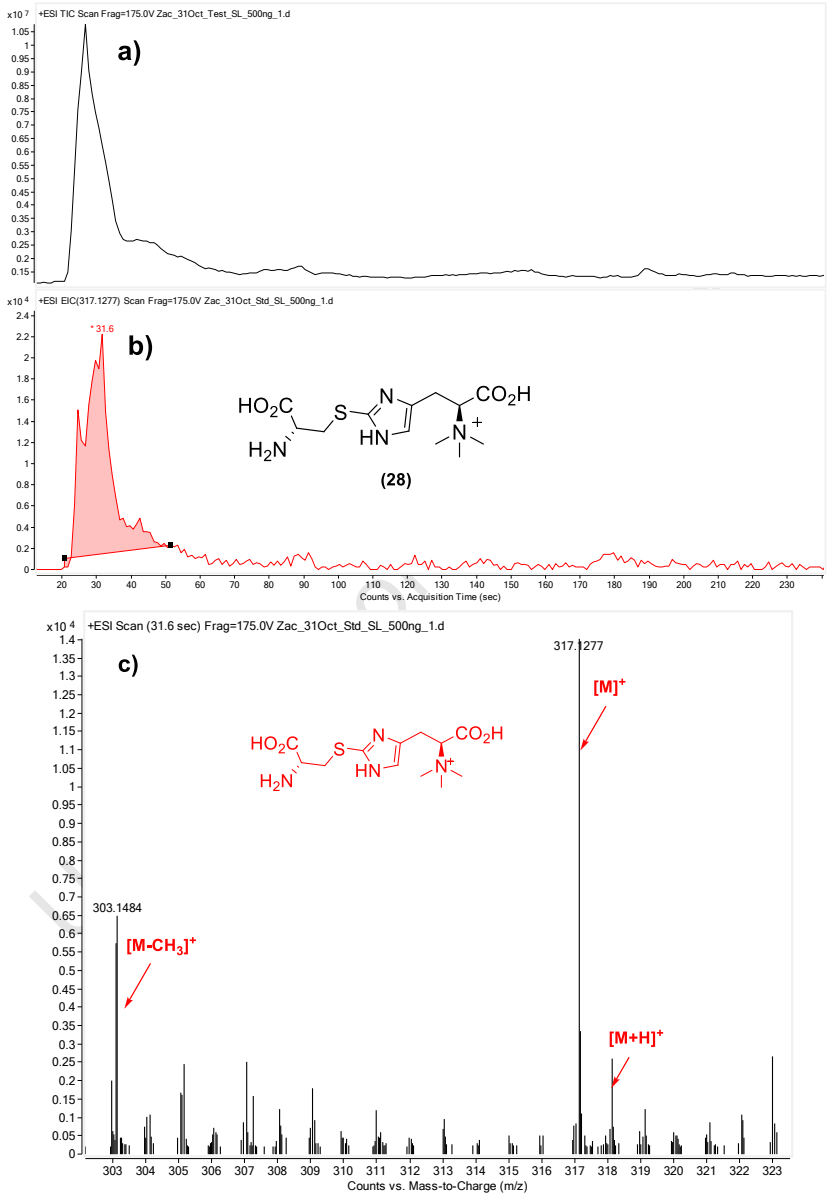

Figure 4.4.(a) TIC/QTOF trace of (*R/S*)-hercynyl cysteine thioether **(28)** (b) EIC/QTOF of (*R/S*)-hercynyl cysteine thioether **(28)** (c) ESI/QTOF mass spectra of hercynyl cysteine thioether **(28)** in positive ion mode. Data acquired by injection 10 µl solution in 3 % acetonitrile, 0.1 % formic acid in milli-Q water.

The ESI QTOF mass spectrum (positive mode) of (*R/S*)-hercynyl cysteine sulfone (**30)** showed peaks at *m/z* 349.1177, 350.1269 corresponding to $[M]^+$, $[M+H]^+$ ions respectively, the accurate mass determination gave a *m/z* 349.1177 which requires *m/z* 349.1182 for $C_{12}H_{21}N_4O_6S^+$ $[M]^+$ (Figure 4.5)

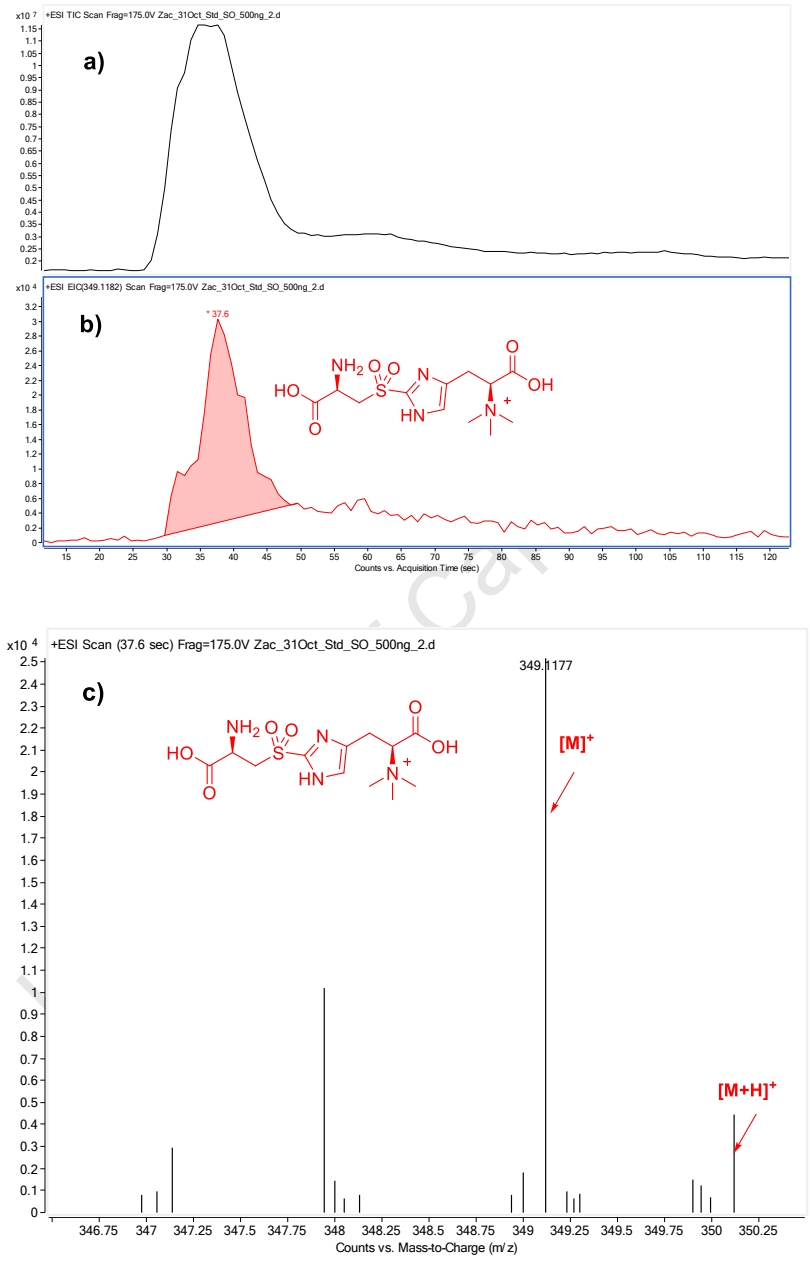

Figure 4.5 (a) TIC/QTOF trace of (*R/S*)--hercynyl cysteine sulfone **(30)** (b) EIC/QTOF of (*R/S*)-hercynyl cysteine sulfone **(30)** (c) ESI/QTOF mass spectra of (*R/S*)-hercynyl cysteine sulfone **(30)** in positive ion mode. Data acquired by injection 10 µl solution in 3 % acetonitrile, 0.1 % formic acid in milli-Q water.

4.2.2.4. Ergothioneine (8) and deuterated ergothioneine [(2*S*)-*N*,*N*,*N*-2-trimethylamino-d_3-3-[2-mercapto-1*H*-imidazol-4-yl) propanoic acid (9)]

In order to establish a calibration curve for the quantification of ESH, five different concentrations (2, 4, 8, 16, 32 ng/ml) of ESH were prepared (figure 4.6). The ESH detection was performed in triplicate, giving a limit of detection (LOD) of 0.56 ng/ml for ESH.[7, 8] Since our experiment was quantitative in design, the limit of quantitation (LOQ) was not optimised.

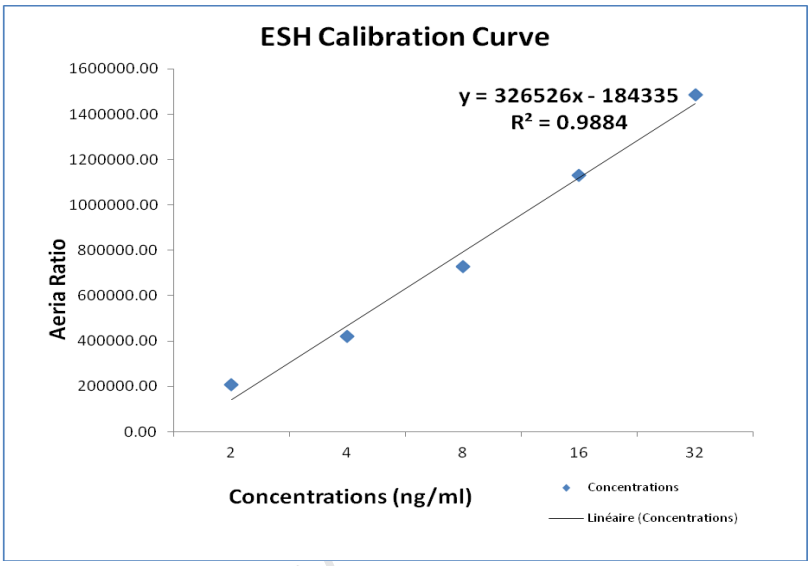

Figure 4.6 Calibration curve of ESH.

The ESI QTOF mass spectrum (positive mode) of ESH (standard) showed peaks at *m/z* 230.0958, 231.0980 and 232.0946 corresponding to $[M]^+$, $[M+H]^+$ and $[M+2H]^+$ ions respectively, the accurate mass found *m/z* 230.0958 requires *m/z* 230.0963 for $C_9H_{16}N_3O_2S^+$ $[M]^+$ (figure 4.7), the similar fragmentation pattern was also observed by *Ey et al.*[9] in their experimental MS spectrum of ergothioneine disulfide. The quantitation was performed on the molecular ion $[M]^+$ which displayed a very intense signal.

University

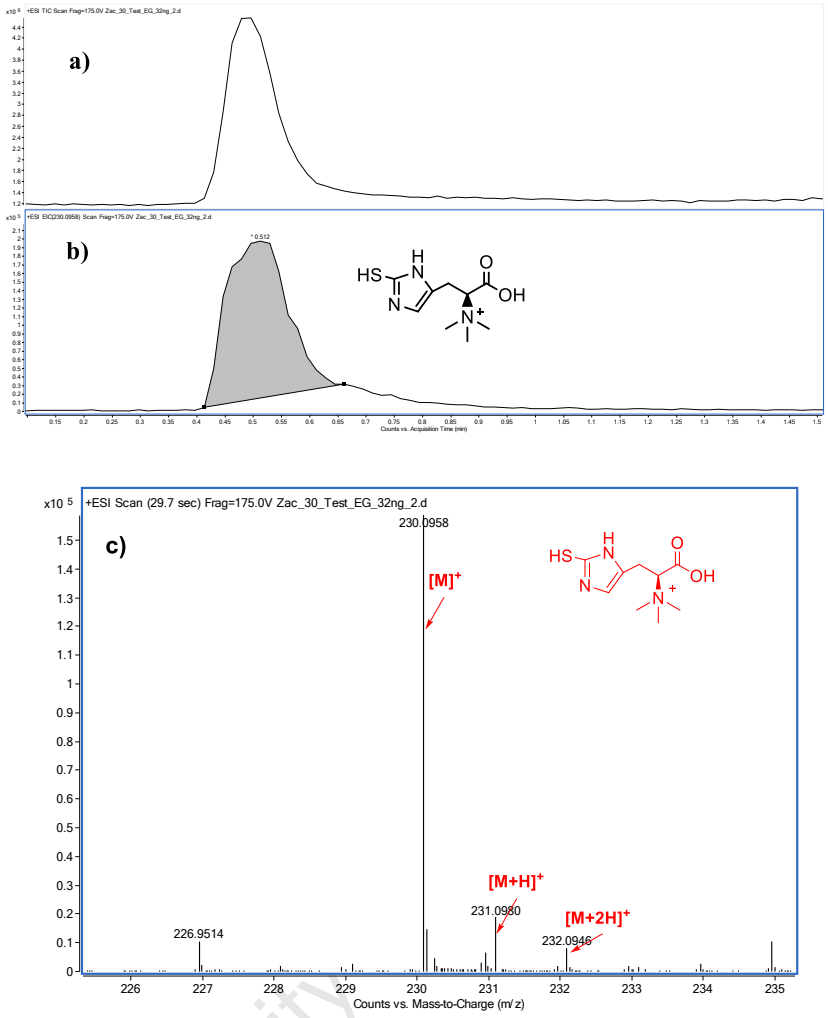

Figure 4.7 (a) TIC/QTOF trace of ESH standard **(8)** (b) EIC/QTOF of ESH standard **(8)** (c) ESI/QTOF mass spectra of ESH standard **(8)** in positive ion mode. Data acquired by injection 10 µl solution in 3 % acetonitrile, 0.1 % formic acid in milli-Q water.

The deuterated ergothioneine **(9)** displayed a similar fragmentation pattern as that observed for ESH, the ESI QTOF mass spectrum (positive mode) of deuterated ESH showed peaks at *m/z* 233.1161 and 189. 1261 corresponding to $[M\text{-}d_3]^+$ and $[M\text{-}d_3\text{-}CO_2]^+$ ions respectively.

The accurate mass determination gave a *m/z* 233.1161 which requires *m/z* 233.1152 for $C_9H_{13}D_3N_3O_2S^+[Md_3]^+$ (Figure 4.8).

University

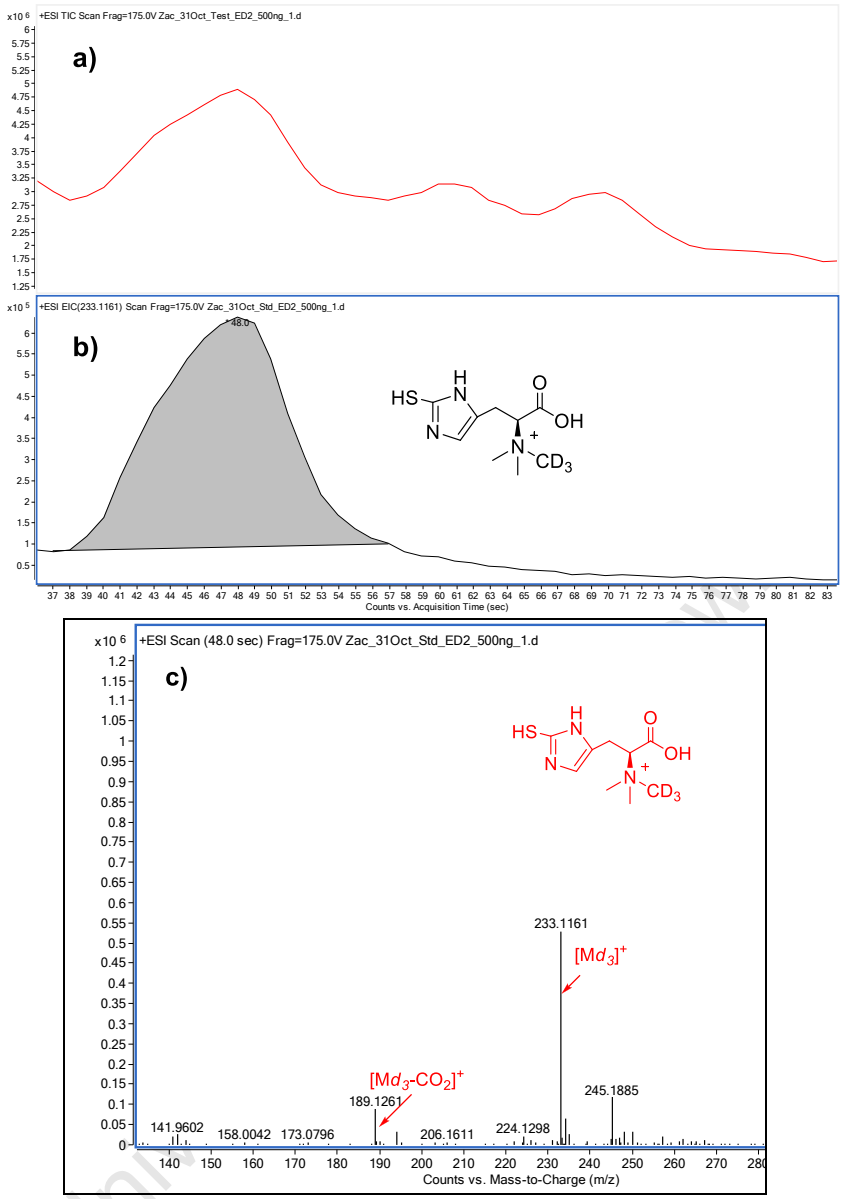

Figure 4.8 (a) TIC/QTOF trace of deuterated ergothioneine **(9)** (b) EIC/QTOF of deuterated ergothioneine **(9)** (c) ESI/QTOF mass spectra of deuterated ergothioneine **(9)** in positive ion mode. Data acquired by injection 10 µl solution in 3 % acetonitrile, 0.1 % formic acid in milli-Q water.

4.3. Crude enzyme mediated biosynthesis of ESH.

With the crude *M. smegmatis* enzyme lysate in hand, the enzyme assay was attempted**.** The enzymatic transformation of the substrate to ergothioneine was evaluated by the production of ESH as analyzed by LCMS.

ESH precursor metabolites, deuterated hercynine (**18**), (*R/S*)-hercynyl cysteine methyl ester sulfoxide (**26**), *R/S*-(*β*-amino-*β*-carboxyethyl) ergothioneine sulfide (**28**) and *S/R*-(*β*-amino-*β*-carboxyethyl) ergothioneine sulfone (**30**) were incubated with the crude cell free extract at

37° C, pH = 7.4 for 1 day, and analyzed by LCMS (Eclipse + C18 RRHD 1.8 µm.2.1 X 50 column, direct injection of 10 µl in 3 % acetonitrile, 0.1 % formic acid in milli-Q water).[9]

The identity of ESH was based on its LC retention time (0.5 minute) and its mass analysis (Figure 4.7).

The control reaction containing only the crude *M. smegmatis* cell free extract was also treated under the same conditions as the four metabolites. The concentration of ESH thus obtained was 0.58 ng /ml, which was equated to that of endogenous ESH. This concentration was at the limit of detection (0.56 ng/ml), thus any increase in the concentration of ESH in the experiment was ascribed to biotransformation of the respective substrates by the crude endogenous enzymes of the ESH pathway.

4.3.1. Biosynthesis of ESH using deuterated hercynine (18) as substrate.

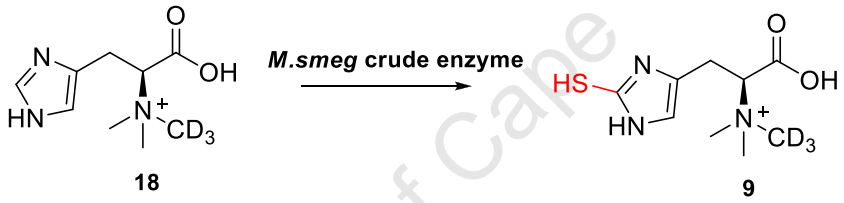

Scheme 4.1. Enzymatic synthesis of ESH using deuterated hercynine **(18)** as substrate.

When deuterated hercynine (**18)** was used as substrate, as expected, no change in natural ESH was observed. However, as expected, the LCMS analysis of the mixture revealed the production of deuterated ergothioneine **(9)** eluting at a retention time of 0.5 min. The HRMS (ESI^+) displayed a peak at *m/z* 233.1161 corresponding to $[M\text{-}d_3]^+$). Peaks values at *m/z* 230.0958 $[M]^+$ or at *m/z* 231.0980 $[M+H]^+$ belonging to the natural ergothioneine were not revealed in the chromatogram. This clearly shows that the crude *M. smeg*. transformed deuterated hercynine into deuterated ESH (Figure 4.9).

University of Cape Town

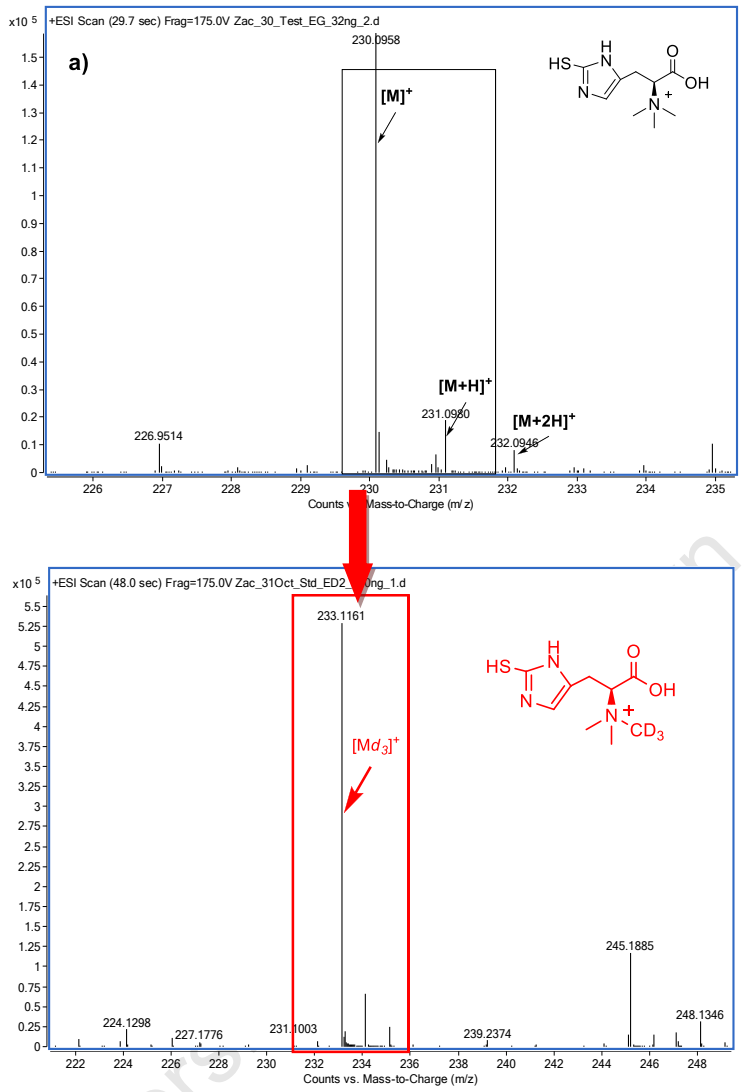

Figure 4.9. LCMS spectrum of ESH *in-vitro* reconstititued experiment using hercynine deuterated **(18)** as substrate (a) ESI/QTOF mass spectra of natural ESH standard **(8)** and (b) ESI/QTOF mass spectra of deuterated ESH deuterated producedfrom deuterated hercynine in the reaction mixture.

4.3.2. Biosynthesis of ESH using hercynyl cysteine methyl ester sulfoxide (26) as substrate.

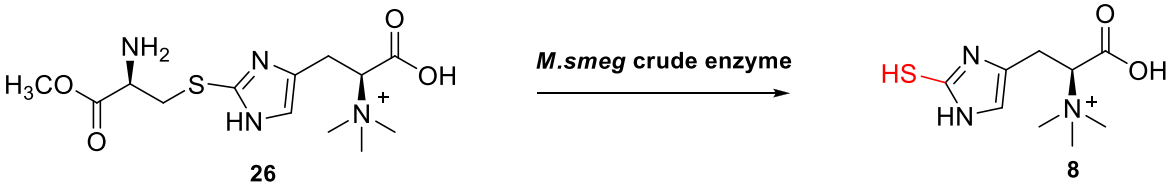

26 **8**

Scheme 4.2. Enzymatic synthesis of ESH using hercynyl cysteine sulfoxide methyl ester **(26)** as substrate

($S_{R/S}$)-hercynyl cysteine sulfoxide methyl ester (**26)** used as substrate gave slight increase in the ESH concentration (0.72 ng/ml) (Figure 4.10). Thus, indicating insignificant biotransformation to ESH. This result is indicative that ($S_{R/S}$)-hercynyl cysteine sulfoxide methyl ester (**26)** could be weak substrate, if any. The carboxyl group of the natural substrate may be involved in critical enzyme active site binding. However, this finding needs further substantiation in the absence of a protein crystal structure of EgtE.

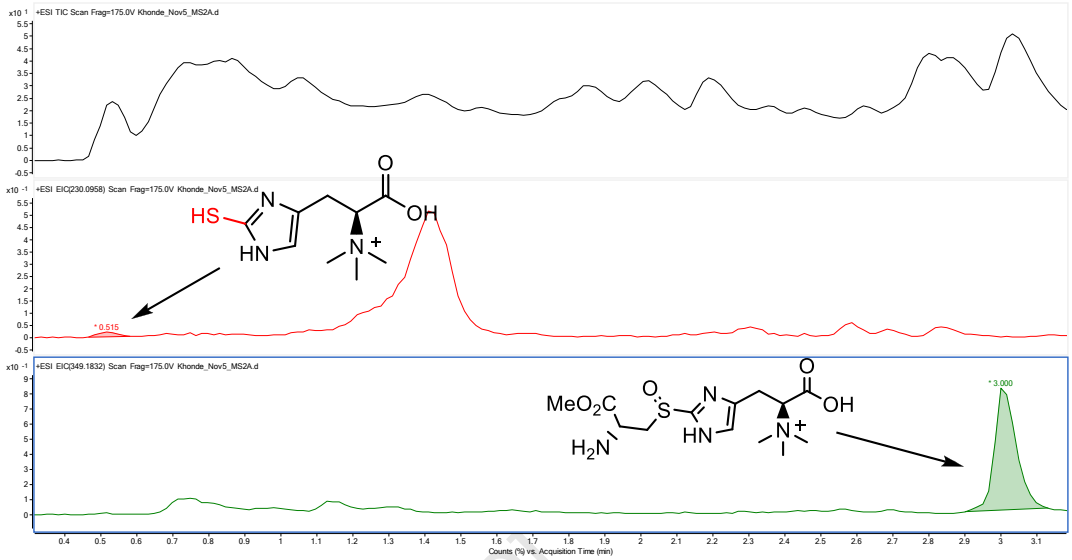

Figure 4. 10. LCMS spectrum of ESH *in-vitro* reconstititued experiment using ($S_{R/S}$)-hercynyl cysteine methyl ester sulfoxide **(26)** as substrate.

4.3.3. Biosynthesis of ESH using *R/S*-(*β*-amino-*β*-carboxyethyl)-ergothioneine sulfide (28) and *R/S*-(*β*-amino-*β*-carboxyethyl) ergothioneine sulfone (30) as substrate.

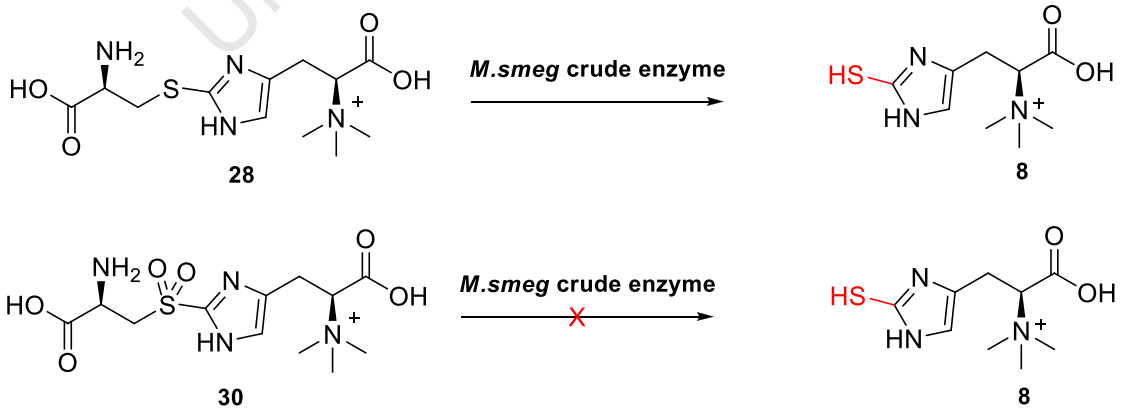

Scheme 4.3. Enzymatic synthesis of ESH using *R/S*-(*β*-amino-*β*-carboxyethyl) ergothioneine sulfide **(28)** and *R/S*-(*β*-amino-*β*-carboxyethyl) ergothioneine sulfone **(30)** as substrate.

University of

(*R/S*)-hercynyl cysteine thioether (**28**) biosynthetically produced the highest concentration of ESH (2.77 ng/ml). The thioether (**28**) appeared to be a better substrate than the ($S_{R/S}$)-hercynyl cysteine methyl ester sulfoxide **(26)** or the (*R/S*)-hercynyl cysteine sulfone (**30**) (Figure 4.11).

When sulfone substrate (**30)** was evaluated, only an insignificant increase of ESH concentration was detected (0.99 ng/ml). The LCMS chromatogram spectrum (Figure 4.12) displayed a peak belonging to basal ESH and the substrate respectively, clearly showing that no enzymatic reaction occurred. The sulfone is not expected to undergo β-lyase mediated cleavage due to its stability. Furthemore the methylene protons adjacent to the sulfone would be relatively acidic, and if deprotonated will result in resonance structures that further stabilises the C-S bond.

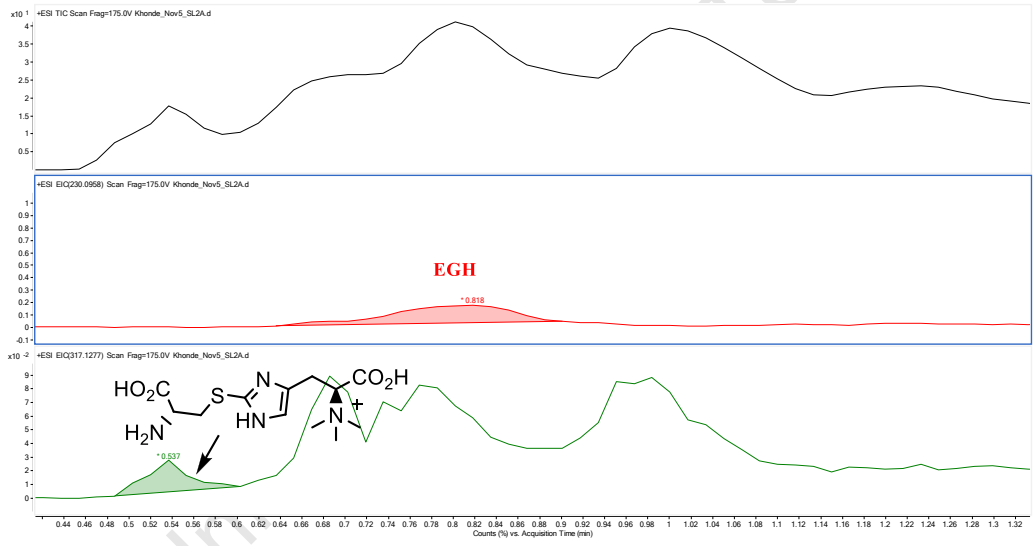

Figure 4. 11. LCMS spectrum of ESH *in-vitro* reconstititued experiment using ($S_{R/S}$)-hercynyl cysteine thioether **(28)** as substrate.

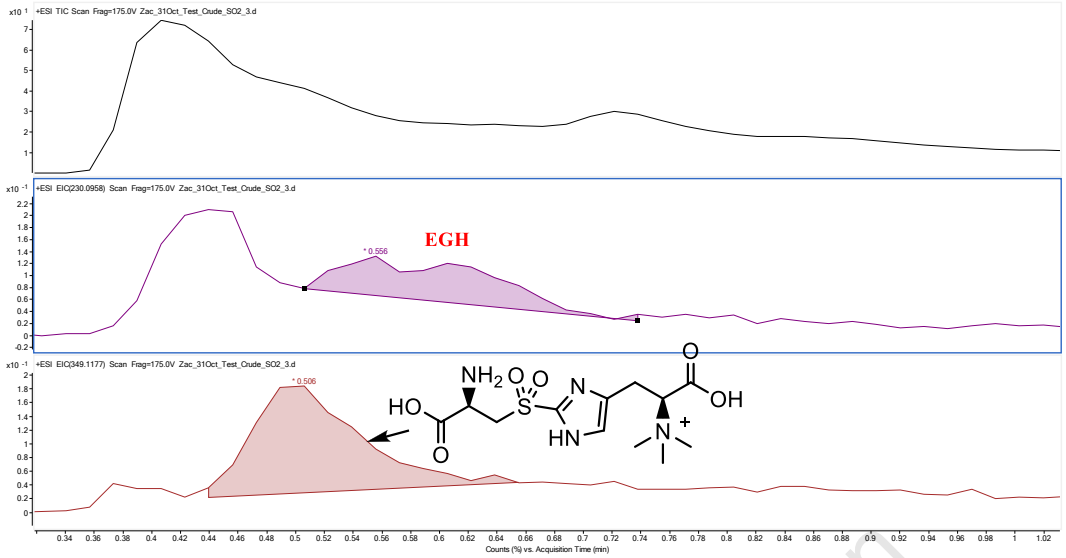

Figure 4. 12. LCMS spectrum of ESH *in-vitro* reconstititued experiment using ($S_{R/S}$)-hercynyl cysteine sulfone **(30)** as substrate.

Krupka et al.[10] in their research on elucidating the crystal structure of cystalysin (PLP dependent enzyme) from *treponema denticola*, they found guanidinium groups Arg 401 and Arg 369 in the active site which makes strong hydrogen bonds with the carboxylate moiety of the substrate, suggesting that the free carboxylic acid moiety is required for the C-S lyase enzyme activity. The presence of a methyl ester could be the reason why the methyl ester sulfoxide (**26)** gave poor conversion compare to the free carboxylic acid of the hercynyl cysteine thioether (**28)**. Due to the unavailability of the hercynyl *L*-cysteine sulfoxide, we could not establish this fact.

The LCMS spectrum (Figure 4.11) displayed a significant conversion of the (*R/S*)-hercynyl cysteine thioether (**28**) into ESH.

University of Cape Town

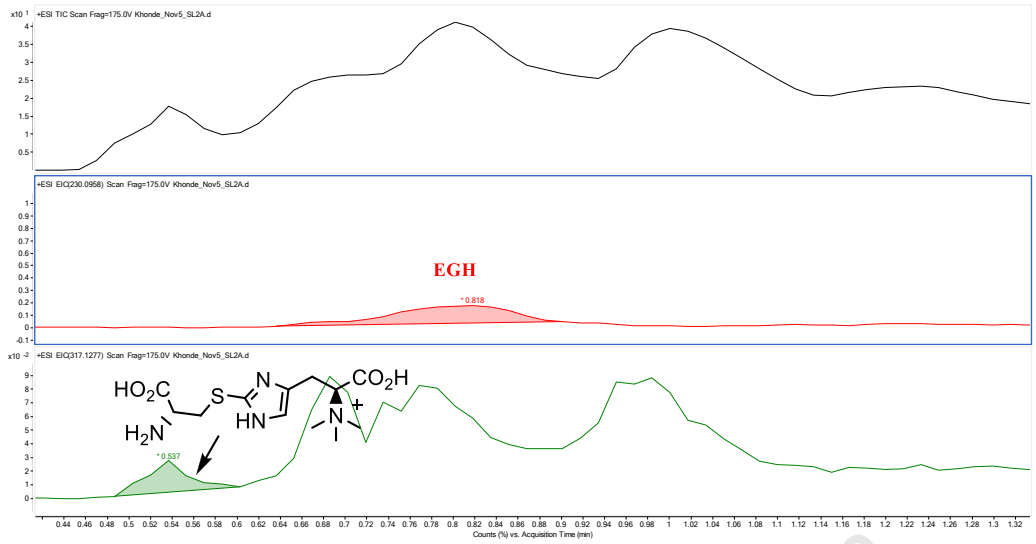

Figure 4. 11. LCMS spectrum of ESH *in-vitro* reconstititued experiment using (*R/S*)-hercynyl cysteine thioether **(28)** as substrate.

From these experiments two important conclusions have been deducted. Firstly, the free carboxylic acid moiety seems to be required for the enzymatic activity. Only the sulfide (**28)** produced a significant 2.77 ng/ml where asproduced 0.99 ng/ml of ESH, thus better enzymatic activity was observed compared to the methyl ester sulfoxide substituted derivative (**26)**, which exhibited poor ESH conversion (0.72 ng/ml).

Secondly the sulfone substrate (**30)** did not lead to ESH, suggesting that the degree of oxidation in the sulfur atom of the substrate could be crucial for the activity (Figure 4.13). Chemical lysis through a beta-elimination process of the sulfone requires strong basic or acidic medium and hence is not possible under the present conditions. Still further research needs to be conducted to successfully express, purify and crystallize EgtE, which would allow a better understanding of enzyme-substrate binding interaction.

University of Cape Town

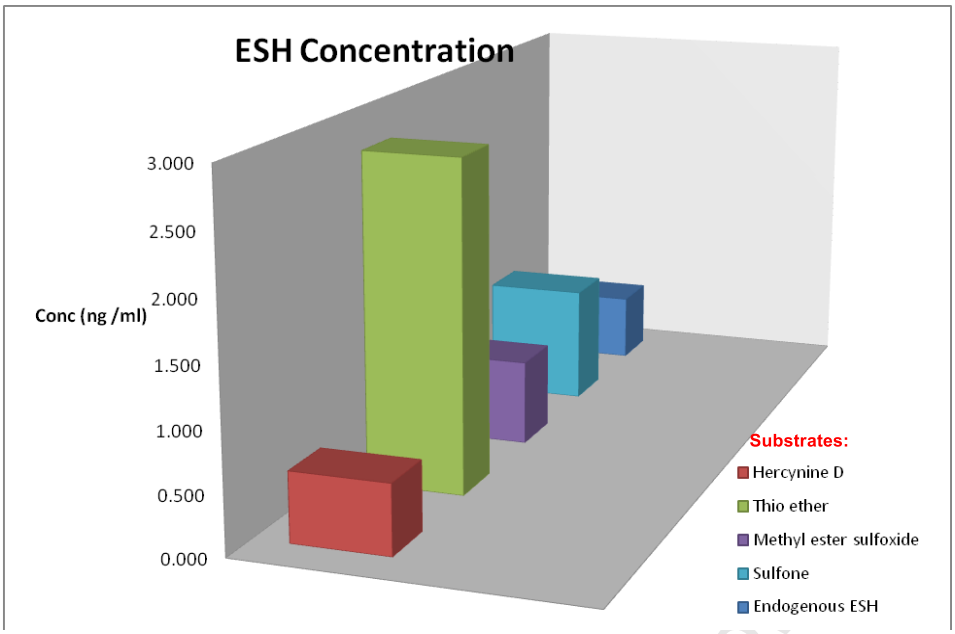

Figure 4.13 *In vitro* reconstitution of ESH graph (500 µl reactions containing 20 mM Tris HCl pH = 7.4, 20 mM NaCl, 0.2 Mm $FeSO_4.7\ H_2O$, 0.5 mM mercaptoethanol, 250 µl of crude *M. smeg*. enzymes and 50 mM of substrates either (1) ($S_{R/S}$)-hercynyl cysteine thioether **(28)** (2) ($S_{R/S}$)-hercynyl cysteine sulfone **(30)** (3) deuterated hercynine **(17)** or (4) ($S_{R/S}$)-hercynyl cysteine methyl ester sulfoxide **(26))**

University of Cape Town

Table 4.1. *In vitro* biosynthesis of ESH table.

Compounds	Structures	ESH Concentration (ng/ml)
Hercynine-d_3 (18)	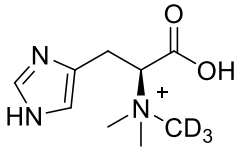	**0.58**
Hercynine cysteine thioether (28)	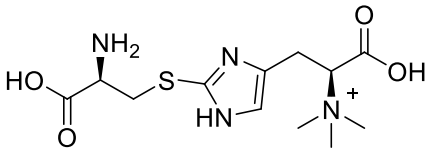	**2.77**
Hercynine cysteine methyl ester sulfoxide (26)	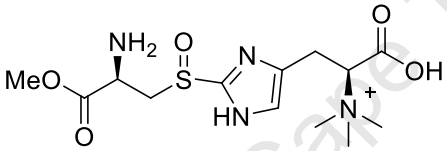	**0.72**
Hercynine cysteine sulfone (30)	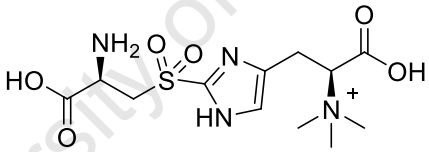	**0.99**
Endogenous ESH (17)	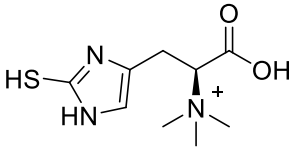	**0.57**

University of Cape Town

Due to the lack of pure ergothioneine enzymes, the biotransformation of four ergothioneine enzymes substrates **(18, 26, 28, and 30)** to ergothioneine was performed using a crude *M. smeg.* enzymatic preparation, and the production of ergothioneine was monitored by LCMS technique. The table 4.1 above displayed the average results of the experiment as it was performed in triplicate and repeated several times (more than 3 times); despite the reproducibility of these results, a deep investigation still needs to be fulfilled.

4.4. References

1. Seebeck, F.P., *J. Am. Chem. Soc*., **2010**, 132, 6632.
2. Nguyen, T.H.; Giri, A.; Ohshima, T., *Food Chem.,* **2012**, 585.
3. Melville, D.B., *Vitamines and hormones*, **1959**, 17, 155.
4. Stowell, *In organic sulphur compounds*, Pergamon Press, Oxford, London, Paris, **1961.**
5. Bello, M.V.; Barrera, P.V.; Morin, D.; and Epstein, L., *Fungal gen. & boil*., **2012**, 160.
6. Ashraf S. A., El-Sayed, *J. of Basic Microbiol.,* **2010**, 331.
7. Squellerio, I.; Caruso, D.; Porro, B.; Veglia, F.; Tremoli, E.; Calvalca, V., *J. Pharm. Biomed. Anal.,* **2012**, 71, 111.
8. Klein, M.; Ouerdane, L.; Bueno, M. and Pannier, F., *Metallomics*, **2011**, 3, 513.
9. Ey, J.; Schomig, E. and Taubert, D., *J. Agric. Food. Chem.,* **2007**, 55, 6466
10. Krupka, H.I.; Huber, R.; Holt, S.C. and Clausen, T., *The Embo J.*, **2000**, 19, 3168.

University of Cape Town

Chapter 5 Conclusion

This thesis focussed the synthesis and cell-free reconstitution of ergothioneine biosynthesis *M. tb* enzyme substrates implicated in ergothioneine biosynthetic pathway as published recently by *Seebeck.*[1] A yet undiscovered oxidase converts the synthesized substrate, hercynyl cysteine sulfide **(26)** into the EgtE substrate, hercynyl cysteine sulfoxide. Thus, this work contributes to the preparation of tools in order to better understand the role of ergothioneine in survival of *Mycobacteria*.

The focus of the project was in the last step of biosynthetic pathway, whereby EgtE (PLP dependent enzyme) catalysed the C-S lyase of hercynyl cysteine sulfoxide to form ergothioneine. This step could be crucial for future ergothioneine inhibition studies, which could lead to ergothioneine *M. tb* drug discovery, although the vital protective role of ergothioneine in *M. tb* still needs to be proven.

PLP is easily the most versatile coenzyme, derived from vitamine B_6.[2] PLP enzymes catalyzes a wide range of biochemical reactions depending on the substrate specificity and these enzymes synthesize, degrade, and interconvert amino acids.[2] *Breitinger et al* [3] elucidated the crystal structure of cystathionine *β*-lyase, a PLP-dependent enzyme that catalyzes the C-S cleavage of *L*-cystathione (Scheme 5.1)

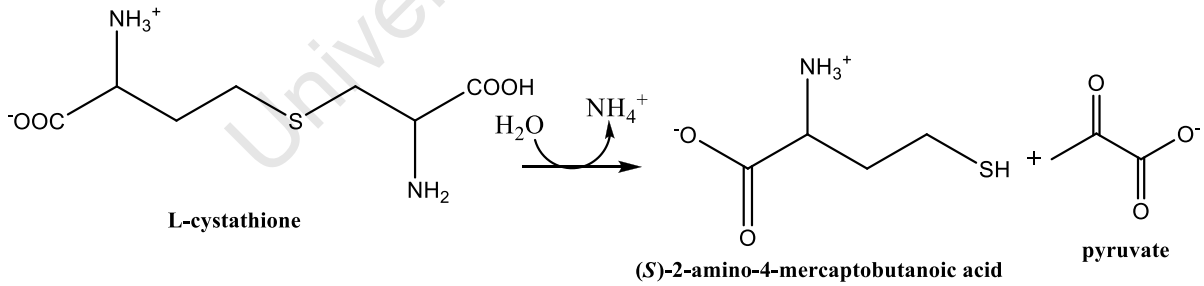

Scheme 5.1 Cleavage of cystathione by cystathionine *β*-lyase.

Yamada et al [4] elucidated the crystal structure of *L*-serine dehydratase (EC 4.3.1. 17) from rat liver, which catalyses the dehydration of *L*-serine to yield pyruvate and ammonia (Scheme 5.2).

University of Cape Town

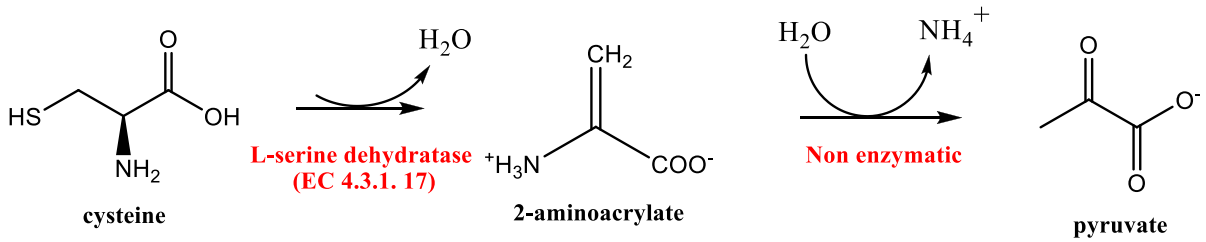

Scheme 5.2 Formation of pyruvate catalysed by *L*-serine dehydratase (EC 4.3.1.17) enzyme.[4].

Elucidation of the crystal structure of PLP-enzymes and modelling remain powerful tools toward the understanding of enzyme-substrate interaction, which is required for the development of modern-drug discovery programmes.

Gannon et al [5] found that *L*-serine dehydratase (EC 4.3.1.17) is specific for the *L*-cysteine only, substituting (*L*-cysteine) substrate by the *D*-cysteine enantiomer resulted in a drastic drop in the enzyme activity, thus suggesting that the *D*-cysteine could be an enzyme inhibitor. Therefore the synthesis of hercynyl-*D*-cysteine sulfoxide (non-natural diastereoisomeric EgtE substrate analogue) was attempted, hoping that it may act as an EgtE enzyme inhibitor. However due to the unsuccessful attempt to hydrolyse the ester, this activity was not determined.

The inhibition of PLP-enzyme has led to the design of drugs against many diseases; Difluoromethylornithine (DFMO), an efficient drug against African Human African trypanosomiasis (HAT), constitutes a successful example of the development of a PLP inhibitor-based drug (Figure 1.9). DFMO inhibits ornithine decarboxylase (ODC), a PLP-dependent enzyme implicated in the first step of the trypanothione (TSH) biosynthetic pathway.[6] Based on the success of DFMO fluorinated hercynyl cysteine sulfoxide, and fluorinated hercynyl cysteine sulfone EgtE substrate derivatives as well as simple *D*-diastereoisomer analogue of the same EgtE substrate could be developed in the future as a potential EgtE *M. tb* enzyme inhibitors (Scheme 5.3). Thus mechanism based designed inhibitors based on the ergothioneine biosynthetic pathway would be the key to *M. tb* drug discovery.

University of Cape Town

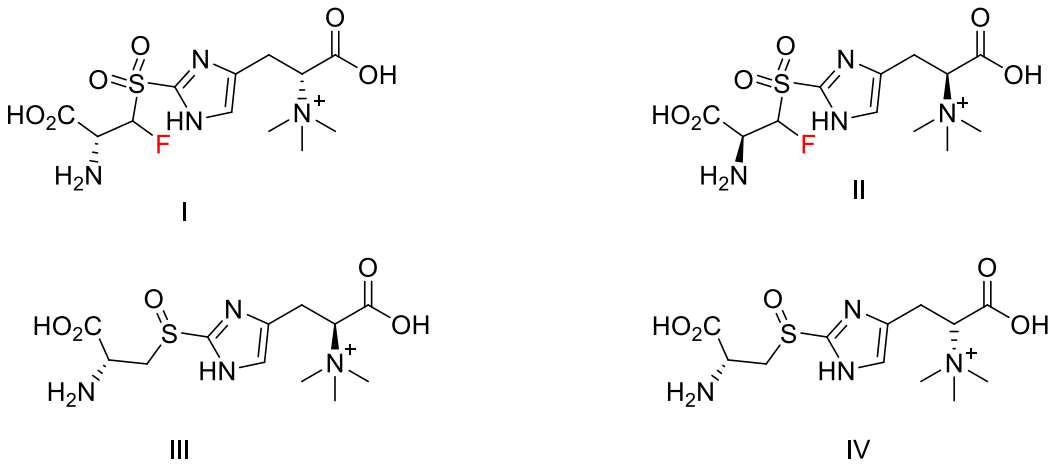

Scheme 5.3 Potential EgtE enzyme inhibitors

Seebeck et al. [1] unsuccessfully attempted to isolate the EgtE enzyme, this result was due to a solubility problem of PLP enzyme. Using a classical method for the EgtE purification could lead to the elucidation of its crystal structure, which is important for the future drug discovery program.

With the lack of pure EgtE *M. tb* enzyme, crude *M. smeg.* enzymes was assayed instead to enzymatically convert substrates to ergothioneine, LCMS was used to establish the production of the product, ergothioneine. It has been found that the ESH assay which utilized mass spectrometry (MS), is one of the best quantification techniques, although is not suitable for rapid and routine analysis in biological materials, without prior derivatisation the presence of ionic ESH adducts (sodiated, potassated, etc) in biological material made the quantification of ESH by MS very complex.[7]

The results of this thesis have established a platform development toward *M. tb* ergothioneine inhibitory studies required for the future *M. tb* drug discovery based on the ergothioneine biosynthetic pathway.

This thesis displays in detail the total synthesis of ergothioneine, as well as its enzymatic synthesis using crude *M. smeg.* enzyme preparation.

University of Cape Town

5.1. References

1. Seebeck, F.P., *J. Am. Chem. Soc*., **2010**, 132, 6632.
2. Christen, P., Mehta, P.K, *The Chem. Record*, **2001**, 1, 436
3. Breitinger, U.; Clasen, T.; Ehlert, S.; Huber, R.; Laber, B.; Schmidt, F.; Pohl, E. and Messerschmidt, A., *Plant Phys.,* **2001**, 126, 631
4. Yamada, T.; Komoto, J.; Takata, Y.; Ogawa, H.; Pitot, H.C. and Takusagawa, F.; *Biochem.*, **2003**, 42, 12854.
5. Gannon, F.; Bridgeland, E.S. and Jones, K.M., *Biochem. J.,* **1977**, 161.
6. Alain, H.F., *Trends. Parasitol.,* **2003**, 19, 488.
7. Nguyen, T.H.; Giri, A.; Ohshima, T., *Food. chem.,* **2012**, 585.

University of Cape Town

Chapter 6 Experimental Section

6.1. General Procedures

All solvents were dried by appropriate techniques and freshly distilled before use. All commercially available reagents were purchased from Sigma-Aldrich and Merck and were used without further purification.

Unless otherwise stated, reactions were performed under an inert atmosphere of nitrogen in oven dried glassware and monitored by thin-layer chromatography (TLC) carried out on Merck silica gel 60-F_{254} sheets (0.2 mm layer) pre-coated plates and products visualized under UV light at 254 nm or by spraying the plate with an ethanolic solution of ninhydrin (2% v/v) followed by heating.

Column chromatography was effected by using Merck Kieselgel silica gel 60 (0.040-0.063 mm) and eluted with an appropriate solvent mixtures. All compounds were dried under vacuum before yields were determined.

Nuclear magnetic resonance spectra (^{1}H and ^{13}C) were recorded on a Varian Mercury 300 MHz (75 MHz for ^{13}C), Varian Unity 400 MHz (101 MHz for ^{13}C) or a Bruker unity 400 MHz (101 MHz for ^{13}C) and were carried out in $CDCl_3$, DMSO-d_6 and D_2O as the solvent unless otherwise stated. Chemical shifts are given in ppm relative to tetramethylsilane (TMS, δ = 0.00 ppm), which is used as internal standard. Assignments were confirmed by COSY, APT and HSQC analysis, when required. Coupling constants (*J*) are reported in Hertz (Hz). The spin multiplicities are indicated by the symbol s (singlet), d (doublet), dd (doublet of doublets), t (triplet), m (multiplet), q (quartet) and br (broad).

Optical rotations were obtained using a Perking Elmer 141 polarimeter at 20°C. The concentration *c* refers to g/100ml.

Melting points were determined using a Reichert-Jung Thermovar hot-plate microscope and are uncorrected. Infra Red spectra were recorded on a Perkin-Elmer FT-IR spectrometer (in cm^{-1}) from 4000 cm^{-1} to 450 cm^{-1}.

Mass spectra were recorded on a JEOL GC MATE II magnetic sector mass spectrometer and the base peaks are given, University of Cape Town.

LCMS analyses were carried out with a UHPLC Agilent 1290 Infinity Series (Germany), accurate mass spectrometer Agilent 6530 Qradrupole Time Of Flight (QTOF) equipped with an Agilent jet stream ionization source (positive ionization mode) (ESI^{+}) and column (Eclipse + C_{18} RRHD 1.8 µm.2.1 X 50, Agilent, Germany).

University of Cape Town

Enzymatic reactions were allowed to incubate in Nuaire incubator (DH Autoflow CO_2 Air – jarcketed Incubator), and centrifuged in Eppendhorf centrifuge (Model 5810R, Germany), Tygerberg Stellenbosch University, Cape Town, South Africa

6.2. Compounds synthesized.

***(S, Z)*-methyl 2, 4, 5-tris (benzamido) pent-4-enoate (2) [1]**

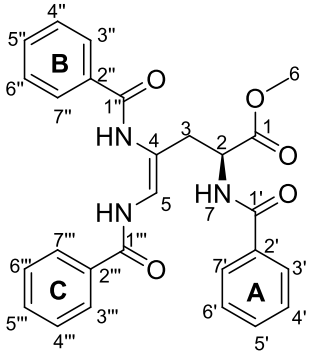

In a mixture of THF:H_2O (10:90, 67 ml) was added histidine methyl ester dihydrochloride (5.0 g; 20.6 mmol). This solution was allowed to stir at 10°C followed by the addition of sodium bicarbonate (13.7 g; 163mmol) and then benzoyl chloride (13.7 g; 113 mmol), drop wise over a period of 30-60 minutes with efficient stirring. The resulting mixture was allowed to equilibrate to room temperature and subsequently allowed to stir for an 18-24 hr period. Upon settling, the organic layer was separated, washed with brine, dried (anhydrous $MgSO_4$) and filtered. The filtrate was evaporated under vacuum. The resultant solid was mixed with 60 ml of diethyl ether and left overnight at -10 °C. The diethyl ether was decanted, the solid residue dissolved in 30 ml of absolute ethanol and mixed with 3.3 ml of triethylamine. The resulting solid was dissolved in 60 ml of diethyl ether and allowed to crystallize for an 18-24 hour period at -10 °C. The resultant crystals were filtered and washed with 8 ml diethyl ether and air dried. The tribenzoyl Bamberger intermediate, (*S, Z*)-methyl 2, 4, 5-tris (benzamido) pent-4-enoate was obtained as a white powder (8.0 g; 82 %). Mp:207-210 °C literature 213-215°C**[1];** ν_{max} (KBr)/cm^{-1} 3316s (NH) 1748s 1202vs ($RCOOCH_3$) 1671s (RCONHR') 804m (Bz), ^{1}H NMR (400 MHz, $CDCl_3$) δ 9.91 (d, *J* = 8.7 Hz, 1H, NH-7), 8.84 (s, 1H, NH), 8.07 – 8.02 (m, 2 H, H-3' H-7'), 7.93 – 7.89 (m, 2 H, H-3" H-7"), 7.82 – 7.78 (m, 2 H, H-3''' H-7'''), 7.60 – 7.39 (m, 9 H, meta, para rings A, B & C), 7.16 (d, *J* = 6.8 Hz, 1 H, NH), 6.78 (d, *J* = 9.0 Hz, 1H, H-5), 4.94 (q, *J* = 6.0 Hz, 1 H, H-2), 3.82 (s, 3 H, OCH_3-6), 3.02 (dd, *J* = 14.9, 5.7 Hz, 1H, H-3a), 2.80 (dd, *J* = 14.9, 5.7 Hz, 1H., H-3b), ^{13}C NMR (101MHz, $CDCl_3$) δ 172.1 (C-1') , 170.9 (C-1), 167.8 (C-1"), 166.2 (C-1'"), 164.1 (C-2'), 134.8 (C-2'"), 133.0 (C-

University of Cape Town

2"), 132.7 (C-5'), 132.1 (C-4''' C-6'''), 131.9 (C-5"), 131.7 (C-4' C-6'), 129.8 (C-3' C-7'), 128.6 (C-3''' C-7'''), 128.4 (C-5'''), 128.1 (C-3" C-7"), 127.7 (C-4" C-6"), 127.2 (C-2'''), 127.1 (C-3"C-6"), 115.8 (C-4), 115.0 (C-5), 53.1 (C-6), 45.1 (C-2), 38.3 (C-3)**.** LRMS (EI^+) *m/z* calculated for $C_{27}H_{26}N_3O_5$ $[MH]^+$ 471.2 found 471.1 ($[MH]^+$, 11 %).

(*S,Z*)-Methyl 2,5-bis(benzamido)-4-hydroxypent-4-enoate (3b) [2, 3]

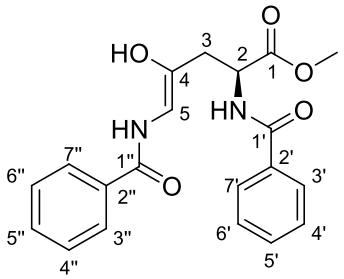

Acetyl chloride (19 ml) was added drop wise to methanol (85 ml) with cooling, resulting in a concentrated solution of methanolic HCl.

(S, Z)-methyl 2, 4, 5-tris (benzamido) pent-4-enoate **(2)** (6.02 g; 12.8 mmol) was added to cold methanolic HCl (prepared as described above). A clear solution was achieved within a 5 hour period. The resultant solution was concentrated on a rotary evaporator to give an oily residue which was mixed with diethyl ether (23 ml) and ice-water (76 ml) and the mixture was left at 0-5 °C, overnight. The resulting crystals were washed with 5 ml water followed by 2 ml of diethyl ether and then allowed to air dry. The *(S,Z)*-methyl 2,5-bis(benzamido)-4-hydroxypent-4-enoate **(3b)** was obtained as a white solid (4.50 g; 95.5 %). Mp: 161-164 °C (literature 156-158 °C)[1]; ^{1}H NMR (400 MHz, $CDCl_3$) δ 9.93 (s, 1H, NH), 8.82 (s, 1H, NH), 8.21 – 7.72 (m, 4H, H-3' H-7' H-3" H-7"), 7.49-7.44 (m, 6H, H-4' H-5' H-6' H-4" H-5" H-6"), 7.14 (brs, 1H, OH), 6.81 (s, 1H, H-5), 5.10 – 4.80 (m, 1H, H-2), 3.83 (s, 3H, OCH_3), 2.95 (m, 2H, H-3). MS (EI^+) *m/z* calculated for $C_{20}H_{20}N_2O_5$ 368.1 found 367.8 ($[M]^+$; 1.3 %), 354.9 ($[M- H_2O]^+$; 9.1 %].

University of Cape Town

***(2S)*-2-amino-3-(2-mercapto-1*H*-imidazol-4-yl) propanoic acid (4)[1]**

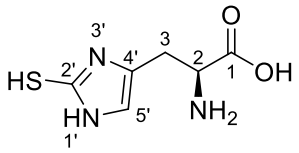

(*S*,*Z*)-methyl 2,5-bis(benzamido)-4-hydroxypent-4-enoate (**3b**) (4.5 g; 12 mmol) was dissolved in a mixture of concentrated HCl (31 ml, 32 %) and 26 ml of water. The resulting solution was allowed to stir at 90-93°C, for a 15 hr period, where-upon it was allowed to cool to 1-5°C. Benzoic acid (crystals) was obtained, which was filtered and washed with cold water (8 ml at 5°C) in order to remove the occluded product. The resulting aqueous solution was lyophilised to dryness. The crude residue was dissolved in water (12 ml) followed by the addition of KSCN (3.34 g, 34.4 mmol) and heating at 80-90°C for 4-5 hr. The solution was allowed to cool followed by treatment with sodium acetate (2.82 g). The mixture was kept at 5 °C overnight, after which the aqueous layer was separated and the pH adjusted with amberlyst 15 (H^+ form) (pH 5 to 1). The amberlyst 15 (H^+ form) was filtered and the filtrate lyophilised to dryness to give compound *(2S)*-2-amino-3-(2-mercapto-1*H*-imidazol-4-yl) propanoic acid **(4)** as a white powder (2.01 g; 87.8 %). Mp: 206-208°C (with decomposition) Literature 204-206°C (with decomposition)[4]; ν_{max} (KBr)/cm^{-1} 3465s + 1634s + 1129w (RNH_2 Free) 2073s (N=C-S) 1383m ($RCOO^-$), ^{1}H NMR (400 MHz, D_2O+DCl) δ 6.87 (s, 1H, H-5'), 4.31 (t, *J* = 6.6 Hz, 1H, H-2), 3.28 (dd, *J* = 16.1, 6.6 Hz, 1H, H-3a), 3.17 (dd, *J* = 16.1, 6.6 Hz, 1H, H-3b), Carboxylic acid and amine protons signals were exchanged with a D_2O. ^{13}C NMR (101 MHz, D_2O) δ 170.5 (C-1), 156.6 (C-2'), 123.3 (C-4'), 116.1 (C-5'), 51.9 (C-2), 25.4 (C-3). LRMS (EI^+) *m/z* calculated for $C_6H_9N_3O_2S$ 187.0 found 187.0 ($[M]^+$; 92.7 %).

***(2S)*-2-amino-3-(2-(*tert*-butylthio)-1*H*-imidazol-4-yl) propanoic acid (5) [1]**

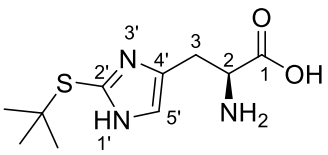

In distilled H_2O (18 ml) was added *(2S)*-2-amino-3-(2-mercapto-1*H*-imidazol-4-yl) propanoic acid **(4)** (2.27 g; 12.1 mmol), followed by the addition of *t*-butanol (2.34 g; 31.5 mmol) and concentrated hydrochloric acid (4 ml, 37 %). The resulting mixture was heated to 85-90°C and kept at this temperature for a 3 - 4 hr period. Subsequently, the reaction mixture was concentrated by lyophilisation. The free amino acid was liberated by adjusting the pH of the

University of Cape Town

solution to 5.0 with aqueous sodium acetate, followed by lyophilisation to dryness, where after the amino acid was extracted with warm 2-propanol. The product **(5)** was obtained as a yellow crystal (1.85 g; 62.7 %). $[\alpha]^{20}_D$ = +14.1° (*c* = 0.7, H_2O) lit.$[\alpha]^{25}_D$ = +13° (*c* = 1, H_2O)[1]; ν_{max} (KBr)/cm^{-1} 3448s + 1561s + 1051w (RNH_2 Free) 2237w (N=C-S) 1703m (RCOOH) 1337m (CH_3) 643 (S-R), ^{1}H NMR (400 MHz, D_2O) δ 7.60 (brs, 1H, H-5'), 4.18 (t, *J* = 3.0 Hz, 1H, H-2), 3.39 (dd, *J* = 11.0, 3.0 Hz, 1H, H-3a), 3.30 (dd, *J* = 11.0, 3.0 Hz, 1H, H-3b), 1.44 (s, 9H, *t-butyl*); LRMS (EI^+) *m/z* calculated for $C_{10}H_{17}N_3O_2S$ 243.1 found 243.1 ($[M]^+$; 4.2%), 199.1 ($[M–CO_2]^+$; 7.1 %), 142.0 ($[M–CO_2–C(CH_3)_3]^+$; 4.2%).

***(2S)*-3-(2-(*tert*-butylthio)-1*H*-imidazol-4-yl)-2-(dimethylamino) propanoic acid (6).[1]**

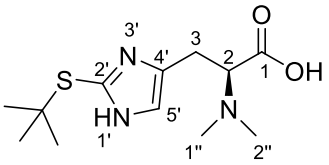

In a solution of THF (19 ml) was dissolved *(2S)*-2-amino-3-(2-(*tert*-butylthio)-1*H*-imidazol-4-yl) propanoic acid **(5)** (1.57 g, 6.45 mmol) followed by the addition of formalin (37 %, 2.04 g, 25.13 mmol) portion wise. The resulting mixture was allowed to equilibrate to room temperature and then sodium triacetoxyborohydride (3.76 g, 17.7 mmol) was added while the reaction temperature was maintained at 0-5°C. The resulting suspension was allowed to stir at 10°C for 6-8 hr. The reaction mixture was cooled to -10°C, and acidified with 2 N HCl (pH ≤1). The resulting solution was lyophilised and the residue was mixed with a 13 ml methanol followed by filtration of the undesired inorganic salts. The filtrate was lyophilised to yield the dihydrochloride salt. The free amine was liberated by triturating with aqueous sodium acetate to pH 5.0 evaporated to dryness, and extraction into 2-propanol, from where it was crystallized. The product **(6)** was obtained as colourless crystals (590 mg; 33.7 %). ^{1}H NMR (300 MHz, D_2O) δ 6.30 (s, 1H, H-5'), 3.45 (d, *J* = 10.7 Hz, 1H, H-2), 3.08 (m, 2H, H-3), 3.01 (s, 6H, H-1" H-2"), 1.50 (s, 9H, *t-butyl*).

University of Cape Town

Ergothioneine (8), (2*S*)-*N,N,N*-2-trimethylethanaminium (2-mercapto-1*H*-imidazol-4-yl) propanoic acid chloride salt (8).[1]

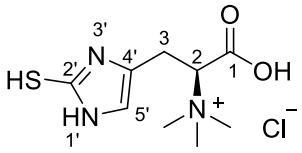

(S)-3-(2-(*tert*-butylthio)-1*H*-imidazol-4-yl)-2-(dimethylamino)propanoic acid **(6)** (590 mg; 1.71 mmol) was dissolved in MeOH (10 ml) and the pH was adjusted to 8.8-9.0 with ammonium hydroxide, followed by the addition of iodomethane (362 mg, 2.57 mmol) and the solution was allowed to stir at room temperature for 24 h. The mixture was concentrated under vacuum and the resulting white solid (ammonium chloride) was filtered and the cake was washed with methanol. The combined filtrates were evaporated to dryness to afford crude *S*-(*tert*-butyl) ergothioneine **(7).** In the presence of 2-mercaptopropionic acid (227 ml; 272 mg; 2.57 mmol), the crude product **(7)** was dissolved in 10 ml H_2O followed by the addition of HCl (7.25 ml, 32%). The resulting mixture was refluxed for 21 hours. After cooling the reaction mixture was extracted with EtOAc (4 x 25 ml) and then the aqueous layer was adjusted to pH 7 with a solution of ammonia (25% v/v) followed by lyophilisation. The residue was again extracted with ethyl acetate (4 x 30 ml) followed by partitioning in a mixture of distilled water: ethyl acetate 50:50 (v/v). The aqueous layer was retained and the organic phase discarded. The aqueous phase was lyophilised to dryness and the solid residue was allowed to stir overnight at room temperature in ethanol. The slurry was then filtered to afford the crude ergothioneine. *L*-(-)-ergothioneine **(8)** was recrystallized from a mixture of ethanol / water (10:1) to yield **(8)** as a white powder (107 mg; 27.3 % over 2 steps). Mp:276-279 °C literature 275-277°C; $[\alpha]^{20}_D$ = +138.21° (*c* = 1; H_2O)[1]; R_f silica gel 0.3 (methanol/water 9:1); ^{1}H NMR (400 MHz, D_2O) δ 7.05 (m, 1H, H-5'), 3.76 (dd, *J* = 11.7, 4.0 Hz, 1H, H-2), 2.88 (m, 2H, H-3), 2.75 (s, 9H, NMe_3); ^{13}C NMR (101 MHz, D_2O)δ 177.0 (C-1), 161.2 (C-2'), 128.9 (C-4'), 103.4 (C-5'), 60.6 (C-2), 55.6 (NMe_3), 24.9 (C-3); ν_{max} (KBr)/cm^{-1} 3138s (NH) 1746s (RCOOH), 1995m (N=C-S), 1403s (C=C aromatic ring); HRMS (ESI$^+$): *m/z* 230.0963 $[M]^+$. Calculated for $C_9H_{16}N_3O_2S^+$, found 230.0958 $[M]^+$.

University of Cape Town

[*(2S)*-*N*,*N*,*N*-2-trimethylamino-*d*$_3$-3-(2-mercapto-1*H*-imidazol-4-yl)propanoic acid (Deuterated ergothioneine) (9)

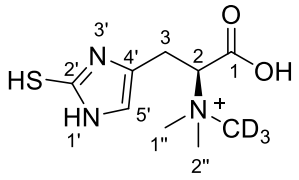

(2S)-3-(2-(*tert*-butylthio)-1*H*-imidazol-4-yl)-2-(dimethylamino)propanoic acid **(6)** (110 mg ; 0.405 mmol) was dissolved in MeOH (3 ml) and the pH was adjusted to 8.8-9.0 with ammonium hydroxide, followed by the addition of iodomethane deuterated (70 mg, 0.61 mmol) and the solution was allowed to stir at room temperature for 24 h. The mixture was concentrated under vacuum and the resulting white solid (ammonium chloride) was filtered and the cake was washed with methanol. The combined filtrates were evaporated to dryness to afford a crude, deuterated *S*-(*tert*-butyl) ergothioneine**.** In the presence of 2-mercaptopropionic acid (1.70 g; 16.1 mmol), crude deuterated *S*-(*tert*-butyl) ergothioneine was dissolved in 2 ml H_2O followed by the addition of HCl (1 ml, 32%). The resulting mixture was refluxed for 21 hours. After cooling the reaction mixture was extracted with EtOAc (3 x 15 ml) and then the aqueous layer was adjusted to pH 7 with a solution of ammonia (25 % v/v) followed by lyophilisation. The residue was again extracted with ethyl acetate (3 x 20 ml) followed by partitioning in a mixture of distilled water: ethyl acetate 50:50 (v/v). The aqueous layer was retained and the organic phase discarded. The aqueous phase was lyophilised to dryness. Purification by reverse chromatography (C18) and recrystallization afforded the product **(9)** as a yellow solid (127 mg; quantitative). Mp:158-160 °C (dec); ^{1}H NMR (400 MHz, D_2O) δ 6.95 (s, 1H, H-5'), 4.34 – 4.13 (m, 1H, H-2), 3.73 – 3.43 (m, 6H, H-1" H-2"), 3.41 (dd, *J* = 11.3, 8.5 Hz, 2H, H-3); ^{13}C NMR (101 MHz, D_2O)δ 180.3 (C-1), 134.9 (C-2'), 119.1 (C-4'), 115.8 (C-5'), 75.5 (C-2), 52.5 (C-1" C-2"), 22.7 (C-3); HRMS (ESI$^+$): *m/z* 233.1152 $[M]^+$. Calculated for $C_9H_{13}D_3N_3O_2S^+$, found 233.1161 $[M]^+$.

(*S*)-Methyl 2-(*tert*-butyloxycarbonylamino)-3-hydroxypropanoate (10) [5, 6, 7, 8]

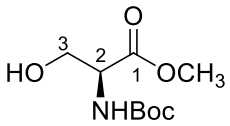

Acetoyl chloride (64.5 ml) was added dropwise to methanol (10 ml) with cooling, resulting in a concentrated solution of methanolic HCl. The solution was allowed to stir for 5 min and then the solid *(L)*-serine (5g; 47.58 mmol) was added in one portion and the solution heated

University of Cape Town

to reflux. After refluxing for 2 h, the reaction mixture was allowed to cool and the solvent removed by evaporation under reduced pressure to give the crude serine methyl ester hydrochloride as a colourless crystalline solid which was used without further purification (7.20 g; approx 100%). Serine methyl ester hydrochloride (7.20 g, 60.4 mmol) was suspended in THF (144 ml) followed by the addition of Et_3N (10.1 g; 99.7 mmol). The resulting suspension was cooled to 0°C and a solution of $(Boc)_2O$ (10.3 g, 47.2 mmol) in THF (72 ml) was added drop wise over 30 min. The mixture was allowed to warm to rt while stirring for 6 h, thereafter, the reaction temperature was raised to 50°C for further 2 h. The solvent was removed in vacuum, and the residue partitioned between Et_2O (100 ml) and H_2O (100 ml). The aqueous phase was extracted with Et_2O (4 x 40 ml) and the combined organic phases washed with 3 % HCl (80 ml), 5% $NaHCO_3$ (80 ml) and brine (100 ml). Dried over $MgSO_4$ and the solvent was evaporated to afford (*S*)-methyl 2-(*tert*-butyloxycarbonylamino)-3-hydroxypropanoate **(10)** as a colorless oil (7.58 g; 34.6 mmol; 72.6 %). ν_{max} $(CH_2Cl_2)/cm^{-1}$ 3607w + 1054s + 1340m (Primary alcohol) 3431m (R_2NH) 1742s + 1245s (RCOOMe); $[\alpha]^{20}_D$ = -25.7 (*c* = 5, MeOH), *L*-(-)-isomer literature $[\alpha]^{20}_D$ = -18 °(*c* = 5, MeOH) (Sigma Aldrich) and $[\alpha]^{20}_D$ = -18.9°(*c* = 5, MeOH)[5]; ^{1}H NMR (400 MHz, $CDCl_3$) δ 5.44 (brs, 1H, NH), 4.39 (br. s, 1H, H-2), 3.96 (dd, *J* = 4.0 Hz, 3.9 Hz, 3H, H-3a), 3.90 (dd, *J* = 3.9 Hz, 4.0 Hz, 1H, H-3b), 3.78 (s, 3H, OCH_3), 2.11 (brs, 1H, OH), 1.45 (s, 9H, Boc). LRMS (EI^+) *m/z* calculated for C_9H17NO_5 219.1 found 219.9 ($[M]^+$; 8.4 %), 119.9 ($[M - Boc]^+$; 30.9 %).

***(S)*-allyl 2-(*tert*-butyloxycarbonylamino)-3-hydroxypropanoate (11)** [9, 10]

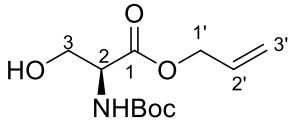

L-(-)-serine **(9)** (1.5 g; 14 mmol) was dissolved in a mixture of THF and 2M NaOH (20 ml; 1:1), and then Boc_2O (4.75g, 21.8 mmol) was added portionwise. The resulting reaction mixture was allowed to stir at room temperature until completion (ca 7h). The reaction mixture was diluted with water (100 ml) and extracted with EtOAc (3 x 50 ml). Subsequently the aqueous layer was adjusted to pH 3 using HCl (5%) followed by extraction with EtOAc (4 x 50 ml). The combined organic layers were dried over $MgSO_4$ and the solvent was evaporated under vacuum to afford yellow oil as crude *N*-Boc-serine, which was used in the next step without further purification.

The crude mixture (2.75 g; assumed to be 13.4 mmol) was dissolved in MeOH (20 ml) followed by the addition of Cs_2CO_3 (2.41 g; 7.39 mmol). The resulting mixture was allowed

University of Cape Town

to stir at room temperature for 3 hr and then the solvent was removed under vacuum. DMF (20ml) was added to the residue, followed by the addition of allylbromide (1.64 g; 13.6 mmol), the resulting reaction mixture was allowed to stir at room temperature for 20 hr. The cesium salts were filtered through celite and the DMF filtrate was evaporated to dryness, whereby EtOAc (50 ml) was added and the organic layer was washed with an aqueous solution of 5% citric acid (2 x 25 ml), followed by brine (3 x 25 ml). The ethyl acetate layer was dried over $MgSO_4$, filtered, and then evaporated under vacuum. The crude product was purified by flash chromatography on silica gel (hexane: EtOAc 3:1 to 1:1) to afford *(S)*-allyl 2-(*tert*-butyloxycarbonylamino)-3-hydroxypropanoate **(11)** as a light yellow oil (2.10 g; 8.56 mmol; 60.0 % over 2 steps); ^{1}H NMR (400 MHz, $CDCl_3$) δ 5.91 - 5.76 (m, 1H, H-2') 5.39 (m, 1H, NHBoc) 5.22 (dq, *J* = 11.2, 1.5 Hz, 2H, H-3') 4.46 - 4.34 (m, 2H, H-1') 4.07 - 4.14 (m, 1H, H-2) 3.78 (dd, *J* = 10.0, 3.2 Hz, 1H, H-3a) 3.66 (dd, *J* = 10.0, 3.2 Hz, 1H, H-3b) 1.45 (s, 9H, Boc).

***(S)*-Methyl 2-(*tert*-butoxycarbonylamino)-3-chloropropanoate (12)** [9, 11]

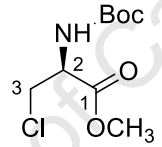

2, 4, 6-Trichloro-[1, 3, 5] triazine (1.87 g; 10.1 mmol) was added portion wise in DMF (2ml) at an internal temperature was maintained at 25 °C. After the formation of a white solid, the reaction was monitored (TLC) until complete disappearance of TCT, thereafter CH_2Cl_2 (25 ml) was added, followed by the addition of *(S)*-methyl 2-(*tert*-butyloxycarbonylamino)-3-hydroxypropanoate **(10)** (2.22 g; 10.1 mmol). The resultant mixture was allowed to stir at room temperature, monitored (TLC pet-ether: EtOAc, 1:1) until completion (ca 4 h). The reaction mixture was diluted with water (20 ml) and washed with saturated aqueous sodium carbonate solution (2 × 15 ml) followed by 1 N HCl and brine. The combined organic phases were dried (Na_2SO_4), filtered and concentrated under vacuum. The residue was purified by flash column chromatography (petroleum ether: EtOAc 1:1) and was crystallized and recrystallized in a mixture of petroleum ether (40-60°C) and ethyl acetate to afford *(S)*-methyl 2-(*tert*-butoxycarbonylamino)-3-chloropropanoate **(12)** as a white solid (736 mg; 30.5 %). Mp: 59-61 °C; ν_{max} (KBr) / cm^{-1} 3362s (NH) 2991s + 2943s (C-H, aliphatic) 1739s 1294s (RCOOMe) 809s + 852m (C-Cl); $[\alpha]^{20}_D$ = +32.5° (*c* = 0.15; $CHCl_3$); ^{1}H NMR (300 MHz, $CDCl_3$) δ 5.43 (s, 1H, NH), 4.69 (br.s, 1H, H-2), 3.96 (dd, *J* = 4.6 Hz, 3.4 Hz, 1H, H-3a), 3.84

University of Cape Town

(dd, *J* = 4.6 Hz, 3.4 Hz, 1H, H-3b), 3.80 (s; 3H, OCH_3), 1.46 (s, 9H, Boc); LRMS $(EI)^+$ *m/z* calculated for $C_9H_{15}Cl^{35}NO_4$ 236.1 found 235.8 ($[^{35}M\text{-}H]^+$; 5.3 %), 138.0 ($[^{35}M^+$- Boc]; 11 %), 140.0 ($[^{37}M^+$- Boc]; 2.6 %).

***(R)*-Methyl 2-(*tert*-butoxycarbonylamino)-3-chloropropanoate (13) [11]**

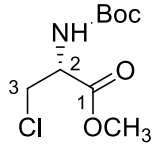

2, 4, 6-Trichloro-[1, 3, 5] triazine (1.83 g; 10.0 mmol) was added portionwise in DMF (2ml) at an internal temperature of 25 °C. After the formation of a white solid, the reaction was monitored (TLC) until complete disappearance of TCT, thereafter CH_2Cl_2 (25 ml) was added, followed by the addition of *β*-hydroxyl, [(*tert*-butoxycarbonyl) amino] -α, methyl propionate (2.20 g; 10.0 mmol). The resultant mixture was allowed to stir at room temperature, monitored (TLC pet-ether: EtOAc, 1:1) until completion (ca 4 h) The reaction mixture was diluted with water (20 ml) and washed with saturated aqueous sodium carbonate solution (2 × 15 ml) followed by 1 N HCl and brine. The combined organic phases were dried (Na_2SO_4), filtered and concentrated under vacuum. The residue was purified by flash column chromatography (petroleum ether: EtOAc, 1:1) and was crystallized and recrystallized in a mixture of petroleum ether (40-60°C) and ethyl acetate to afford *(R)*-methyl 2-(*tert*-butoxycarbonylamino)-3-chloropropanoate **(13)** as a white crystal (336 mg; 14.14 %) Mp: 60-62°C; ν_{max} (KBr)/cm^{-1} 3367s (NH) 2985s (C-H, aliphatic) 1745s + 1245s (RCOOMe) 849m + 875m (C-Cl); $[\alpha]^{20}_D$ = -35.7° (*c* = 1, $CHCl_3$), *D*-(-)-isomer, ^{1}H NMR (400 MHz, $CDCl_3$) δ 5.41 (brs, 1H, NH), 4.74 – 4.67 (m, 1H, H-2), 3.97 (dd, *J* = 8.3, 3.4 Hz, 1H, H-3a), 3.84 (dd, *J* = 8.4, 3.3 Hz, 1H, H-3b), 3.80 (s, 3H, OCH_3), 1.45 (s, 9H, Boc); ^{13}C NMR (101 MHz, $CDCl_3$) δ 169.6 (C-1), 155.0 (C=O (Boc)), 80.5 (C(Boc)), 54.5 (C-2), 52.8 (C-OCH_3), 45.5 (C-3), 28.3 (3C,(Boc)); LRMS $(EI)^+$ *m/z* calculated for $C_9H_{15}{}^{35}ClNO_4$ 236.1 found 236.1 ($[^{35}M\text{-}H]^+$; 3.5 %), 135.9 ($[^{35}M^+$- Boc]; 2.6 %).

***(R)*-allyl 2-(*tert*-butoxycarbonylamino)-3-chloropropanoate (14)[11, 12]**

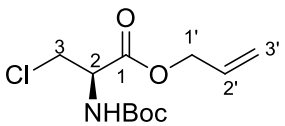

2, 4, 6-Trichloro-[1, 3, 5] triazine (577 mg; 3.13 mmol) was added portion wise in DMF (1ml) at an internal temperature was maintained at 25 °C. After the formation of a white

University of Cape Town

solid, the reaction was monitored (TLC) until complete disappearance of TCT, thereafter CH_2Cl_2 (20 ml) was added, followed by the addition of *(S)*-allyl 2-(*tert*-butyloxycarbonylamino)-3-hydroxypropanoate **(11)** (768 mg; 3.13 mmol). The resultant mixture was allowed to stir at room temperature, monitored (TLC pet-ether: EtOAc, 2:1) until completion (ca 10 h) The reaction mixture was diluted with water (20 ml) and washed with saturated aqueous sodium carbonate solution (2 × 15 ml) followed by 1 N HCl and brine. The combined organic phases were dried (Na_2SO_4), filtered and concentrated under vacuum. The residue was purified by flash column chromatography (petroleum ether: EtOAc 2:1) to afford *(R)*-allyl 2-(*tert*-butoxycarbonylamino)-3-chloropropanoate **(14)** as a yellow oil (729 mg; 2.76 mmol; 88.5 %); $[\alpha]^{20}_D$ = +23.94° (*c* = 0.35, CH_2Cl_2); R_f 0.75 (hexane/EtOAc 2: 1); ^{1}H NMR (400 MHz, $CDCl_3$) δ 5.91 – 5.75 (m, 1H, H-2'), 5.37 (brs, 1H, NH), 5.27 – 5.12 (m, 2H, H-3'), 4.52 - 4.45 (m, 2H, H-1') 4.39 - 4.30 (m, 1H, H-2), 3.96 (dd, *J* = 8.1, 3.8 Hz, 1H, H-3a), 3.91 (dd, *J* = 8.1, 3.8 Hz, 1H, H-3b), 1.45 (s, 9H, Boc); ^{13}C NMR (101 MHz, $CDCl_3$)δ 171.3 (C-1), 154.3 (C=O Boc), 114.1 (C-2'), 72.4 (C-3'), 70.1 (C(Boc)), 63.7 (C-2), 52.7 (C-1'), 30.5 (C-3), 28.4 (3C, (Boc)); LRMS (EI^+) *m/z* calculated for $C_6H_8ClNO_2$ 161.0 for Cl^{35} and 162.0 for Cl^{37} found 160.1 ([M Cl^{35}-Boc - H]$^+$; 30 %), 162.1 ([M Cl^{37}-Boc - H]$^+$, 10 %); 133.0 ([M Cl^{35} - Boc – CH_2=CH_2 - H]$^+$; 100 %).

***(2S)*-Methyl 2-(dimethylamino)-3-(1*H*-imidazol-4-yl) propanoate (15)[13, 14, 15]**

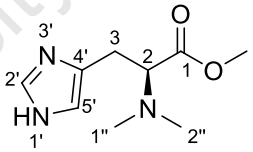

Histidine methyl ester dihydrochloride (1.5 g; 6.2 mmol) was dissolved in a solution of THF (20 ml), followed by the addition in one portion of formaldehyde (37.0 %; 650 mg; 21.7 mmol). The resulting mixture was allowed to equilibrate to room temperature and sodium triacetoxyborohydride (2.62 g; 12.4 mmol) was added at an internal temperature was maintained at 0-5°C and acetic acid glacial (200 µl) was added as a catalyst. The solution was allowed to stir at room temperature for 18-24 h period. The reaction was quenched with 20 ml of saturated $NaHCO_3$, extracted with EtOAC (5 x 25 ml), and the remaining water layer was retained for recycling. The organic layer was separated, washed with brine, dried (anhydrous $MgSO_4$) and filtered. The filtrate was evaporated under vacuum. The resultant oil was purified by silica gel chromatography (CH_2Cl_2: MeOH 80:20) to afford (*S*)-Methyl 2-(dimethylamino)-3-(1*H*-imidazol-4-yl) propanoate **(15)** as a yellowish oil (1.02 g; 83.6 %).

University of Cape Town

ν_{max} (CH_2Cl_2) / cm^{-1} 3456w + 1604m (N-H) 1277 (C-N) 1733m + 1255s (RCOOMe); $[\alpha]^{20}_D$ = + 0.6° (*c* = 6.77, CH_2Cl_2); ^{1}H NMR (400 MHz, $CDCl_3$) δ 7.85 (s, 1H, H-2'), 6.99 (brs, 1H, NH), 6.90 (s, 1H, H-5'), 3.69 (s, 3H, OCH_3), 3.55 (t, *J* = 7.5 Hz, 1H, H-2), 3.08 (dd, *J* = 15.3, 7.5 Hz, 1H, H-3a), 2.98 (dd, *J* = 15.3, 7.5 Hz, 1H, H-3b), 2.39 (s, 6H, H-1" H-2"); ^{13}C NMR (101 MHz, $CDCl_3$)δ 171.5 (C-1), 133.9 (C-2'), 131.5 (C-4'), 118.8 (C-5'), 67.0 (C-2), 51.4 (C-OCH_3), 41.6 (C-1" C-2"), 25.5 (C-3); LRMS (EI^+) *m/z* calculated for $C_9H_{15}N_3O_2$ 197.1 found 197.1 ($[M]^+$; 4.3 %) 136.1 ($[M\text{-}COOCH_3]^+$; 66.4 %).

(2*S*)-Methyl *N*,*N*,*N*-2-trimethylethanaminium-3-(1*H*-imidazol-4-yl) propanoate (16) [13]

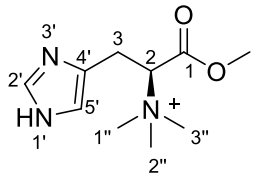

(S)-Methyl 2-(dimethylamino)-3-(1*H*-imidazol-4-yl) propanoate **(15)** (217 mg; 1.10 mmol) was dissolved in methanol (20 ml), and the pH was adjusted to 8-9 with a concentrated solution of NH_4OH (25 %, 40 µl), followed by the addition of methyl iodide (250 mg; 1.76 mmol). The resultant solution was allowed to stir at room temperature for 24 hours. The solvent was evaporated to dryness to afford a crude product **(16)** which was recrystallized in a mixture of warm methanol and diethyl ether to afford (2*S*)-methyl *N*,*N*,*N*-2-trimethylethanaminium-3-(1*H*-imidazol-4-yl) propanoate **(16)** as a yellow crystal (87 mg; 37 %); Mp: 223-225 °C (245 °C dec);^{1}H NMR (400 MHz, DMSO) δ 8.98 (s, 1H, H-2'), 8.44 (brs, 1H, NH), 7.44 (s, 1H, H-5'), 4.89 – 4.81 (m, 1H, H-2), 3.67 (s, 3H, OCH_3), 3.32 (s, 9H, H-1" H-2" H-3"), 3.15 (dd, *J* = 9.8, 3.4 Hz, 1H, H-3a) 3.05 (dd, *J* = 9.8, 3.4 Hz, 1H, H-3b); ^{13}C NMR (101 MHz, DMSO)δ 166.8 (C-1), 135.2 (C-2'), 126.9 (C-5'), 118.3 (C-4'), 72.6 (C-2), 52.7 (C-OCH_3),40.0 (3C, C-1"C-2"C-3"overlapped by DMSO-d_6 signal), 23.0 (C-3); LRMS (EI+) *m/z* calculated for $C_{10}H_{19}N_3O_2^+$ 213.1 $[MH]^+$ found 213.0 ($[MH]^+$; 1.0 %), 141.8 ($[M\text{-}COOCH_3\text{-}2\ CH_3]^+$; 100 %).

University of Cape Town

(2*S*)-*N*,*N*,*N*-2-trimethylethanaminium-3-(1*H*-imidazol-4-yl)propanoic acid (17), *L*-hercynine (17)[14]

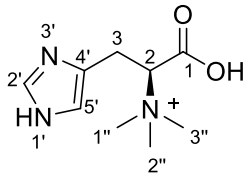

(S)-3-(1*H*-imidazol-4-yl)-1-methoxy-*N*,*N*,*N*-trimethyl-1-oxopropan-2-aminium **(16)** (653 mg; 3.08 mmol) was dissolved 6 N HCl (40 ml) and the solution was allowed to reflux overnight. Where upon the solution was allowed to cool at room temperature, thereafter the volatile components were removed under vacuum. The residue was dissolved in a minimum amount of water (20 ml), treated with a charcoal, filtered through celite, washed with water (3 x 10 ml) and the combined aqueous extracts were lyophilised to dryness. The crude solid was recrystallized in a mixture of warm methanol and diethyl ether to yield dihydrochloride salt form of *L*-hercynine (**17)** as a white solid (489 mg; 60.0 %). Mp: 240-242°C (with decomposition) Lit. 237-239 °C (with dec)[13]; ν_{max} KBr /cm^{-1} 3435s (N-H) 1632m (RCOOH) 1496 w (C=C Aromatic) 1335w (C-N); $[\alpha]^{20}_{D}$ = +48.7° (*c* = 0.9, 5 N HCl); ^{1}H NMR (400 MHz, D_2O) δ 8.76 (s, 1H, H-2'), 7.51 (d, *J* = 12.7 Hz, 1H, H-5'), 4.02 – 3.83 (m, 1H, H-2), 3.49 (s, 9H, H-1"H-2"H-3"), 3.12 (dd, *J* = 12.7, 4.1 Hz, 1H, H-3a) 3.06 (dd, *J* = 12.7, 4.1 Hz, 1H, H-3b) ^{13}C NMR (101 MHz, D_2O)δ 166.8 (C-1), 135.5 (C-2'), 134.3 (C-5'), 118.3 (C-4'), 72.7 (C-2), 53.0 (C-1"C-2"C-3"), 22.3 (C-3); LRMS (EI+) *m/z* calculated for $C_9H_{17}N_3NaO_2^+$ 223.1 found 223.6 ([M+H+Na]$^+$; 20.4%).

Hercynine (17) synthesis (one pot) [16]

L-histidine (293 mg; 1.6 mmol) was dissolved in NaOH (10 %, 4 ml) followed by the addition of Me_2SO_4 (0.4 ml; 532 mg; 4.2 mmol). The reaction was allowed to stir for 30 min at 0°C and for further 30 min at room temperature. The solution was neutralized with 0.5 N HCl, and lyophilised to dryness. The residue was triturated with Et_2O, to yield the *L*-hercynine (**17)** as white solid (300 mg; 94.6 %), which was used without further purification.

University of Cape Town

(2*S*)-*N*,*N*,*N*-2-trimethylamino-d_3-3-(1*H*-imidazol-4-yl)propanoic acid (deuterated hercynine) (18)

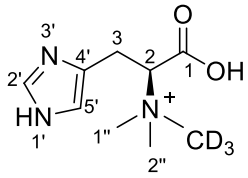

L-histidine (200 mg; 1.29 mmol) was dissolved in CH_3CN (10 ml), followed by the addition in one portion of formaldehyde (37 %; 157 mg; 145 µl; 1.93 mmol. The solution was allowed to equilibrate to room temperature, thereafter sodium triacetoxyborohydride (615 mg; 2.90 mmol) and acetic acid glacial (73 µl) were added at an internal temperature was maintained at 0-5°C. The resulting solution was allowed to stir at room temperature for 18-24 h period. The reaction was quenched with 5 ml of HCl 5 % to pH ≤ 1 and then extracted with EtOAC (5 x 20 ml), the remaining water layer was retained for recycling. The organic layer was separated, washed with brine, dried (anhydrous $MgSO_4$) and filtered. The filtrate was evaporated under vacuum to obtain crude *N*,*N*-dimethyl *L*-histidine which was used without further purification.

To the crude *N*,*N*-dimethyl *L*-histidine (374; assumed to be 2.023 mmol) dissolved in MeOH (5 ml) adjusted to pH 9-10 with a solution of concentrated ammonia (25%), followed by the addition of methyl iodate deuterated (489 mg; 3.034 mmol). The solution was allowed to stir at room temperature for 24 hours. The solvent was evaporated under high vacuum to dryness. Reverse phase chromatography (C18) and recrystallization in mixture of warm EtOH/H_2O afforded deuterated hercynine (**18)** as a yellow solid (249 mg; 61.3%); Mp: 142-145 °C (dec); ^{1}H NMR (400 MHz, D_2O) δ 8.70 (s, 1H, H-2'), 7.45 (s, 1H, H-5'), 4.44 (d, *J* = 7.7 Hz, 1H, H-2), 3.74 – 3.30 (m, 8H, H-1" H-2" & H-3); HRMS (ESI$^+$): *m/z* 201.1431 $[M]^+$.Calculated for $C_9H_{13}D_3N_3O_2^+$ found 201.1414 $[M]^+$.

***(2S)*-*N*,*N*,*N*-2-trimethylammonium-3-[2-((2*R*)-2-(*tert*-butoxycarbonylamino)-3-methoxycarbonyl)- ethylthio)-1*H*-imidazol-4-yl)] propanoic acid (19) [17]**

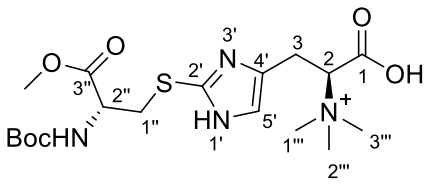

N-Boc-*β*-chloro-*L*-alanine methyl ester **(12)** (93 mg; 0.39 mmol) was dissolved in a mixture of DCM: H_2O (50:50; 4 ml) followed by the addition of Et_3N (0.4 mL) which adjusted the pH

University of Cape Town

of the solution to 9-10. The resulting mixture was allowed to stir at room temperature for 30 min and subsequently followed by the addition of ergothioneine **(8)** (89 mg; 0.34 mmol). The solution was allowed to stir at 30 °C for 5 hours. The solvent was removed under high vacuum to dryness and the crude product was purified by reverse chromatography (C18) to afford *(2S)-N,N,N*-2-trimethylammonium-3-[2-((2*R*)-2-(*tert*-butoxycarbonylamino)-3-methoxycarbonyl)- ethylthio)-1*H*-imidazol-4-yl)] propanoic acid **(19)** as a pale yellow solid (92 mg; 0.20 mmol; 51%); ^{1}H NMR (400 MHz, D_2O) δ 5.95 (s, 1H, H-5'), 4.51 - 4.43 (m, 1H, H-2), 4.27 - 4.19 (m, 2H, H-1''), 4.10 (dd, *J* = 10.0, 4.0 Hz, 1H, H-3a) 4.05 (dd, *J* = 10.0, 4.0 Hz, 1H, H-3b), 3.36 - 3.25 (m, 1H, H-2''), 2.49 (s, 3H, OCH_3), 1.59 (s, 9H, H-1''' H-2''' H-3'''), 1.56 (s, 9H, Boc); LRMS *m/z* calculated for $C_{18}H_{31}N_4O_6S^+$ 431.2 found 431.8 ([M^+]; 2.5 %).

***(2S)-N,N,N*-2-trimethylammonium-3-[2-((2*S*)-2-(*tert*-butoxycarbonylamino)-3-methoxycarbonyl)- ethylthio)-1*H*-imidazol-4-yl)] propanoic acid (20)** [17]

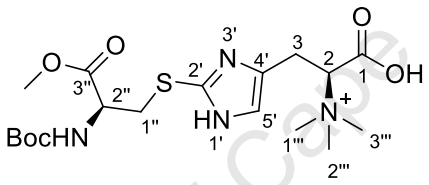

N-Boc-*β*-chloro-*D*-alanine methyl ester **(13)** (54 mg; 0.23 mmol) was dissolved in a mixture of DCM: H_2O (50:50; 3 ml) followed by the addition of Et_3N (0.3 ml) which adjusted the pH of the solution to 9-10. The resulting mixture was allowed to stir at room temperature for 30 min and subsequently followed by the addition of ergothioneine **(8)** (61 mg; 0.23 mmol). The solution was allowed to stir at 30 °C for 5 hours. The solvent was removed under high vacuum to dryness and the crude product was purified by reverse chromatography (C18) to afford *(2S)-N,N,N*-2-trimethylammonium-3-[2-((2*S*)-2-(*tert*-butoxycarbonylamino)-3-methoxycarbonyl)- ethylthio)-1*H*-imidazol-4-yl)] propanoic acid **(20)** as a yellow very hygroscopic solid (36 mg; 0.08 mmol; 33 %); ^{1}H NMR (400 MHz, D_2O) δ 6.22 - 6.28 (m, 1H, H-5') 3.16 - 3.25 (m, 9H, H-1''' H-2''' H-3''') 1.45 (s, 3H, OCH_3) 1.29 (s, 9H, Boc). Other signals were overlapped by huge water peak; LRMS (EI$^+$) *m/z* calculated for $C_{18}H_{31}N_4O_6S^+$ 431.2 found 431.2 ([M] $^+$; 1.9 %).

University of Cape Town

***(2S)-N,N,N*-2-trimethylammonium-3-[2-((2*R*)-2-(*tert*-butoxycarbonylamino)-3-allyloxycarbonyl)- ethylthio)-1*H*-imidazol-4-yl)] propanoic acid (21)** [17]

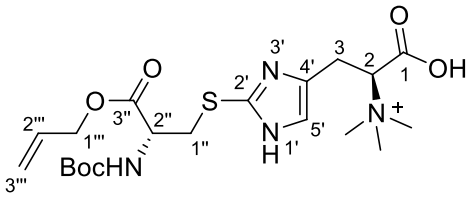

N-Boc-*β*-chloro-*L*-alanine allyl ester **(14)** (728 mg; 2.76 mmol) was dissolved in a mixture of THF:H_2O (66:34; 15 ml) followed by the addition of Et_3N (0.5 ml) which adjusted the pH of the solution to 9-10. The solution was allowed to stir at room temperature for 30 min and subsequently followed by the addition of ergothioneine **(8)** (729 mg, 2.76 mmol). The solution was allowed to stir at 30 °C for 5 hours. The solvent was removed under high vacuum to dryness and the crude product was purified by reverse chromatography (C18) to afford *(2S)-N,N,N*-2-trimethylammonium-3-[2-((2*R*)-2-(*tert*-butoxycarbonylamino)-3-allyloxycarbonyl)- ethylthio)-1*H*-imidazol-4-yl)] propanoic acid **(21)** as yellow hygroscopic solid (1.12 g; 2.27 mmol; 82.4%). Mp: 195-197 °C; ν_{max} (CH_2Cl_2)/cm^{-1}) 3350m (NH) 1732s + 1163s + 1046 (RCOOR) 895s (N=C-S); ^{1}H NMR (300 MHz, DMSO) δ 6.88 (brs, 1H, H-5'), 5.98 – 5.80 (m, 1H, H-2'''), 5.32 (dd, *J* = 10.3 ,1.5 Hz, 1H, H-3'''a), 5.20 (dd, *J* = 10.3, 1.5 Hz, 1H, H-3'''b), 4.95 (m, 1H, H-2''), 4.58 (t, *J* = 7.8 Hz, 1H, H-2), 4.07 (m, 2H, H-1''), 3.66 (t, *J* = 4.8 Hz, 2H, H-1'''), 3.05 (s, 9H, NMe), 2.98 (m, 2H, H-3), 1.38 (s, 9H, Boc); ^{13}C NMR (101 MHz, DMSO) δ 171.1 (C-3''), 155.7 (C-1, C=O(Boc)), 132.8 (C-2', C-3'''), 117.7 (C-2''', C-4') 111.4 (C-5'), 78.7 (C-2), 65.0 (*C*(Boc)), 61.6 (C-1'''), 56.8 (C-2''), 45.8 (C-1''), 44.2 (NMe_3), 28.5 (3C(Boc)), 18.9 (C-3).

***(2S)-N,N,N*-2-trimethylammonium-3-[2-((*R*)-2-(*tert*-butoxycarbonylamino)-3-hydroxycarbonyl)- ethylthio)-1*H*-imidazol-4-yl)] propanoic acid (22)** [18]

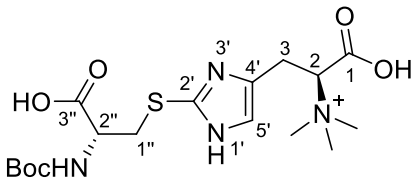

(2S)-N,N,N-2-trimethylammonium-3-[2-((2*R*)-2-(*tert*-butoxycarbonylamino)-3 allyloxycarbonyl)-ethylthio)-1*H*-imidazol-4-yl)] propanoic acid **(21)** (304 mg; 0.617 mmol) was dissolved in a mixture of EtOH: H_2O (80:20, 6 ml) followed by the addition of $RhCl(PPh_3)_3$ (17mg; 0.019 mmol). The solution was allowed to reflux at 90°C for overnight. The solvent was evaporated under high vacuum to dryness. The crude product was purified

University of Cape Town

by reverse chromatography (C18) to afford *(2S)-N,N,N*-2-trimethylammonium-3-[2-((2*R*)-2-(*tert*-butoxycarbonylamino)-3-hydroxycarbonyl)-ethylthio)-1*H*-imidazol-4-yl)]propanoic acid **(22)** as a yellow solid (252 mg; 90.1%). Mp: 267-270°C (277°C dec); ν_{max} (KBr)/cm^{-1} 3139s (NH) 2939s (C-H) 1744s (COOH) 1401vs (C=C aromatic ring)1168w (RNH) 664w (S-R alkyl); ^{1}H NMR (400 MHz, DMSO) δ 7.50 (s, 1H, H-5'), 3.15 (s, 1H, H-2"), 3.04 (s, 9H, NMe_3), 1.21 (s, Boc). Others signals were overlapped by huge H_2O signal 3.35-3.30 (brs, 5H, H-1" H-3-H-2). ^{13}C NMR (101 MHz, DMSO)δ 158.0 (C-3" C-1), 123.0 (C-2'), 115.5 (C-4', C-5'), 74.0 (C-2), 67.8 (C(Boc)), 45.7 (NMe_3), 36.6 (C-2"), 28.8 (C-1"), 18.8 (C-3). Boc signals were overlapped by DMSO peaks (40.6 - 39.3 ppm); LRMS (EI^+) *m/z* calculated for $C_{17}H_{29}N_4O_6S^+$ 417.2 found 379.3 ([M- $2H_2O$ – 2H] $^+$; 1.8 %); 351.3 ([M- CO]$^+$; 1.4 %)

_(2S)-N,N,N_-2-trimethylammonium-3-[2-((2_R_)-2-(_tert_-butoxycarbonylamino)-3-hydroxycarbonyl)- ethylthio)-1_H_-imidazol-4-yl)] propanoic acid (23)

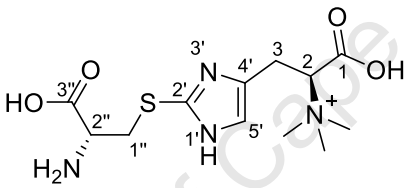

(2S)-N,N,N-2-trimethylammonium-3-[2-((2*R*)-2-(*tert*-butoxycarbonylamino)-3-hydroxycarbonyl)-ethylthio)-1*H*-imidazol-4-yl)] propanoic acid **(22)** (135 mg; 0.298 mmol) was dissolved in a mixture of H_2O:DCM (50:50, 4 ml) followed by the addition of TFA (5 ml) with cooling in a ice bath (0-5°C). The solution was allowed to stir at room temperature for 20 hours, the solvent was evaporated under high vacuum to dryness, and the residue was treated with Et_2O to remove any by product of the reaction. Purification by reverse chromatography (C18) afforded *(2S)-N,N,N*-2-trimethylammonium-3-[2-((2*R*)-2-(*tert*-butoxycarbonylamino)-3-hydroxycarbonyl)- ethylthio)-1*H*-imidazol-4-yl)] propanoic acid **(23)** as pale yellow hygroscopic solid (100 mg; 0.283 mmol; 95.2 %); Mp:162-165°C; ν_{max} (KBr)/cm^{-1} 3409 br.m (RNH_2, amine) 3142 br.m (OH) 3024 (C-H, aromatic ring) 1675vs (C=O) 598w (R-S, sulfur); ^{1}H NMR (400 MHz, D_2O) δ 7.62 (s, 1H, H-5'), 4.11 – 4.01 (m, 1H, H-2), 3.91 (t, *J* = 9.6 Hz, 1H, H-2"), 3.30-3.20 (s, 9H, NMe_3), 3.15 (dd, *J* = 9.6, 4.1 Hz, 1H, H-3a), 2.90 (dd, *J* = 9.6, 4.1 Hz, 1H, H-3b), 2.82 (m, 2H, H-1"); LRMS (EI^+) *m/z* calculated for $C_{12}H_{21}N_4NaO_4S^+$ 341.1 found 341.0 ([MH +Na]$^+$; 1.1 %); 288.3 ([M - CO_2]$^+$; 1.9 %).

University of Cape Town

***(2S)-N,N,N*-2-trimethylammonium-3-[2-((2*R*)-2-(*tert*-butoxycarbonylamino)-3-methoxycarbonyl)- ethylsulfinyl)-1*H*-imidazol-4-yl)] propanoic acid (24)**

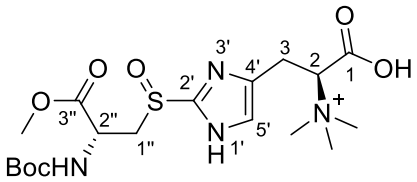

(2S)-N,N,N-2-trimethylammonium-3-[2-((2*R*)-2-(*tert*-butoxycarbonylamino)-3 methoxycarbonyl)-ethylthio)-1*H*-imidazol-4-yl)] propanoic acid **(19)** was dissolved in a mixture of H_2O: DCM (50:50; 4 ml) followed by the addition of *m*CPBA (13 mg; 0.06 mmol; 77 %). The solution was allowed to stir at 0-5°C for 3-5 hours until completion (TLC). The solution was partitioned in a separator funnel, water layer was returned and organic layer discarded. Water layer was treated with amberlyst (H^+ form) to neutral and then extracted with DCM to remove any organic impurities. Water layer was returned and lyophilised to dryness. The residue was purified by reverse phase chromatography (C18) to afford *(2S)-N,N,N*-2-trimethylammonium-3-[2-((2*R*)-2-(*tert*-butoxycarbonylamino)-3-methoxycarbonyl)-ethylsulfinyl)-1*H*-imidazol-4-yl)] propanoic acid (**24)** as a pale yellow crystal (25 mg; 0.06 mmol; 96 %). ^{1}H NMR (400 MHz, D_2O) δ 6.10 (s, 1H, H-5') 4.07 (brs., 1H, H-2) 3.89 (m, 2H, H-3) 3.77 (s, 3H, OCH_3) 3.72 -3.67 (m, 1H, H-2") 3.60 (dd, *J* = 11.72, 6.41 Hz, 1H, H-1"a) 3.42 (dd, *J* = 11.72, 6.41 Hz, 1H, H-1"b) 2.98 (s, 9H, NMe_3) 1.47 (s, 9H, Boc); MS (EI^+) *m/z* calculated $C_{18}H_{31}N_4O_7S^+$ 447.2 found 450.4 ($[M + 3H]^+$, 1.5 %)

***(2S)-N,N,N*-2-trimethylammonium-3-[2-((2*S*)-2-(*tert*-butoxycarbonylamino)-3-methoxycarbonyl)- ethylsulfinyl)-1*H*-imidazol-4-yl)] propanoic acid (25) [19]**

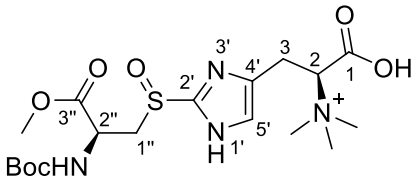

(2S)-N,N,N-2-trimethylammonium-3-[2-((2*S*)-2-(*tert*-butoxycarbonylamino)-3-methoxycarbonyl)-ethylthio)-1*H*-imidazol-4-yl)] propanoic acid **(20)** (20 mg; 0.046 mmol) was dissolved in a mixture of H_2O: DCM (50:50; 4 ml) followed by the addition of *m*CPBA (10 mg; 0.05 mmol; 77 %). The resulting solution was allowed to stir at 0-5°C for 5 hours, as indicated by TLC (completion). The solution was partitioned in a separator funnel, the water layer was returned and organic layer discarded. Water layer was treated with amberlyst (H^+ form) to neutral and then extracted with DCM to remove any organic impurities. Water layer

University of Cape Town

was returned and lyophilised to dryness, the residue was purified by reverse phase chromatography (C18) to afford compound *(2S)-N,N,N*-2-trimethylammonium-3-[2-((2*S*)-2-(*tert*-butoxycarbonylamino)-3-methoxycarbonyl)-ethylsulfinyl)-1*H*-imidazol-4-yl)] propanoic acid **(25)** as a white crystal (15 mg; 0.026 mmol; 73%); ^{1}H NMR (400 MHz, D_2O) δ 6.47 (s, 1H, H-5'), 4.10 – 4.05 (m, 2H, H-1"), 3.92 (s, 3H, OCH_3), 3.88 – 3.84 (m, 1H, H-2"), 3.75 (dd, *J* = 11.7, 3.7 Hz, 1H, H-3a), 3.67 (dd, *J* = 11.7, 3.7 Hz, 1H, H-3b), 3.45 – 3.41 (m, 1H, H-2), 3.06 (s, 9H, NMe_3), 1.46 (s, 9H, Boc).

(2*S*)-*N,N,N*-2-trimethylammonium-3-[2-((2*R*)-2-amino-2-methoxycarbonyl) ethylsulfinyl)- 1*H*-imidazol-4-yl] propanoic acid (26).

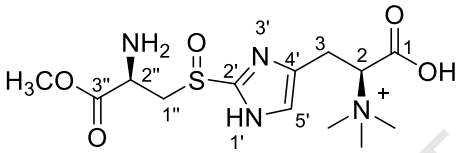

(2S)-N,N,N-2-trimethylammonium-3-[2-((2*R*)-2-(*tert*-butoxycarbonylamino)-3-methoxycarbonyl)-ethylsulfinyl)-1*H*-imidazol-4-yl)] propanoic acid **(24)** (45 mg, 0.10 mmol) was dissolved **i**n distilled H_2O (1 ml) followed by the addition of trifluoroacetic acid (1 ml) with cooling in a ice bath. The solution was allowed to stir at 0-5°C until completion (monitored by TLC). The solvent was concentrated by lyophilisation and the residue was extracted with DCM to remove any by product and lyophilised to dryness. The crude product was crystallized in ethanol to afford (2*S*)-*N,N,N*-2-trimethylammonium-3-[2-((2*R*)-2-amino-2-methoxycarbonyl)ethylsulfinyl)-1*H*-imidazol-4-yl] propanoic acid **(26)** as a pale yellow and hygroscopic crystal (25 mg; 0.07 mmol; 70%). Mp:108-110°C; ν_{max} (KBr)/cm^{-1} 3409s (RNH_2) 2086m (N=C-S) 1688vs (COOH) 1434s (C=C aromatic ring) 1206s (C-N) 1142s (S=O); $[\alpha]^{20}_{D}$ = -30.26° (*c* = 0.39, H_2O); ^{1}H NMR (400 MHz, D_2O) δ 7.38 (brs, 1H, H-5'), 4.08 (dd, *J* = 9.9, 4.7 Hz, 2H, H-1" major diastereoisomer), 4.02 (dd, *J* = 9.6, 4.6 Hz, 2H, H-1", minor diastereoisomer), 3.89 (d, *J* = 4.2 Hz, 1H, H-2), 3.86 (s, 3H, OCH_3), 3.77 (dd, *J* = 11.5, 4.2 Hz, 1H, H-3a), 3.67 (dd, *J* = 11.05, 4.2 Hz, 1H, H-3b), 3.45 – 3.40 (m, 1H, H-2"), 3.05 (s, 9H, NMe_3); ^{13}C NMR (101 MHz, D_2O) δ 162.6 (C=O), 162.9 (C=O), 163.3 (C=O), 163.6 (C=O), 120.9 (C-2'), 118.0 (C-4'), 115.1 (C-5'), 72.2 (C-2), 66.0 (C-1" major diastereoisomer), 62.9 (C-1" minor diastereoisomer), 63.8 (OCH_3), 43.8 (C-2"), 43.4 (NMe_3), 36.5 (C-3); HRMS (ESI$^+$): *m/z* 348.1462 $[M+H]^+$. Calculated for $C_{13}H_{24}N_4O_5S^+$ found 348.1465 $[M+H]^+$.

University of Cape Town

(2*S*)-*N*,*N*,*N*-2-trimethylammonium-3-[2-((2*S*)-2-amino-2-methoxycarbonyl) ethylsulfinyl)-1*H*-imidazol-4-yl] propanoic acid (27).

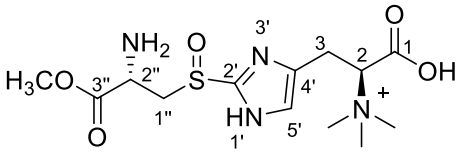

Same procedure for the synthesis of compound **(26)** was followed as described above. (2*S*)-*N*,*N*,*N*-2-trimethylammonium-3-[2-((2*S*)-2-amino-2-methoxycarbonyl)ethylsulfinyl)-1*H*-imidazol-4-yl] propanoic acid **(27)** was isolated as brownish and hygroscopic solid (15 mg; 73.2 %).

(2*S*)-*N*,*N*,*N*-2-trimethylammonium-3-[2-((2*R*)-2-amino-2-hydroxycarbonyl)ethylthio)-1*H*-imidazol-4-yl] propanoic acid trihydrochloride salt (28) [20, 21]

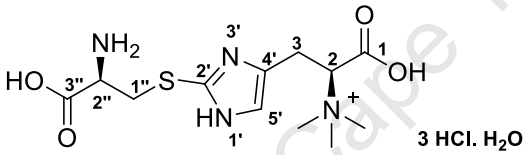

L-hercynine (**17)** (100 mg, 0.50 mmol) was dissolved in distilled H_2O (5 ml), followed by the addition of concentrated HCl (37 %, 28 mg, 74 µl, 0.76 mmol). The solution was allowed to cool in an ice bath, thereafter Br_2 (104 mg, 0.65 mmol) was added drop wise, followed by the addition of cysteine monohydrate chloride (439 mg, 2.50 mmol) 5 min later. The reaction mixture was allowed to stir for 90 min at 0°C. Purification by Dowex chromatography (gradient 0.5-2N HCl, Dowex (50WX8-100) and reverse phase chromatography (C18) afforded (2*S*)-*N*,*N*,*N*-2-trimethylammonium-3-[2-((2*R*)-2-amino-2-hydroxycarbonyl) ethylthio)-1*H*-imidazol-4-yl] propanoic acid trihydrochloride salt **(28)** as a pale yellow hygroscopic solid, in trihydrochloride hydrate salt form (193 mg, 46.6 %). Mp: 79°C (dec), Lit. 77° C (dec)[20]; ^{1}H NMR (400 MHz, D_2O) δ 8.77 (d, *J* = 7.6 Hz, 0.5H, H-5'), 7.47 (d, *J* = 10.5 Hz, 0.5H, H-5'), 4.53 (dd, *J* = 7.6, 4.3 Hz, 1H, H-2), 4.42 (t, *J* = 4.3 Hz, 1H, H-2"), 4.02 – 3.88 (m, 1H, H-3a), 3.55 (dt, *J* = 18.2, 7.6 Hz, 1H, H-3b), 3.41 (m, 2H, H-1"), 3.31 – 3.16 (m, 9H, NMe_3); ^{13}C NMR (101 MHz, D_2O) δ 170.8 (C-3"), 170.3 (C-1), 134.6 (C-2'), 122.5 (C-4'), 118.5 (C-5'), 67.7 (C-2), 54.6 (C-2"), 52.0 (NMe_3), 36.7 (C-3), 24.0 (C-1"); HRMS (ESI$^+$): *m/z* 317.1284 $[M]^+$. Calculated for $C_{12}H_{21}N_4O_4S^+$ found 317.1277 $[M]^+$.

University of Cape Town

(2*S*)-*N*,*N*,*N*-2-trimethylammonium-3-[2-((2*R*)-(*tert*-butoxycarbonylamino)-3-butoxycarbonyl)ethylthio)-1*H*-imidazol-4-yl] benzyl propanoate (29).[22]

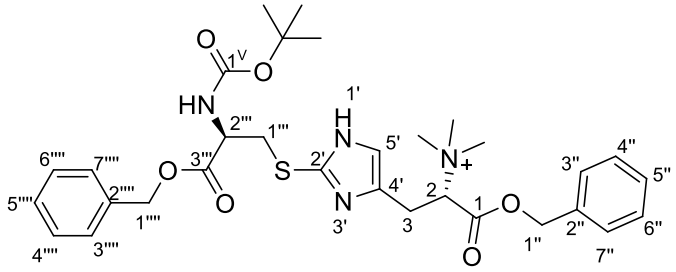

(2*S*)-*N*,*N*,*N*-2-trimethylammonium-3-[2-((2*R*)-2-amino-2-hydroxycarbonyl)ethylthio)-1*H*-imidazol-4-yl] propanoic acid trihydrochloride salt **(28)** (765 mg, 2.51 mmol) was dissolved in a mixture of distilled H_2O:CH_3CN (1:1, 10 ml), followed by the addition portion wise of NaOH (100 mg, 2.51 mmol). *Tert-butyl* dicarbonate (602 mg, 2.76 mmol) was added and the solution was allowed to stir overnight at room temperature. The solvent was evaporated under high vacuum to dryness, and the residue was triturated with Et_2O, dried under vacuum. The crude solid was dissolved in DMF (5ml) followed by the addition of benzyl bromide (943 mg, 5.52 mmol). The solution was allowed to stir overnight at room temperature. The solvent was removed under high vacuum to dryness. Purification by chromatography using silica gel column (CH_2Cl_2:MeOH, 70:30) afforded (2*S*)-*N*,*N*,*N*-2-trimethylammonium-3-[2-((2*R*)-(*tert*-butoxycarbonylamino)-3-butoxycarbonyl)ethylthio)-1*H*-imidazol-4-yl]benzylpropanoate **(29)** as a brown gum (563 mg, 37.6 %). $[\alpha]^{20}_D$ = +0.084° (*c* = 6.67, MeOH), ^{1}H NMR (400 MHz, DMSO) δ 8.63 – 8.24 (m, 10H, 2Ph), 7.90 (s, 1H, H-5'), 4.72 (s, 2H, H-1"), 5.32 (brs, 2H, NH), 4.44 (s, 2H, H-1""), 3.73 (d, *J* = 3.1 Hz, 1H, H-2), 3.66 (dd, *J* = 4.1, 2.7 Hz, 1H, H-2'"), 3.30 (dd, *J* = 11.1, 3.1 Hz, 1H, H-3a), 3.25 (dd, *J* = 16.8, 4.1 Hz, 1H, H-1'"a) 3.18 (dd, *J* = 16.8, 4.1 Hz, 1H, H-1'"b), 3.15 (dd, *J* = 11.1, 3.1 Hz, 1H, H-3b), 2.84 (s, 9H, NMe_3), 2.68 (s, 9H, Boc); ^{13}C NMR (101 MHz, DMSO) δ 169.4 (C=O), 169.2 (C=O), 168.7 (C=O), 138.3 (C-2'), 136.4 (C-4'), 129.7, 129.1, 128.8, 128.5, 128.0, 127.8, 127.1, 126.9 (8C, 2Ph), 125.57 (C-5'), 70.4 (C-1"), 69.5 (C-1""), 68.0 (C(Boc)), 53.7 (C-2), 51.7 (NMe_3), 51.3 (C-2'"), 37.7 (C-3), 36.3 (3C(Boc)), 25.4 (C-1'"); LRMS (EI^+) *m/z* calculated for $C_{25}H_{31}N_4O_4S^+$ 483.2 [M-Boc- CH_3]$^+$ found 483.7 ([M- Boc- CH_3]$^+$, 2 %).

University of Cape Town

(2*S*)-*N*,*N*,*N*-2-trimethylammonium-3-[2-((2*R*)-2-amino-2-hydroxycarbonyl) ethylsulfonyl)- 1*H*-imidazol-4-yl] propanoic acid (30)

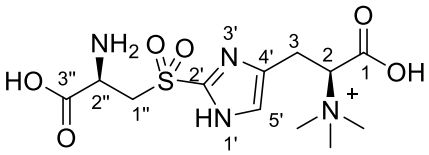

(2*S*)-*N*,*N*,*N*-2-trimethylammonium-3-[2-((2*R*)-2-amino-2-hydroxycarbonyl)ethylthio)-1*H*-imidazol-4-yl] propanoic acid trihydrochloride salt **(28)** (924 mg, 2.04 mmol) was dissolved in distilled H_2O (1ml) followed by the addition of H_2O_2 (30 %, 231mg, 2.04 mmol). The reaction mixture was allowed to stir at room temperature for 4 hours. The solution was lyophilized to dryness, the residue was recrystallized in a mixture of EtOH/H_2O to afford the (2*S*)-*N*,*N*,*N*-2-trimethylammonium-3-[2-((2*R*)-2-amino-2-hydroxycarbonyl)ethylsulfonyl)-1*H*-imidazol-4-yl] propanoic acid **(30)** as white hygroscopic needles (889 mg, 93%). Mp: 62-64°C; ν_{max} (KBr)/cm^{-1} 3517s (RNH_2) 1737vs 1632vs (COOH) 1441s (C=C aromatic ring) 1204s (SO_2); ^{1}H NMR (400 MHz, D_2O) δ 8.91 – 8.64 (m, 0.5H, H-5'), 7.44 (dd, *J* = 27.3, 10.8 Hz, 0.5H, H-5'), 4.61 – 4.50 (m, 1H, H-2), 3.92 (m, 2H, H-3), 3.86 (dd, *J* = 11.3, 7.4 Hz, 1H, H-1"a) 3.75 (dd, *J* = 11.3, 7.4 Hz, 1H, H-1"b), 3.70 – 3.37 (m, 9H, NMe_3), 3.34 (d, *J* = 7.4 Hz, 1H, H-2"); ^{13}C NMR (101 MHz, D_2O) δ 172.3 (C=O), 169.8 (C=O), 137.5 (C-2'), 136.0 (C-4'), 122.4 (C-5'), 74.8 (C-2), 52.5 (C-2"), 49.9 (NMe_3), 49.3 (C-3), 49.0 (C-1"); HRMS (ESI^+): *m/z* 349.1177 $[M]^+$. Calculated for $C_{12}H_{21}N_4O_6S^+$, found 349.1192 $[M]^+$.

6.3. Total Protein extraction and purification from *Mycobacterium smegmatis.*

6.3.1. Mc^{2}155 (*M. smegmatis*) growth conditions.

M. smeg culture (800 ml) were grown to exponential phase, and then dried to obtain 10 g of dry cells. The obtained pellets of *M. smeg* cells were thereafter stored at -80°C until it was required.

6.3.2. Total protein extraction.

M.smeg cells was sonicated for 35minutes at 4°C (25 pulsars), followed by the addition of potassium phosphate buffer (60 ml; pH 7). The solution was allowed to stir at 4°C for 10 minutes and thereafter centrifuged at 3000 rpm for 20 min. The supernatant was collected, measured and then the appropriate amount of ammonium sulphate gradually added while stirring at 4 °C overnight to obtain 60-70 % saturation.[23]

University of Cape Town

After precipitation of total protein the suspension was centrifuged at 4°C at 3000 rpm for 20 min and stored at -20°C.

6.3.3. Preparation of buffers.

6.3.3.1. Preparation of potassium phosphate buffer.

In distilled H_2O (1000 ml) was dissolved NaOH (2g; 50 mmol) to obtain solution A (NaOH 50 mM; 1000 ml). In distilled H_2O (1000 ml) was dissolved KH_2PO_4 (6.8 g; 50 mmol) to obtain solution B (KH_2PO_4 50 mM; 1000 ml). To solution A (291 ml) of was added of solution B (500 ml) and mixed thoroughly to obtain a solution C (potassium phosphate buffer 50 mM; pH approx 7)

6.3.3.2. Preparation of a dialysis Buffer.

To a solution C (791 ml; Potassium buffer 50 mM) was added a solution of pyridoxal 5'-phosphate (150 ml; 20 µM) and EDTA (50 ml) to obtain the dialysis buffer (1000 ml; pH approx 7)

6.3.4. Total protein purification.

The complex total protein ammonium salts precipitate was resuspended in dialysis buffer mixture (20 ml; pH 7) containing pyridoxal phosphate (10 ml; 20µM), potassium phosphate buffer (8 ml; 50 mM; pH 7) and (2 ml; 1mM EDTA). Thereafter the suspension was dialyzed against the same buffer until complete removal of ammonium sulphate as confirmed by a barium chloride test.[23, 24]

6.3.5. Total protein concentration.

6.3.5.1. Protein calibration curve

The Protein Dc Assay was used to obtain protein concentrations

- Create dilution series (0mg/ml-1mg/ml) with BSA. The following standards were used;

Conc (c2) (mg/ml)	**0**	**0.1**	**0.2**	**0.4**	**0.6**	**1**
BSA (v1) (µl)	0	5	10	20	30	50
H_2O (µl)	100	95	90	80	70	50

Where c1 = 2mg/ml and v2 = 100µl

University of Cape Town

- Mix together 1ml Reagent A and 20µl Reagent S for every 4 samples and label it "Reagent A".
- Dilute the protein (10% SDS) 1 in 10 and make sure to have a final volume of 50µl.
- Pipette 50µl of the standards and protein into 15ml tubes.
- Add 250µl Reagent A to each tube and vortex.
- Add 2ml Reagent B to each tube and vortex immediately.
- Let the reaction proceed for 15 min.
- After a few minutes have elapsed, transfer each sample to a cuvette.

Read the absorbance at 750 nm and calculate the concentration using the standard curve (excel doc).

6.3.5.2. Results

Supernatant: 0.009 µg/µl

Protein precipitate: 0.17 µg/µl

6.4. *In vitro* reconstituted biosynthesis of ergothioneine in *Mycobacteria smegmatis.*

Four sets of 500 µl reactions (1-4) containing 20 mM Tris HCl pH= 7.4, 20 mM NaCl , 0.2 Mm $FeSO_4.7\ H_2O$, 0.5 mM mercaptoethanol, 250 µl of crude enzymes and 50 mM of either (1) hercynyl cysteine thioether **(28)** (2) hercynyl cysteine sulfone **(30)** (3) deuterated hercynine **(17)** or (4) hercynyl cysteine methyl ester sulfoxide **(26)**. The reaction was stopped by heating the mixture at 90°C for 2 min followed by lyophilisation. The crude enzyme reactions were incubated for 1 day at 37° C. The reaction was stopped by heating the mixture at 90°C for 2 min followed by lyophilisation and sunsequent reconstitution in LC buffer before analysis by LC/MS.

Control

Containing 250 µl of 20 mM Tris HCl pH = 7.4, 20 mM NaCl, 0.2 mM $FeSO_4.7\ H_2O$, 0.5 mM mercaptoethanol, H_2O distilled and 250 µl of crude enzymes.

University of Cape Town

6.5. HPLC –ESI/MS (QTOF) analysis.

Analyses were carried out with a UHPLC Agilent 1290 Infinity Series (Germany), accurate mass spectrometer Agilent 6530 Qradrupole Time Of Flight (QTOF) equipped with an Agilent jet stream ionization source (positive ionization mode) (ESI^+) and column (Eclipse + C_{18} RRHD 1.8 µm.2.1 X 50, Agilent, Germany).

To optimise the MS signal, direct injection of 10 µl of standard solutions was dissolved in 3 % acetonitrile, 0.1 % formic acid in milli-Q water. Analyte separation was attempted in 3 % acetonitrile, 0.1 % formic acid in milli-Q water as mobile phase in an isochratic flow rate of 0.4 ml/min.

The system was controlled with the software packages Mass Hunter workstation software (Qualitative and Quantitative version B.05.00; Build 5.0.519.0, Agilent 2011, Germany).

University of Cape Town

6.6. References.

1. Trampota, M., *United States Patent*, **2010**, US 7,767,826, B2.
2. Garner, P.; Park , J-M., *J. Org. Chem.*, **1987**, 52, 2361.
3. Health, H.; Lawson, A.; Rimington, C., *J. Chem. Soc.*, **1951,** 2215.
4. Keheller, F. and Proinsias, O.K., *Tetrahedron letters*, **2007**, 48, 4879.
5. Mc Killop, A.;Taylor , R. J.K.; Watson, R.J.; Lewis, N., *Synthesis* , **199**4, 31
6. Crosignani, S.; White, P.D. and Linclau, B., *J.org. Chem*, **2004**, 69, 5897.
7. Collier, P.N.; Campbell, D.A.; Patel, I.; Raynham, T.M. and Taylor, R.J.K., *J.Org. Chem.*, **2002**, 67, 1802.
8. Garner, P.; Park, J-M., *Org. Syn. Coll*, **1998**, 9, 300.
9. Bregant, S. and Tabor, A. B., *J.Org. Chem.*, **2005,** 70, 2430.
10. Alsina, J.; Rabanal, F.; Chiva, C.; Giralt, E. and Albericio, F., *Tetrahedron*, **1998**, 54, 10125.
11. Lidia, D.L.; Giampaolo, G., and Porcheddu, A., *Org Lett*, **2002,** 4,553.
12. Collier, P.N.; Campbell, D.A.; Patel, I.; Raynham, T.M. and Taylor, R.J.K., *J.Org. Chem.*, **2002**, 67, 1802.
13. Reinhold, V.N; Ishikawa, Y. and Melville, D.B., *J. Med. Chem*, **1968,** 11(2), 258.
14. Cundy, D.; Gurr, P.A.; Knill, A.M., *Arkivoc*, **2000**, 158.
15. Halle, J.C. and Simonnin, M.P., *J. Biol. Chem.*, **1981**, 8569.
16. Fattori, D.; Rossi, C.; Fincham, C.I.; Caciagli, V.; Catrambone, F. and Quartara, L., *J. Med. Chem.*, **2007**, 50, 550.
17. Ishikawa, Y.; Israel, S.E. and Melville, D.B., *J. Biol. Chem.*, **1974**, 279, 4420.
18. Navickas, V.; Ushakov, D. B.; Maier, M. E.; Stroebele, M. and Meyer, H-J, *Org. Let.*, **2010**, 12, 3418.
19. Kano, N., Daicho Y. and Kawashima, T., *Org. Lett*., **2006**, 8, 4625.
20. Erdelmeier, I.; Daunay, S.; Lebel, R.; Farescour, L. and Yadan, J.C., *Green Chem.*, **2012**, 14, 2256.
21. Erdelmeier, I., *Patent WO2011/042480 A1*, **2011.**
22. Arnaud, O.; Koubeissi, A.; Ettouati, L.; Terreux, R.; Alame, G.; Grenot, C.; Dumontet C.; Pietro, A.D.; Paris, J. and Falson, P., *J. Med. Chem.*, **2010**, 53, 6720.
23. Ashraf, S. A., *J. Basic Microbiol.*, **2010**, 331.
24. Ashraf, S. A., *J. Microbiol.*, **2011**,130.

University of Cape Town